THESIS APPROVAL

GRADUATE SCHOOL, KASETSART UNIVERSITY

Master of Science (Chemistry)
DEGREE

Chemistry
FIELD

Chemistry
DEPARTMENT

TITLE: Preparation, Characterization and Photocatalytic Application of Nitrogen and Sulfur co-doped TiO_2 Photocatalyst

NAME: Miss Wanlapa Chitchiaranai

THIS THESIS HAS BEEN ACCEPTED BY

THESIS ADVISOR
(Associate Professor Apisit Songsasen, Ph.D.)

THESIS CO-ADVISOR
(Mr. Boonthana Wannalerse, Ph.D.)

DEPARTMENT HEAD
(Associate Professor Supa Hannongbua, Dr.rer.nat.)

APPROVED BY THE GRADUATE SCHOOL ON _____

DEAN
(Associate Professor Gunjana Theeragool, D.Agr.)

THESIS

PREPARATION, CHARACTERIZATION AND PHOTOCATALYTIC APPLICATION OF NITROGEN AND SULFUR CO-DOPED TiO_2 PHOTOCATALYST

WANLAPA CHITCHIARANAI

A Thesis Submitted in Partial Fulfillment of
the Requirements for the Degree of
Master of Science (Chemistry)
Graduate School, Kasetsart University
2011

Wanlapa Chitchiaranai 2011: Preparation, Characterization and Photocatalytic Application of Nitrogen and Sulfur co-doped TiO_2 Photocatalyst. Master of Science (Chemistry), Major Field: Chemistry, Department of Chemistry. Thesis Advisor: Associate Professor Apisit Songsasen, Ph.D. 132 pages.

N-S co-doped TiO_2 photocatalyst was prepared by the sol-gel method, which studied in term of effect on type of titania precursors and solvent in the step of preparation. The titania precursors used are titanium(IV) tetraisopropoxide and titanium(IV) tetra-n-butoxide. The solvents which were studied in this work are methanol, ethanol and isopropanol. The crystallite size and phase composition of the prepared photocatalyst were characterized by TGA, Raman and XRD. The XRD and Raman results indicated that the anatase transform to the rutile phase when increase temperature. The co-doped elements were incorporated into the TiO_2 structure due to the expansion of crystal lattice. SEM/EDX and TEM results showed that nitrogen and sulfur were dispersed in TiO_2 structure and its surface morphology was spherical like fluffy powders. Elemental Analysis and UV-Vis/DR results also suggested that nitrogen and sulfur could be dormant in the TiO_2 lattice and had effect on the narrowing of the band gap in the structure. These improved properties that could enhanced the photocatalytic activity of N-S co-doped TiO_2 under visible light. For the photocatalytic activity, N-S co-doped TiO_2 by titanium(IV) tetraisopropoxide used isopropanol as a solvent calcined at 400°C succeeded in degrading benz[a]anthracene and methylene blue with the highest efficiency.

Student's signature Thesis Advisor's signature ___ / ___ / ___

ACKNOWLEDGEMENTS

I would like to express my profound appreciation to my supervisor, Associate Professor Dr. Apisit Songsasen for introducing me to an interesting research theme. I wish appreciate his valuable guidance and encouragement throughout the span of my study and research. I also wish to express my sincere gratitude to Dr. Boonthana Wannalerse, member of the committee and Mr. Suchat Suwannatus, inventing the photoreactor used in my research.

I would like to thank the Center of Excellent for Innovation in Chemistry: Postgraduate Education and Research Program in Chemistry (PERCH-CIC) for financial support and the Department of Chemistry, Faculty of Science, Kasetsart University for all research facilities.

Finally, I am specially appreciated my parents for continuously boosting my morale and giving me financial assistance. I would like to thank all my colleagues and my friends for devoting their valuable time to helping me during my graduate study.

Wanlapa Chitchiaranai

September, 2011

TABLE OF CONTENTS

Page

TABLE OF CONTENTS (Continued)

Page

LIST OF TABLES

LIST OF TABLES (Continued)

LIST OF TABLES (Continued)

LIST OF TABLES (Continued)

LIST OF FIGURES

LIST OF FIGURES (Continued)

LIST OF FIGURES (Continued)

LIST OF FIGURES (Continued)

LIST OF FIGURES (Continued)

LIST OF FIGURES (Continued)

LIST OF FIGURES (Continued)

LIST OF FIGURES (Continued)

LIST OF ABBREVIATIONS

EA	=	Elemental Analysis
JCPDS	=	Joint Committee on Powder Diffraction Standard
PAHs	=	Polycyclic Aromatic Hydrocarbons
SEM	=	Scanning Electron Microscopy
TEM	=	Transmission Electron Microscopy
TGA	=	Thermal Gravimetric Analysis
TPO	=	Temperature-Programmed Oxidation
EPA	=	The American Environmental Protection Agency
UV-Vis/DR	=	UV-Vis Diffuse Reflectance Spectrophotometry
XRD	=	X-ray Diffraction

PREPARATION, CHARACTERIZATION AND PHOTOCATALYTIC APPLICATION OF NITROGEN AND SULFUR CO-DOPED TiO_2 PHOTOCATALYST

INTRODUCTION

1. Titanium dioxide (TiO_2)

Titanium dioxide (TiO_2), also known as Titania, is naturally occurring oxide of titanium. It occurs generally in the mineral sources such as ilmente, rutile, anatase and brookite. Ilmenite or titanic iron ore is a grey mineral to use as a source of titanium metal, white pigment, welding rod coating and other products. It was firstly discovered at Ural Ilmen Mountain (Russia) in 1827 by Kupffer who named it. Rutile is the most stable from of titanium dioxide and major ore of titanium was discovered in 1803 by Werner in Spain. It is commonly reddish brown but also sometimes yellowish or violet and contains up to 10% of iron and other impurities. The main uses for rutile are the manufacture of refractory ceramic, as a pigment, or the production of titanium metal. Anatase, earlier called octahedrite, was named by R.J. tlauy in 1801. It is always found as small, isolated and sharply developed crystals and a more commonly occurring modification of titanium dioxide. Brookite was discovered by A. Levy in 1825. Its crystals are dark brown to greenish black mineral mainly consisting of titanium dioxide but brookite occurs rarely compared to the anatase and rutile from titanium dioxide phase (Crap *et al*., 2004).

1.1 Crystal structure and properties

Titanium dioxide can naturally occur in three crystal structures, anatase, rutile and brookite (Figure 1). Anatase and rutile both are tetragonal structures, whereas brookite is orthorhombic (Gopal *et al*., 1997). All three crystal structure consists of octahedral (TiO_6), where each Ti^{4+} ion is surrounded by an octahedral of six O^{2-} ions (Chen *et al*., 2007). They still differ from one another by distortion of

each octahedral and by assembly pattern of the octahedral chains. Anatase is corner-sharing octahedral and they are connected with their edges with the plane of octahedral below. In rutile, two opposite edges of each octahedral are sharing and chains are then linked to each other by sharing corner oxygen atoms. These differences in lattice structures cause different mass densities and electronic band structures between the two forms of TiO_2 (Chen *et al*., 2007). The structure of brookite is more complex and connected by corner and edge sharing in the orthorhombic system.

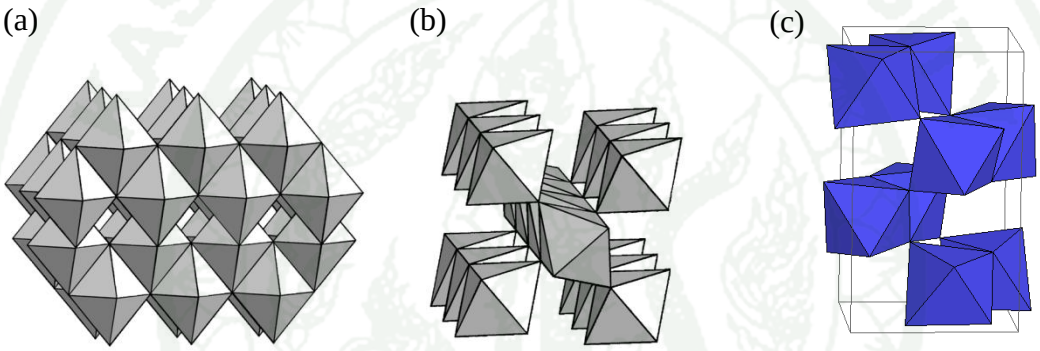

Figure 1 Crystal structures of (a) anatase, (b) rutile and (c) brookite

Source: Gopal *et al*. (1997)

Furthermore, phase stability in a thermodynamic, rutile is the most stable phase of titanium dioxide while anatase and brookite are metastable phase. The metastable structures are almost as stable as rutile at normal pressure and temperature because of small difference in the Gibbs free energy (4-20 kJ/mol) between three phase (Crap *et al*., 2004). Additionally, some researchers reported that the small TiO_2 nanoparticles (<50 nm), anatase phase seemed more stable. Other crystal properties of all three structures of TiO_2 are shown in Table1.

Table 1 Some crystal properties of the three crystal structures of TiO_2

Crystal structure	System	Space group	Lattice constants (nm)			Density (kg/m^3)	Band gap (eV)
			a	b	c		
Anatase	Tetragonal	$I4_1/amd$	0.3733	0.3733	0.937	3830	3.26
Rutile	Tetragonal	$P4_2/mmm$	0.4584	0.4584	0.2953	4240	3.05
Brookite	Orthorhombic	Pbca	0.5436	0.9166	0.5134	4170	-

Source: Carp *et al*. (2004)

1.2 TiO_2 applications

TiO_2 has been the most widely used for many fields and has attracted great attention due to its nontoxicity, inexpensiveness, chemical stability and favorable optoelectronic properties. It has found applications in various fields such as photovoltaic, photocatalysis, self-cleaning coating and pigments. In photocatalysis, TiO_2 has semi-conducting properties which make it an attractive material to be used as a photocatalyst. Among the three crystal structures of TiO_2 (anatase, rutile and brookite), anatase usually exhibits higher photocatalytic activity than rutile. The higher adsorption affinity toward organic compound, along with the lower electron-hole recombination rate of anatase, phase makes it a superior photocatalyst (Periyat *et al*., 2009). Good catalytic property depends on surface area and crystallinity of the photocatayst. The high crystallinity helps to prolong the recombination rate of the photo-excited electron and positive hole. The high surface area helps to facilitate adsorption of the target molecules onto the surface of the catalyst; as higher numbers of molecules are adsorbed the faster the rate reaction (Kanna *et al*., 2008).

The photocatalytic activity of TiO_2 originates from semiconductor band between the valence band (VB) and the conduction band (CD). The energy difference between the VB and CD is known as the "band gap". When TiO_2 absorb UV irradiation or illuminated light source which has equal or higher energy than band gap energy of TiO_2 (3.2 eV for the anatase phase) producing an electron-hole pair on the surface of TiO_2 as schematized in Figure 2. An electron is promoted to the conduction band creating the negative-electron (e^-) while a positive hole (h^+) is formed in the valence band. After reaction with water and oxygen in the environment, these holes can produce hydroxyl radicals or active species with high redox oxidizing potential. Depending upon the exact conditions, the holes, OH radicals, O^{2-}, H_2O_2 and O_2 itself can important roles in the photocatalytic reaction (Zaleska, 2008). The organic compounds are decomposed by reaction with the active species on the TiO_2 surface.

The usually proposed of the photocatolytic reactions at the surface of TiO_2 are as followed (Gnaser *et al*., 2005):

Electron–hole pair formation:

$TiO_2 + h\nu \rightarrow TiO_2 (e^- + h^+)$ (1)

Oxidation of adsorbed water by holes:

$(H_2O)ads + h^+ \rightarrow H^+ + OH^\bullet$ (2)

Adsorbed oxygen by electrons:

$(O_2)ads + e^- \rightarrow O_2^{\bullet -}$ (3)

Oxidation of adsorbed hydroxide ions by holes:

$2(OH^-)ads + h^+ \rightarrow OH^- + OH^\bullet$ (4)

Transient formation of hydroperoxide radicals via Eq. (3) and the further reactions:

$O_2^{\bullet -} + H^+ \rightarrow HOO^\bullet$ (5)

$2HOO^\bullet \rightarrow H_2O_2 + O_2$ (6)

$H_2O_2 + e^- \rightarrow OH^- + OH^\bullet$ (7)

Oxidation of organics by $OH^\bullet$ radicals, or directly by holes:

$R H + OH^\bullet \rightarrow R^\bullet + H_2O$ (8)

$R + h^+ \rightarrow R^{+\bullet} \rightarrow$ degradation products (9)

Moreover, excited-state electrons and holes can recombine and dissipate the input energy as heat, get trapped in metastable surface states, or react with electron donors and electron acceptors adsorbed on the semiconductor surface or within the surrounding electrical double layer of the particles (Zaleska, 2008).

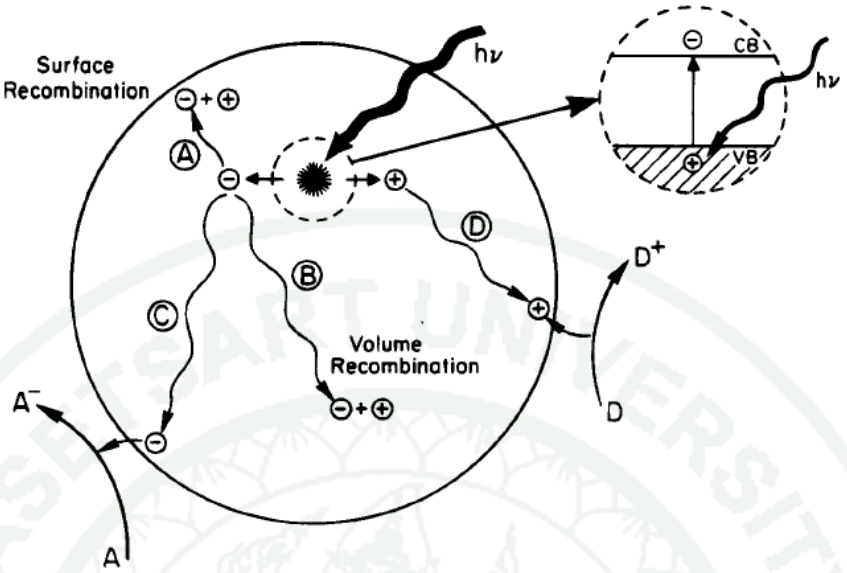

Figure 2 photocatalytic process on the TiO_2 particle; (dash line) e^- and h^+ generation, (C) reduction of acceptor, (D) oxidation of donors, and (A) and (B) e^- and h^+ recombination at surface and in bulk, respectively.

Source: Linsebigler *et al*. (1995)

1.3 Modification of TiO_2 photocatalyst.

The development of TiO_2 photocatalyst that show a high photoactivity under visible light irradiation is needs in order to utilize sunlight or rays from artificial sources more effectively in photocatalytic reaction (Ohno *et al*., 2004). However, TiO_2 can be activated only under UV-light irradiation due to its wide band gap of 3.2 eV for anatase phase, which is a small fraction (about 3-5%) of the sunlight (Sheng *et al*., 2008). Several methods have been devoted to enhance the photoactivity, among which, non metal doping such as nitrogen, sulfur, fluorine, bromine, carbon and boron. The doping of TiO_2 lattice to modifies its electronic band gap and shift its absorption edge to the visible light region (Yang *et al*., 2010). For example, N-doping was found to be effective in decreasing the band gap of TiO_2 by generating an isolated N 2p narrow band above the O 2p valence (Huang *et al*., 2006). Smith *et al*., 2007 prepared S doped TiO_2 by oxidative annealing of TiS_2 powder, has been found to

have a lower band gap than pure TiO_2, giving a higher photoactivity under visible light. They suggested that sulfur on the surface in the form of SO_4 and S defects in the bulk (most likely S interstitials).

Recently, many researchers reported that the doping of TiO_2 with double non-metal elements has attracted more attention. Huang *et al*., 2006 found that N, F co-doped TiO_2 photocatalyst had a higher visible light photocatalytic activity than TiO_2 doped solely with nitrogen or fluorine. This can be ascribed to the doped N atoms improved the visible light absorption and the doped F atoms led to the enhancement of surface acidity and the adsorption of reactant. Chen *et al*., 2007 found that C, N co-doped TiO_2 prepared by sol-gel method exhibited the highest photocatalytic activity, which attributed to the N atoms could incorporate into the lattice through substituting the sites of oxygen atoms, while most C atoms could form a mixed layer of deposited active and complex carbonate species at the surface of TiO_2 nanoparticles.

Furthermore, Yu *et al*., 2005 reported that the N, S co-doped TiO_2 exhibited a significant photoactivity under daylight, stronger absorption in the UV-vis light and a red shift in the band gap due to the band gap of N, S co-doped TiO_2 were narrowed by mixing the N 2p and S 3p states with O 2p states. In addition, Wei et al. reported that doping TiO_2 with N and S could also the creation of surface oxygen vacancies and the enhancement of surface acidity.

1.4 Preparation method

A number of methods have been used to prepare TiO_2 photocatalyst, such as electrochemical, hydrothermal, precipitation, sol-gel, chemical vapour decomposition and spin coating. Sol-gel is one of the most sucessful techniques for preparing nanosized materials with high photocatalytic activities. It is used mainly to produce thin film and powder catalyst. Sol-gel has many adventages over method is terms of purity, homogeneity, precise composition control and low-temperature synthesis. Generally, there are two know types of titania precursors, non-alkoxide and

alkoxide, utilized in the sol-gel method. The metal alkoxide are used as a starting material because metal alkoxide precursors are commercially avaible in high purity and are easily hardled at ambient temperature. The former makes use of inorganic salts (such as chlorides, acetyacetonatem etc.), which requires the removal of the inorganic anions after preparation. The sol-gel method is composed of four key steps as follow;

a. Wet solution

This step focuses on gel formation, which is a diphasic material with a solid encapsulating solvent. Before gel formation occurs, a starting material will be hydrolyzed and partially condensed in order to form sol, which is liquid suspension in solid particles. After that, further condensation in three-dimension network is conducive to gel formation. In case of metal alkoxide precursors, the reactions are shown below.

Hydrolysis reaction: $-M-OR + H_2O \longrightarrow -M-OR + R-OH$

Condensation reaction: $-M-OH + XO-M \longrightarrow -M-O-M + X-OH$

Where x is either H or R (an alkyl group)

b. Aging

To further complete the reaction, gel is left to continue constructing its more networks causing stronger cross-linkage. Moreover, some solvent molecules are expelled by the extensive condensation of gel. This step mainly depends on aging time, temperature as well as pH.

c. Drying

In order to remove organic solvent or hydrolyzed molecules, metal oxide needs to be heated at the temperature to dispose them. Furthermore, this step is

involved in the capillary pressure that has an effect on the pore size of metal oxide. Therefore, many factors, such as heating rate, pressure rate and time, are taken into serious consideration with a view to controlling the pore structure of metal oxide.

d. Calcination

This final step emphasizes on crystallization of metal oxide. Calcination is used in order to remove the dormant organic part and to crystallize phase of metal oxide. However, it will inevitably cause a decrease in surface area, loss of surface hydroxyl groups and even phase transformation.

2. Polycyclic aromatic hydrocarbons (PAHs)

Polycyclic aromatic hydrocarbons (PAHs) compounds are a class of complex organic chemicals, which include carbon and hydrogen with a fused ring structure containing at least two benzene ring. The molecular structures of PAHs have been defined as priority pollutants by The American Environmental Protection Agency (EPA) (Henner *et al*., 1997). PAHs, an important class of pollutants, are ubiquitously distributed in the environment, possessing mutagenic, carcinogenic and teratogenic properties (Shen *et al*., 2007). Although only at trace levels, they pose a real threat to human health, especially high molecular weight PAHs.

PAHs are formed from the incomplete combustion or pyrolysis of organic materials such as oil, petroleum gas, coal and wood which are usually used in energy production. They are adsorbed on the solid such as soils and sediments which contents increase in the vicinity of large urban and industrial areas and are carried at long distances by air in the troposphere. As for benz[a]anthracene, is one of the PAHs, consisting of four-member ring structure and a high molecular weight as shown in Table 2. Benz[a]anthracene is probable human carcinogen because it is formed when gasoline, garbage, or any animal or plant materials burns, usually found in smoke and soot.

3. Methylene blue

Dyes are organic compounds for used as dyeing, paper and pulp, textiles, plastics, leather, cosmetics and food industries. A large volume of wastewater generated from the textiles industries. The production of dye is lost during the dyeing and finishing process, which contains suspended solids, dyestuffs (color) and other auxiliary chemicals (Zhou *et al*., 2008). In addition, some dyes are carcinogens and they are affected on aquatic environment and living organisms. The release of these colored wastewaters in the ecosystem is a dramatic source of aesthetic pollution, decrease BOD of water and obstruct the route of photosynthesis. Dyes usually have complex aromatic molecular structures which make them more stable and difficult to degradable. Thus, many researchers to develop a suitable purification method that can degrade the organic pollutant present in wastewater.

Among, the various dyestuffs, methylene blue (MB) is an intensely colored compound and the most commonly employed basic dye (thiazine group) that find enormous application in dyeing and printing industry. It is a common water pollutant. MB is a heterocyclic aromatic chemical compound as shown in Table 2. It appears as a solid, odorless, dark green powder at room temperature and soluble in water and alcohol.

Table 2 The structures and general properties of benz[a]anthracene and methylene blue

structure	Properties			
	Molecular formula	Molecular weight (g/mol)	Melting point (K)	Boiling point (K)
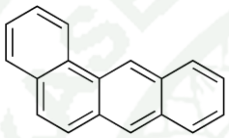	$C_{18}H_{12}$	228.29	158	438
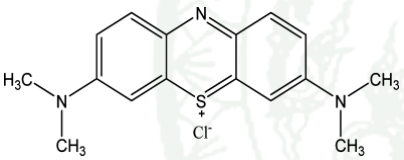	$C_{16}H_{18}N_3SCl$	319.9	100-110	-

Source: Henner *et al*. (1997)

OBJECTIVES

The aim of the present work was to investigate the preparation with sol-gel, characterization with various techniques and photocatalytic application N-S co-doped TiO_2.There are three main objectives that this work focuses on;

1.To study the effect of calcinations temperature on two titania precursors on phase transformation, crystallinity, crystallite size, visible absorption ability as well as the amount of co-doped nitrogen and sulfur.

2.To study the effect of solvent in sol-gel method on the N-S co-doped TiO_2 at fixed calcinations temperature of 400°C in terms of its phase composition, crystallinity, crystallite size and visible absorption ability as well as the amount of co-doped nitrogen and sulfur.

3.To make use of some the N-S co-doped TiO_2 in photocatalytic degradation of benz[a]anthracene and methylene blue, the photocatalytic activites and rate constants of each N-S co-doped TiO_2 were studied.

LITERATURE REVIEW

This section reviews of some previous researchs of the preparation of titanium dioxide doped non-metal by different methods and characterization techniques. The studies on photocatalytic activity of TiO_2 with doping non-metal and its application are also be reviewed.

Ohno *et al*. (2004) synthesized the titanium dioxide photocatalysts in which S substitutes for some of the lattice titanium atoms (S-doped TiO_2), by using titanium isopropoxide as a titania precursors and thiourea as a sulfur precursors. The catalyst was calcined at various temperatures. Diffuse reflectance spectra showed that the photoabsorption in the visible region was strongest when the catalyst was calcined at about 500ºC. From results of XPS spectra indicated that S atoms have 4 oxidation state into the bulk phase of TiO_2. S-doped TiO_2 (calcined at 500ºC) showed high photocatalytic activity in photodegradation of methylene blue, 2-propanol and partial oxidation of adamantine under irradiation at wavelengths longer than 400 nm.

Yu *et al*. (2005) developed titanium dioxide co-doped nitrogen and sulfur (N, S co-doped TiO_2) which prepared by hydrolysis of $Ti(SO_4)_2$ in a $NH_3.H_2O$ solution at room temperature. The catalyst was calcined at various temperatures form 400ºC to 800ºC. The results of XRD investigated the effects of calcination temperature on the phase structures of TiO_2 powders. At 400ºC, the powder was anatase phase. With increasing calcination temperatures (from 400 to 700ºC), the peak intensities of anatase increase and the width of peak becomes narrower. The rutile phase starts to appear at 700ºC. SEM image of the TiO_2 powder calcined at 500ºC found to be fine and slightly agglomerated. The UV-vis absorption spectra of N, S co-doped TiO_2 indicated that a stronger absorption in the UV-vis light region and a red shift in the band gap transition due to N, S doping. The catalyst calcined at 500ºC showed the highest photodegradation of acetone and formaldehyde.

Ho *et al*. (2006) developed the preparation of S-doped TiO_2 photocatalysts by using a one-step low temperature hydrothermal process. The XRD patterns showed

that the crystalline TiO_2 was formed and sulfur could be efficiently doped into the anatase phase and the crystallite size of the S-doped TiO_2 increase with the S dopants. The sulfur atoms are all in the state of S^{2-}, which corresponds to the Ti-S bond formed when some of the oxygen in the TiO_2 lattice are replaced. The photocatalytic activity of the samples were evaluated by degradation of 4-chlorophenol in aqueous solution under visible light irradiation. The results showed that the S-doped TiO_2 prepared by this hydrothermal process possesses much higher photocatalytic activity than that obtained from traditional high-temperature processes.

Huang *et al*. (2006) studied the effect of acidity and solvents on crystallinity, morphology and size of the prepared N-F co-doped TiO_2 powder. The catalyst was prepared by a sol-gel solvothermal method using tetrabutyl titanate as precursor. From XRD patterns, samples prepared in low dielectric constant organic solvents possessed smaller particles than those prepared in high dielectric constant organic solvents. The prepared catalyst was in anatase phase. The effect of medium pH value indicated a too low or too high pH resulted in the formation of smaller particles. The XPS spectrum showed that the N- F co-doped TiO_2 powder contained only Ti, O, F, N elements and a trace amount of carbon. The N and F elements were incorporated into the TiO_2 crystal lattice or were adsorbed on the surface of the crystals. The N-F co-doped TiO_2 powder showed high photocatalytic activity for p-chlorophenol and Rhodamine B under visible light irradiation (400-500 nm).

Katoh *et al*. (2006) prepared titanium dioxide doped sulfur (S-doped TiO_2) by a mixture of titanium (III) chloride and ammonium thiocyanate solution. The powders were calcined at 400 ºC and various concentration of ammonium thiocyanate (0.5, 1 and 13 M). The catalysts were characterized by X-ray photoelectron spectroscopy (XPS), X-ray powder diffractometry (XRD) and UV-Vis diffuse reflectance spectrophotometry. The S-doped TiO_2 (1M) exhibited higher photocatalytic activity than commercial anatase type TiO_2 for degradation of methylene blue in aqueous solution under visible light irradiation.

Shouxin *et al*. (2006) prepared N-doped TiO_2 photocatalyst by using the acid-catalyzed hydrolysis method followed by calcinations in an NH_3/N_2 atmosphere. The catalyst was calcined at 500ºC at various calcinations periods. N-doped TiO_2 was a vivid yellow powder. With the increase in the N doping content, the yellow color of TiO_2 became deeper. The UV-Vis/DRS spectra showed a second absorption edge in the visible region (490-550). When increase the N doping content, the second absorbance edge shifts to the longer wavelength. The effect of the calcinations temperature on the BET surface area and on the crystal size of TiO_2 indicated that the BET surface area increased, whereas the crystal size of TiO_2 decreased with the increase in the calcinations temperature. The N-doped TiO_2 photocatalyst calcined at 500ºC for 5 h exhibited a higher activity than the unmodified TiO_2 and P25 for degradation of phenol in both UV and visible light regions.

Chen *et al*. (2007) prepared C-doped TiO_2, N-doped TiO_2 and C-N co-doped TiO_2 photocatalysts by sol-gel method. XRD results showed that the doping of nitrogen and carbon atoms in TiO_2 can suppress the crystal growth of TiO_2. The lattice parameter and XPS revealed that nitrogen atoms could incorporate in the lattice of anatase through substituting the sites of oxygen atoms, while carbon atoms could form a mixed layer composed of a complex carbonate species at the surface of TiO_2 nanoparticles. C, N co-doped TiO_2 photocatalyst had higher photocatalytic activites than those doped solely with carbon or nitrogen under visible light.

Wei *et al*. (2007) prepared N-S co-doped anatase nanosized TiO_2 photocatalyst (NSTO) by one-step hydrothermal method from a mixed aqueous solution of $Ti(SO_4)_2$ and thiourea. The catalyst was characterized by X-ray powder diffractometry (XRD), X-ray photoelectron spectroscopy (XPS), Elemental analysis (EA), Fourier transform infrared spectroscopy (FT-IR) and UV-Vis diffuse reflectance spectrophotometry. From results of UV-vis, the absorption spectrum of NSTO shows a red shift. XPS, EA and FT-IR studies revealed that N and S were in situ co-doped in the lattice of TiO_2. The photocatalytic tests showed that NSTO exhibited a high activity for decompositions of methyl orange in aqueous solution in both UV-light and vis-light irradiation comparing to S-doped TiO_2 and undoped TiO_2.

Xie *et al*. (2007) prepared N-doped and N-S co-doped anatase TiO_2 photocatalyst by using sol-gel method at 100°C. Titaniumtetrachloride, ammonia and thiourea were used for the synthesis of N-doped and N-S co-doped TiO_2, which N, S co-doped TiO_2 prepared from precursors with different molar ratio of thiourea (3/100, 5/100, 20/100, 40/100 and 100/100). The XRD patterns of N-doped and co-doped TiO_2 indicated the structure of anatase phase. The intensity of (101) peak increase with increasing molar ratio of thiourea/TiO_2 and decrease when the ratio higher than 20/100. This suggests that the addition of thiourea might enhance the formation and growth of TiO_2 anatase phase, but the surplus thiourea might be unfavorable for the formation of anatase. The crystallite sizes of samples are in range of 5-8 nm, which is promising since nanocrystalline has being considered as the more photoactive form of TiO_2. TEM image showed that N-S co-doped TiO_2 has rodlike morphology and SAED analysis confirmed that sample has anatase structure. The UV-Vis/DRS of samples with different molar ratios of thiourea to TiO_2 revealed that the absorption edge shifts from 387 to 510 nm with decreasing initial molar ratio of thiourea/TiO_2 from 100/100 to 3/100. The N, S co-doped TiO_2 (thiourea/TiO_2: 20/100) exhibited the highest photodegradation activity with a methyl orange conversion of 90.6% and 96.6% after 8 and 24 h under visible light irradiation.

Zhang *et al*. (2007) synthesized N-S co-doped TiO_2 montmorillonite (NST-MMT) by impregnating doped titania sol in the interlayers of MMT. Titanium tetrachloride ($TiCl_4$) and thiourea ($CS(NH_2)_2$) were used as the precursors of TiO_2, N and S, respectively and calcined at 300, 350, 400 and 500ºC in air for 2 h. The XRD patterns showed that the (001) peaks of MMT disappeared and the layered structure of MMT was delaminated, which is confirmed by the SEM images. The surface of the layered MMT is smoother and its crystallinity is better but the surface of NST-MMT shows small flakes, which are attributed to delamination of MMT. The anatase phase of TiO_2 apperars at all samples and its crystallinity increase with increasing calcinations temperature. The XPS spectrum of sample which was calcined at 350ºC indicated the substitution of N and S in catalyst. The S atoms are in the state of S^{6+} incorporated into the bulk phase of TiO_2 nanoparticles and the substitution of Ti^{4+} by

S^{6+}. The catalyst obtained at 350ºC exhibited the highest photocatalytic activity for degradation acid red G.

Ksibi *et al*. (2008) studied the preparation of titanium (IV) (diisopropoxide) bis (2, 4-pentadionate) substituted nitrogen and sulfur by sol-gel method, using different nitrogen and sulfur precursors (methyldibenzothiophene, urea, ammonia and thiourea). The catalysts were calcined at 550 ºC for two hours. A thermogravimetric analysis of samples showed that crystallization has been almost completed at this value of calcination temperature. The XRD patterns of the N-S co-doped TiO_2 samples revealed that anatase as the predominant homogeneous crystalline phase. The photocatalytic activity for decolouration of Congo red dye under near visible light indicated that S-doped TiO_2 catalyst has highest activity among the doped TiO_2 powders examined.

Li *et al*. (2008) prepared N-S co-doped TiO_2 photocatalyst by simple sol-gel method. UV-Vis spectra of samples showed a stronger absorption in the visible region and a red shift in the absorption edge which the absorbance decreases with increasing calcinations temperature. It could due to that high calcinations temperature could enlarge the particle size which lead non-metal element atom hard into the TiO_2 lattice. XRD patterns obtained that the particle size increased with the calcinations temperature increased. The cell parameters a and c (calculated according to XRD result) of N-S co-doped TiO_2 sample calcined at 450°C were slightly bigger than those of undoped TiO_2. The photocatalytic activities of N-S co-doped TiO_2 in visible region are about three times higher than that of Degussa P25 is ascribed to synergetic effects of codoping such as red shift in absorption edge and particle size.

Liu and Chen (2008) prepared TiO_2 photocatalyst with sulfur by acid catalyzed hydrolysis method using thiourea (TU) as sulfur source. The catalyst was characterized by DRS, XPS, XRD, FTIR, SEM and S_{BET}. The results showed that cationic S^{6+} was homogeneously incorporated into the bulk phase of TiO_2 and substituted for some of lattice titanium (Ti^{4+}). Doped S could form a new band gap and giving rise to a second absorption edge in the visible light region. For

photodegradation of phenol in aqueous solution under both artificial visible light and solar light irradiation, the catalyst calcinated 600°C with the mass ratio of TU/TiO_2=1 exhibited the highest activity. In addition, doped S also beneficial for TiO_2 crystalline dispersion, large S_{BET} and phase transformation retardation.

Sheng *et al*. (2008) prepared N-Br co-doped TiO_2, N-doped TiO_2 and undoped TiO_2 photocatalyst using a facile hydrothermal method at low temperature (100°C). From the optical properties, the undoped have no absorption in the visible band while the other two samples both have distinctly great absorption in the visible band. The N, Br co-doped TiO_2 showed obvious enhanced absorption in the visible range of 400-600 nm. The broad absorption below 500 nm is because the N 2p orbits are localized above the top of the O 2p valence bands, whereas the absorption above 500 nm is mainly caused by oxygen vacancies. The results of XPS showed the existence of N-Ti-N, O-Ti-N-R, Ti^{3+}, and TiO_xN_y species, indicating the successful codoping of N and Br atoms, which were substituted for lattice oxygen without any influence on the crystalline phase of TiO_2. The photodecomposition of the methylene blue (MB) in aqueous solution was carried out under UV and visible light. For under UV light, Degussa P25 exhibited the higher photodegrade MB than the doped TiO_2. The co-doped TiO_2 showed the highest photodecomposition of MB in visible light. The excellent visible light photocativity of doped TiO_2 because the doped N atoms will result in band gap narrowing and improve the visible light absorption of anatase TiO_2. Moreover, the doped Br atoms can convert Ti^{4+} and Ti^{3+} by charge compensation, and the existence of a certain amount of Ti^{3+} reduces the electron hole recombination rate and further enhanced photocatalytic activity.

Xie *et al*. (2008) studied the effects of synthesis temperature on the structure and photocatalytic activity of N-F co-doped TiO_2 and N-S co-doped TiO_2. The samples prepared at different temperature form 313 to 413 K. The XRD and selective area diffraction (SAED) pattern confirmed that the all of catalyst as anatase phase. The XRD peaks are weak for the sample synthesized at the temperature lower than 353 K and become stronger with increasing temperature. The XRD patterns showed that good crystalline structure could be formed at 373 and 353 K for the N-F co-doped

TiO_2 and N-S co-doped TiO_2. UV-Vis/DRS showed two band transitions for the co-doped samples. The first one in UV region (around 387 nm) is accounted for the titania fundamental band transition. The second in the visible region of 400-620 nm is resultant of non-metal codoping. Furthermore, the absorption edge of new band shifts towards higher wavelength on the whole with decreasing reactive temperature for all the co-doped titania photocatalysts. Photocatalytic decopomposition of methyl orange carried out in the visible region showed that the samples prepared at the temperature of 313 K had the highest photodegradation activity among the N-F co-doped TiO_2 and N-S co-doped TiO_2 photocatalysts and more than three times higher than that of Degussa P25.

Lv *et al*. (2009) studied the preparation, characterization and photocatalytic activity of N-S co-doped TiO_2, N-doped TiO_2 and S-doped TiO_2 photocatalysts by using tetrabutyltitanate was used as a precursor, urea as a nitrogen source and thiourea as a sulfur source. The absorption edges of the doped sample are shifted to the longer wavelength region with respect to that pure TiO_2. The XPS peak of N-S co-doped TiO_2 can be ascribed to the partial substitution of S^{4+} for the Ti^{4+} in the TiO_2 and the formation of Ti-N bond. BET surface area measurements indicated that the specific surface area of the co-doped TiO_2 is slightly higher than that of pure, N-, or S-doped TiO_2. The N-S co-doped TiO_2 showed the higest photocatalytic activity either under visible light or under solar light for photodegradation of metylene blue (MB). The effect of solution pH on the photocatalytic degradation of MB observed that the N-S co-doped TiO_2 exhibited the best photoactivities in both neutral and alkaline solutions.

Periyat *et al*. (2009) studied the preparation of N-S co-doped TiO_2 at high temperature by using titanium isopropoxide (TTIP) as a precursor and ammonium sulfate ($(NH_4)_2SO_4$) as a nitrogen and sulfur source. A stoichiometric modification of 1:8 (TTIP: $(NH_4)_2SO_4$) composition was found to be the most effective in extending the stability of anatase to higher temperature. At 800°C the co-doped sample is 100% anatase phase, whereas the pure TiO_2 was already completely converted to rutile phase at 800°C. The nitrogen adsorption and desorption isotherm of samples and pure

TiO_2, indicating the pore size to be in the micropore range which the surface area and pore volume decrease at the calcinations temperature increase. XPS studied showed that nitrogen is doped as an anion and sulfur as a cation within the TiO_2 lattice. The visible light photocatalytic activity of the sample calcined at 850°C was double that of Degussa P25, and the rate constant calculated by pseudo-first-order kinetics was 0.019 min^{-1} for the N-S co-doped TiO_2 and 0.008 min^{-1} for Degussa P25.

Zhang *et al* (2009) synthesized the N-S co-doped TiO_2 powders through a facile one step sol-gel method by using tetrabutyltitanate and thiourea as precursors. Thiourea was mixed with tetrabutytitanate at a molar ratio of 1:2 in ethanol. The XRD patterns of the N-S co-doped TiO_2 samples and undoped TiO_2 calcined at 500°C showed that the undoped TiO_2 was consistent with mixed phase of anatse and rutile. However, the N-S co-doped TiO_2 was attributed to anatase phase, which showed that the sulfur and nitrogen doping restain the phase transformation from anatase to rutile phase. The photoabsorption of N-S co-doped TiO_2 in the visible region was stronger than that of undoped TiO_2. XPS results indicated that nitrogen and sulfur atoms simultaneously incorporated into the bulk phase of TiO_2. The N-S co-doped TiO_2 calcined at 500°C has the highest efficiency for the degradation of methylene blue.

Zhou *et al*. (2009) prepared the N-I co-doped TiO_2 nanoparticles by hydrolysis method, using ammonia and iodic acid as the doping sources and $Ti(OBu)_4$ as the titanium source. The XPS results showed that N atoms substitute at some of oxygen atoms in TiO_2 lattice (Ti^{4+}, Ti^{3+}) and I exist in I^{7+}, I^- and I^{5+} chemical states in the sample. This result can further improve the visible light response of N, I co-doped TiO_2. I^{7+} can accept e^- and I^- can accept h^+, thus can prevent electron-hole recombination. Moreover, the existence of Ti^{3+} on the surface of N-I co-doped TiO_2 can slow down the recombination of the electron-hole pairs. The N-I co-doped TiO_2 showed the best photocatalytic activity for decoloration of methyl orange, comparing with Degussa P25 and undoped TiO_2. The discolorations rate of codoping as 96.3% under visible light irradiation for 2 h.

Yang *et al*. (2010) synthesized the F-S co-doped TiO_2 and mono (F, S) doped TiO_2 as photocatalysts by using low temperature solvothermal method., The catalysts were characterized by XPS, XRD, FTIR, laser Raman and EPR. The results showed that the solvothermal method produced F-S co-doped TiO_2 with S and F partially substituted the oxygen and gave smaller crystalline sizes than mono (F, S) doped TiO_2. For photodegradation of methylene blue in aqueous solution under visible light irradiation, the F-S co-doped TiO_2 exhibited higher photocatalytic activity than F and S doped TiO_2. The co-doped TiO_2 gives rise to a localized state in the band gap of TiO_2 and creates super oxygen species, thus leading to the enhancement of visible light photoactivities.

Wang *et al*. (2010) investigated mesoporous $TiO_{2-x}A_y$ (A = N, S) thin film using thiourea as a doping resource by a combination of sol-gel and evaporation-induced self-assembly (EISA) process. The samples presented homogeneous mesostructure with a high porosity and a narrow pore distribution. The co-doped TiO_2 showed the strong photoadsorption in the visible region (520 nm) corresponding to 2.38 eV. In order to evaluate the effect of (N-S) co-doping on the decomposition of methyl orange under UV and visible light irradiation compared with that of pure TiO_2, the co-doped TiO_2 showed that higher photocatalytic activity than pure TiO_2. The N-S co-doped TiO_2 films exhibited visible light-induced hydrophilicity and red shift of the absorption edge, which could be attributed to good photocatalytic activity.

MATERIALS AND METHODS

Materials

Reagents

1. Titanium(IV) isopropoxide ($C_{12}H_{28}O_4Ti$, Lab. Grade, Acros, New Jersey, USA)
2. Titanium(IV) tetra-n-butoxide ($C_{16}H_{36}O_4Ti$, Lab. Grade, Merck, Hohenbrunn, Germany)
3. Methanol (CH_3OH, AR. Grade, Mallinckrodt, Phillipsburg, USA)
4. Ethanol (C_2H_5OH, AR. Grade, Merck, Darmstadt, Germany)
5. Isopropanol (C_3H_7OH, AR Grade, Scharlau, Carl Roth, Spain)
6. Methylene blue ($C_{16}H_{18}N_3SCl$, Lab Grade, Fluka, Buchs, Switzerland)
7. Thiourea ($CS(NH_2)_2$, Lab Grade, Merck, Darmstadt,Germany)
8. Benz[a]anthracene ($C_{18}H_{12}$, Lab. Grade, Fluka, Buchs, Switzerland)

Methods

1. Catalyst preparation

N-S co-doped TiO_2 photocatalysts were prepared by sol-gel method using titanium(IV) tetraisopropoxide as a titania precursor, thiourea as a nitrogen and sulfur source. Initially, 1.522 g of thiourea was dissolved in 20 ml of solvent (methanol, ethanol and isopropanol). The mixture was added dropwise in 5.93 ml of titanium precursor under stirring condition. After the addition the mixture was stirred for 2 hours at 30°C. The dried-gel precursor was heated at 120ºC in the oven for 2 hours to evaporate the solvent and some organic by-products generating from the hydrolysis reaction. The white color gel was formed. Finally, the as-prepared N-S co-doped TiO_2 was calcined in the furnace at various temperatures (300-700°C) for 2 hours to obtain about a phase transition and removal of a volatile fraction. The color of catalyst depends on the calcination temperature. Additionally, the N-S co-doped TiO_2 using 6.83 ml of titanium(IV) tetra-n-butoxide instead of titanium(IV) tetraisopropoxides was also studied via sol-gel method.

Table 3 The titania precursors with their volumes, density and equivalent mole of titania

Titania precursors	Chemical formula	Density (g/ml)	Volume (ml)	Amount of titanium (mole)
Titanium(IV) tetraisoproxide	$C_{12}H_{28}O_4Ti$	0.950	5.93	0.02
Titanium(IV) tetra-n-butoxide	$C_{16}H_{36}O_4Ti$	0.999	6.83	0.02

2. Catalyst characterization

2.1 Thermal Gravimetric Analysis

The range of calcination temperature of the as-prepared catalysts was obtained from a TGA 7 Perkin Elmer analyzer. 4.0-5.0 mg of Al_2O_3 as a reference was loaded to protect the damaging effect of samples on an alumina pan. This weight was set as zero and then about 10.0 mg of the powdered sample was added into the pan. The temperature program was set up from 50°C to 700°C with the rate of 10 °C/min.

2.2 X-ray Diffraction (XRD)

2.2.1 Determination of the crystalline phase

The crystalline phase was obtained by a Philips Pw 1830 X-ray diffractometer (XRD) operated at 40 kV and 35 mA and a Philips X´ Pert X-ray diffractometer operated at 40 kV and 30 mA, both of which used Cu Kα radiation source at λ of 1.54 Å. XRD data were collected from 2θ of 20-60 degree. The sample was coated on the inverse side of clear adhesive tape and made its surface smooth by pressing with a spatula or spread on a small piece of glass. The crystalline phase of all samples were identified by comparison with the Joint Committee on Power Diffraction Standards (JCPDS) files.

2.2.2 Determination of the crystallite size

The crystallite size was also calculated by the Sherrer's equation as shown in equation 1 (Xie *et al*., 2008).

$$d = \frac{k\lambda}{\beta \cos\theta_B} \qquad \ldots\ldots (1)$$

where d is the crystallite size (nm)

k is the constant whose value is approximately 0.9

λ is the wavelength of the X-ray radiation source (0.154 nm for Cu Kα)

β is the full width at half maximum intensity (FWHM) (radians)

θ_B is the Bragg angle at the position of the peak maximum

The example of the calculation is shown in the Appendix A.

2.2.3 Determination of the content of anatase.

The content of anatase was also calculated by Spurr-Myers equation as shown in equation 2 (Spurr *et al*., 1957).

$$w_A = \frac{1}{(1+1.26\frac{I_R}{I_A})} \quad \text{..... (2)}$$

where w_A is the weight fraction of anatase in the mixture

I_R is the intensity of the diffraction peak of rutile

I_A is the intensity of the diffraction peak of anatase

The example of the calculation is shown in the Appendix B.

2.2.4 Determination of the unit cell volume

The unit cell volume was calculated from the product among three lattice parameters (a, b and c), which can be equated for the tetragonal system ($a=b\neq c$) as shown in equation 3.

$$\frac{1}{d^2} = \frac{h^2+k^2}{a^2} + \frac{l^2}{c^2} \quad \text{..... (3)}$$

where d is a lattice spacing between the planes in the atomic lattice

h, k and l are the Miller indices

a, b and c are the lattice parameters

The example of the calculation is shown in the Appendix C.

2.3 Raman spectroscopy

The Raman shift of samples were performed on a Renishaw Raman Imaging Microscope operated with green laser. Si plate was used to calibrate Raman, which exhibited the evident Raman shift at 520 cm^{-1}. The sample was deposited on a glass slide. A small amount of acetone solution was dropped to the sample in order to make the sample tightly attached to the glass slide.

2.4 Diffuse Reflectance UV-Vis spectrophotometry

Diffuse Reflectance UV-Vis spectra from 200 nm to 700 nm of all catalysts with slit width of 2 nm were collected on a Perkin Elmer Lambda 650 spectrophotometer. The powdered sample was mounted on a glass by using acetone to help the sample adhere to the glass plate during time. Then, the sample was pressed by a spatula to have a smooth surface and moved into the analysis chamber.

2.5 Scanning Electron Microscopy (SEM) and Energy Dispersive X-ray Spectroscopy (SEM/ EDX)

The morphology and the element constituents of the catalysts were determined by SEM recorded on a JEOL JSM-5600Lv scanning electron microscope fitted with tungsten filament and operated at 13 kV. The sample was spread on a carbon tape mounted on a SEM stub and coated with Au atoms in a sputter coater in order to enhance conductivity before to SEM operation.

2.6 Transmission Electron Microscopy (TEM)

The morphology and particle size of the catalysts were investigated by TEM recorded on a Hitachi-7650 electron microscope fitted with a standard tungsten filament and operated at 100 keV. The samples were diluted in water and deposited onto a 3 mm carbon coated copper grids.

2.7 Elemental Analysis (EA)

The nitrogen and sulfur contents were carried out on LECO CHNS-932 Elemental Analyzer. Before operating, the weight of a blank sample was set up at 2 mg needed to be run for many times until the percentage of C, H, N and S were constant. About 2 mg of Sulfamethazine as a reference was also necessary to be operated in order to check the instrumental accuracy which shows that the percentages of C, H, N and S should be congruent with the standard values. Then set blank again for another time before three-replicated samples weighted in tin capsules about 2 mg in each replica were run.

3. Preparation of benz[a]anthracene/metylene blue solution for photodegradation reaction

3.1 Preparation of benz[a]anthracene solution

25 ml of 1000 ppm stock benz[a]anthracene solution in pure methanol solvent was prepared by dissolving 0.0250 g standard benz[a]anthracene with certain volume in a 25 ml volumetric flask.

500 ml of 20 ppm benz[a]anthracene solution was prepared by diluting 10 ml of stock benz[a]anthracene solution with distilled water and methanol in the volumetric ratio of 1:3. Then, the solution was sonicated in water bath in order to enhance the solutbility of benz[a]anthracene and homogeneity of solution.

3.2 Preparation of methylene blue solution

250 ml of 1000 ppm stock methylene blue solution in distilled water was prepared by dissolving 0.25 g standard methylene blue with certain volume in a 250 ml volumetric flask.

250 ml of 20 ppm methylene blue solution was prepared by diluting 5 ml of stock methylene blue solution with distilled water. After that, the solution was sonicated in water bath in order to enhance the homogeneity of solution.

4. Preparation of benz[a]anthracene/metylene blue solution for linear calibration curves

4.1 The calibration curve of benz[a]anthracene solution

Initially, the series of benz[a]anthracene concentrations (0.1, 0.2, 0.3, 0.4 and 0.5 ppm) were prepared by diluting from 20 ppm of benz[a]anthracene solution with the volume of 0.05, 0.10, 0.15, 0.20 and 0.25 ml, respectively. Then, diluted solution was made up the volume to 10 ml by distilled water. Finally, the solutions were measured fluorescene emission using a Perkin Elmer Lambda 35 luminescence spectrophotometer.

4.2 The calibration curve of methylene blue solution

Initially, the series of methylene blue concentrations (2, 4, 6, 8 and 10 ppm) were prepared by diluting from 1000 ppm of stock methylene blue solution with the volume of 0.02, 0.04, 0.06, 0.08 and 0.10 ml, respectively. Then, diluted solution was made up the volume to 10 ml by distilled water. Finally, the solutions were measured the absorption by using a Perkin Elmer Lambda 35 UV-Vis spectrophotometer.

5. Photocatalytic study

5.1 Photocatalytic degradation of benz[a]anthracene

Initially, 125 ml of 20 ppm benz[a]anthracene solution containing 0.1 g of the prepared catalyst was added into a 400 ml beaker equipped with a UV cut-off filter. Prior to photocatalytic reaction, the suspension was allowed to reach adsorption equilibrium under dark reaction for an hour before the degradation. To follow the reaction, the sample was collected by a syringe in order to measure the amount of initial (before adding the photocatalyst) and remaining concentration of benz[a]anthracene in each period of time. Then, the reaction was operated under artificial light with 190W of the Xe-lamp. The sample was collected every 30 minutes until 4 hours of degradation. Before samples were picked up, the stirrer was switched off by 10 minutes. All the samples were left overnight in dark and then centrifuged about 20 minutes to reduce the dispersion of the fine-powdered catalyst. Finally, 0.2 ml of a sample was picked up an autopipette from the centrifuged sample and made up the volume by distilled water in a 10 ml volumetric flask. The benz[a]anthracene concentrations were measured by using a spectrofluorometer at λ_{em} of 526 nm. All samples were also conducted in three replicates.

5.2 Photocatalytic degradation of methylene blue

Initially, 100 ml of 20 ppm methylene blue solution containing 0.1 g of the prepared catalyst was added into a 400 ml beaker equipped with a UV cut-off filter. The reaction was operated under dark reaction for an hour and then under artificial light with 190 W of Xe-lamp. The dark reaction was done in order to let the system achieve the adsorption equilibrium before the degradation. To follow the reaction, the sample was collected by a syringe in order to measure the amount of initial (before adding the photocatalyst) and remaining concentration of metylene blue in each period of time. The sample was collected every1 hour until 5 hours of degradation. Before samples were picked up, the stirrer was switched off by 10 minutes. All the samples were left overnight in the dark and then centrifuged for 20

minutes to reduce the dispersion of the fine-powdered catalyst. Finally, 4 ml of a sample was picked up an autopipette from the centrifuged sample and made up the volume by distilled water in a 10 ml volumetric flask. The concentration of the samples were measured by using the UV-Vis spectrophotometer at λ_{max} of 664 nm. All samples were also conducted in three replicates.

6. Concentration measurement of benz[a]anthracene/methylene blue

6.1 Luminescence Spectrophotometry

The decreasing concentration of benz[a]anthracene was followed by measuring the absorption at 264 nm on a Perkin Elmer Lambda 35 spectrophotometer. The excitation slit width was 5 nm and emission slit width was 5 nm with scan speed of 1000 nm/min.

6.2 UV-Vis Spectrophotometry

The decreasing concentration of methylene blue was followed by measuring the absorption at 664 nm on a Perkin Elemer Lambda 35 spectrophotometer. Distilled water was used as a blank and reference solution.

7. Photoreactor

The photodegradation reaction of benz[a]anthracene/metylene blue was studied by using a photoreactor as shown in figure 3. 90/100W of the Xe lamp as a light source has been fitted, which can be selected to operate 90W, 100W or 190W per one lamp. The adaptor has necessarily been used for the adjustment of AC 220V to DC 12V. Inside the reactor, it contained a set of magnetic stirrer and a 400 ml beaker equipped with a HOYA UV 385 cut-off filter.

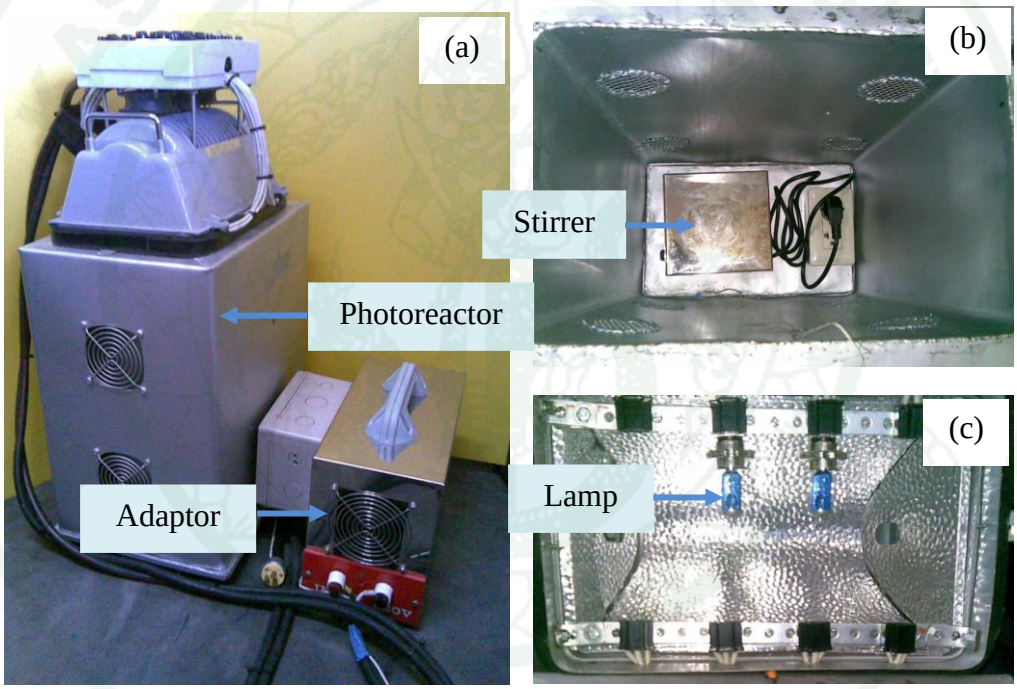

Figure 3 The image of the photoreactor; (a) photoreactor, (b) stirrer and (c) lamp.

RESULTS AND DISSCUSSION

1. Catalyst characterization

1.1 Effect of calcinations temperature

1.1.1 Thermal Gravimetric Analysis (TGA)

In order to obtain the effect of calcination temperature on the thermal decomposition behavior of the as-prepared N-S co-doped TiO_2 sample from the different type of titania precursors, all samples were characterized using thermal gravimetric analyzer.

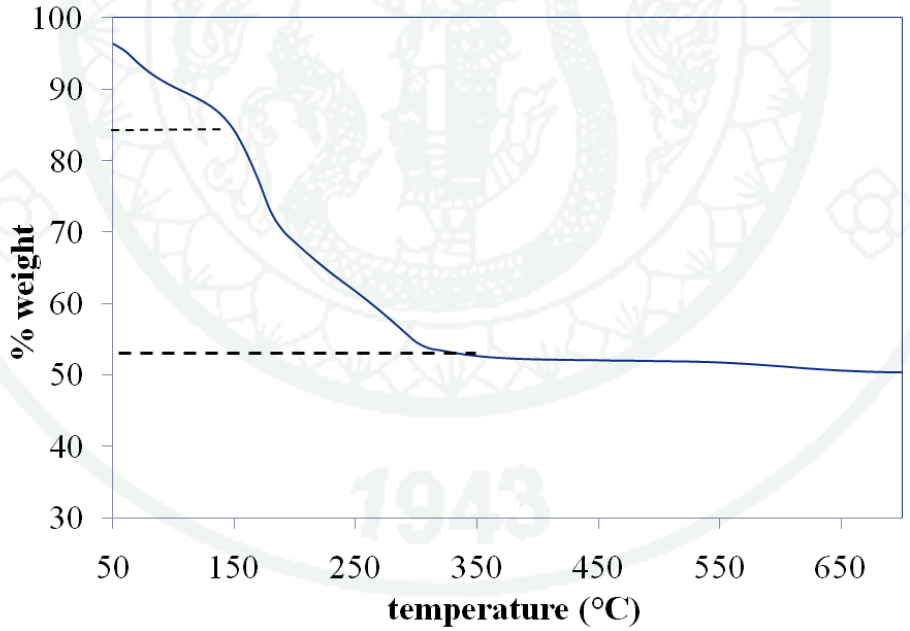

Figure 4 The TG curve of the as-prepared N-S co-doped TiO_2 using titanium(IV) tetraisopropoxide as a titania precursor.

The TG curve (Figure 4) of the as prepared N-S co-doped TiO_2 using titanium(IV) tetraisopropoxide presents two stages of weight loss. The first stage is from 50 to 150°C correspond to 12% of weight loss. This weight loss was due

to weakly-adsorbed water molecule and alcohol which still present in the sample. The second stage is from 150 to 350°C where the weight loss is about 31%. This can be attributed to strongly-bonded water molecule and organic solvent.

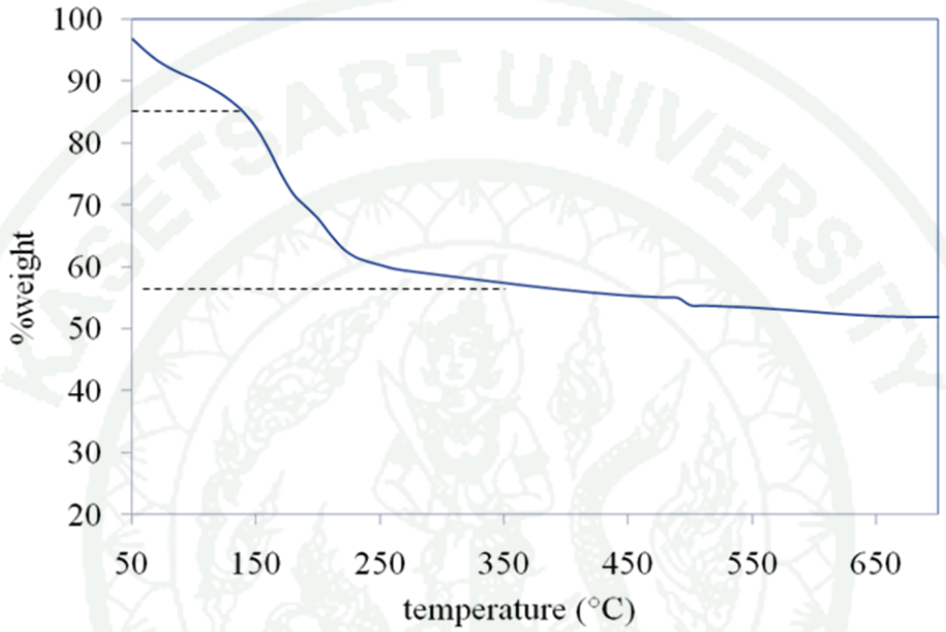

Figure 5 The TG curve of the as-prepared N-S co-doped TiO_2 using titanium(IV) tetra-n-butoxide as a titania precursor.

The TG curve (Figure 5) of the as-prepared N-S co-doped TiO_2 using titanium(IV) tetra-n-butoxide illustrates two significant stages of weight loss. A small amount was lost in the first stages (14% weight loss) from 50°C to150°C which was attributed to the elimination of water and loosely-adsorped species of as-prepared N-S co-doped TiO_2 resulting from the hydrolysis reaction. Second stage, about 25% weight loss from 150° to 300°C indicates the oxidation of organic from the thiourea (m.p.180°C) and butoxide residues of dry gel.

Furthermore, Madarász *et al.* (2008) studied the decomposition of an amorphous precursor by sol-gel method using titanium(IV) tetraisopropoxide and titanium(IV) tetra-n-butoxide as a precursor and thiourea as sulfur source and measured *in situ* by the online TG-FTIR. They found that the evolution of H_2O, CO_2,

COS (carbonyl sulfide) and NH_3 occurred at temperature lower than 200°C. At high temperature, showed that the evolution of SO_2 and strongly-bond of COS and nitrogen species. Moreover, Gombac *et al.* (2007) used the Temperature-Programmed Oxidation experiment (TPO) to study the presence of nitrogen species on as prepared N doped TiO_2. They found that the weakly adsorbed species were eliminated in forms of NO, NH_3, NH_2 etc. at lower temperature. Meanwhile, the higher temperature revealed that the presence of more strongly bonded nitrogen species.

In comparison with the studied previously reported by others researchers, TG results may be confirmed the weight loss of the as-prepared N-S co-doped TiO_2 using two titania precursors. The first stage of weight loss was ascribed to the evolution of weakly-adsorbed species such as H_2O, CO_2, COS, NH_3, NH_2 etc. The second stages were related to the evolution of SO_2 and strongly-bonded of nitrogen and sulfur species on the prepared catalyst.

1.1.2 X-ray powder diffraction (XRD)

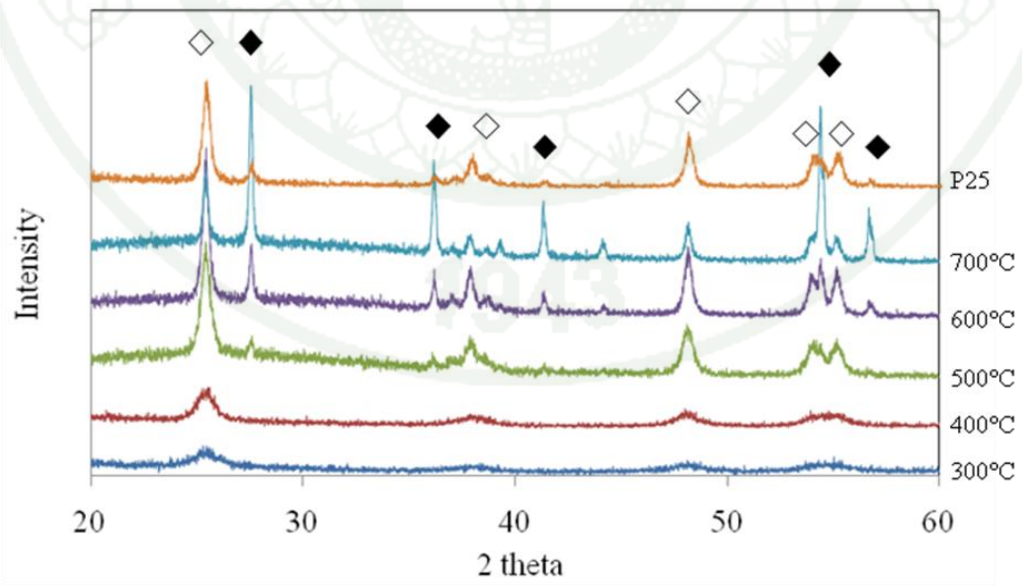

Figure 6 The XRD patterns of N-S co-doped TiO_2 using titanium(IV) tetra isopropoxide as a titania precursor with different calcination temperatures. (◇ for the anatase phase and ◆ for the rutile phase)

The XRD patterns of N-S co-doped TiO_2 at various temperatures are shown in Figure 6, which indicate the effects of calcinations temperature on phase structure of the powders. It can be seen that the calcination temperature obviously influences phase composition of the catalyst. The appearance of the anatase phase started at the calcination temperature of 300°C. The anatase phase was identified at 2θ of 25.4°, 38.1°, 48.2°, 53.9° and 55.1°, respectively, corresponding with the standard XRD pattern (JCPDS file NO.21-1272). With increasing calcination temperature, the peak intensities of anatase increase and the diffraction peak of anatase (2θ =25.4°C) becomes narrower. This can be suggested that crystallite size and the relative crystallinity siginificantly increace. The result implies that the rutile phase was observed at 500°C. The rutile XRD pattern starts appearing at 2θ of 27.6°, 36.2°, 41.5° and 55.6°, respectively (JCPDS file. NO.21-1276). The percentages of anatase and rutile are 70 and 30% as shown in Table 4. The crystallite size of N-S co-doped TiO_2 using titanium(IV) tetraisopropoxide as a precursor which calculated from Sherrer's equation increase from 6 to 25 nm with increasing calcinations temperature.

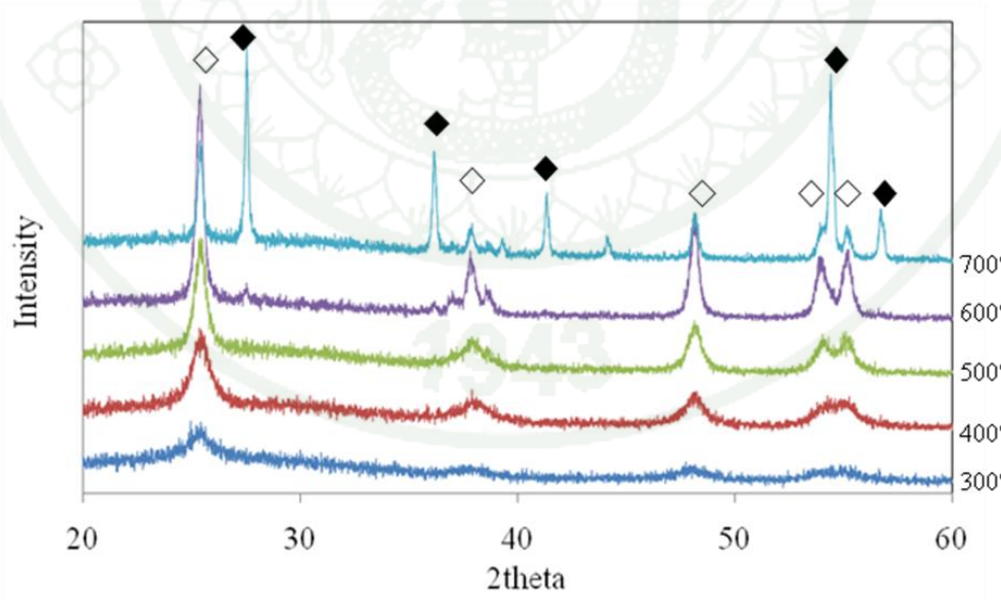

Figure 7 The XRD patterns of N-S co-doped TiO_2 using titanium(IV) tetra-n-butoxide as a titania precursor with different calcination temperatures. (◇ for the anatase phase and ◆ for the rutile phase)

The XRD patterns in Figure 7 shows anatase and rutile phase depended on calcinations temperature. Only anatase phase was observed when the calcination temperature were in the range of 300- 500°C. As the calcinations temperature increase, the anatase peak at 2θ of 25.4° became shaper and more intense, indicative a higher crystalline and larger crystallite size. The catalyst calcined at 500°C exhibited a well-crystallized anatase phase and higher crystallinity than catalyst calcined at 300°C and 400°C. The phase transformation occurred when the catalyst was calcined at 600°C, the rutile phase was detected in the catalyst. The rutile phase is predominant in catalyst calcined at 700°C. The crystallized size of N-S co-doped TiO_2 using titanium(IV) tetra-n-butoxide are in the range of 2-24 nm as shown in Table 4. The crystallite size was calculated by the Scherrer's equation to the full-width at half-maximum of the peak (25.4°) of anatase TiO_2.

In comparison with the XRD patterns of N-S co-doped TiO_2 using two different types of titania precursors, the discussion in term of phase transformation and crystallite size can be as follow;

Firstly, N-S co-doped TiO_2 using titanium(IV) tetraisopropoxide shows phase transformation from anatase to rutile at 500°C while N-S co-doped TiO_2 using titanium(IV) butoxide shows phase changes at 600°C, suggesting that the N-S co-doped TiO_2 using titanium(IV) tetra-n-butoxide was retarded to transform into rutile phase with increasing temperature than N-S co-doped TiO_2 using titanium(IV) tetraisopropoxide. This may be due to the high organic contents in the catalyst, titania precursor which caused more difficult to be hydrolyzed and high contents of nitrogen and sulfur caused the retardation of phase transformation. The catalyst calcined at 700°C using two types of precursors showed the similar results. The percentage of rutile are 69% using titanium(IV) tetraisopropoxide and 68% using titanium(IV) tetraisopropoxide as a precursor. This may be attributed to the content of nitrogen and sulfur co-doping. At high temperature, a smaller amount of nitrogen and sulfur still remained in the catalysts.

Secondly, similar crystallite size are found in the N-S co-doped TiO_2 by using two titania precursors. At the same calcination temperature, the crystallite size of N-S co-doped TiO_2 using titanium(IV) tetra-n-butoxide are smaller than N-S co-doped TiO_2 using titanium(IV) tetraisopropoxide as precursor due to the remaining organic contents blocked the agglomeration of N-S co-doped TiO_2 particles. Moreover, with increasing calcinations temperature, the crystallite sizes of N-S co-doped TiO_2 photocatalysts were increased.

From this experiment, it can be concluded that N-S co-doped TiO_2 prepared from both titania precursors have similar character. The crystallite size of N-S co-doped TiO_2 using titanium(IV) tetra-n-butoxide as a precursor appeared to be smaller than when the titanium(IV) tetraisopropoxide was used.

Table 4 Effect of titania precursors and calcination temperatures on the crystallite sizes and phase content of N-S co-doped TiO_2

Titania precursor	Calcination temperature (°C)	Phase	2θ (degree)	Cosθ	β (degree)	β (radian)	Crystallite size (nm)[a]	Intensity (A)	Intensity (R)	%A[b]	%R[c]
Titanium(IV) tetraisopropoxide	300	A	25.285	0.9758	1.79	0.0312	4.55	-	-	-	-
	400	A	25.535	0.9753	1.13	0.0197	7.21	-	-	-	-
	500	A	25.395	0.9755	0.65	0.0113	12.46	910	303	70	30
		R	27.585	0.9712	2.64	0.0461	3.10				
	600	A	25.425	0.9755	0.38	0.0066	21.53	1113	498	63.95	36.05
		R	27.565	0.9712	0.26	0.0045	31.44				
	700	A	25.405	0.9755	0.34	0.0059	24.08	643	1163	30.50	69.50
		R	27.535	0.9713	0.19	0.0031	43.02				
Titanium(IV) tetra-n-butoxide	300	A	24.955	0.9764	3.07	0.0536	2.65	-	-	-	-
	400	A	25.355	0.9756	1.18	0.0206	6.90	-	-	-	-
	500	A	25.415	0.9755	0.76	0.0133	10.68	-	-	-	-
	600	A	25.385	0.9756	0.42	0.0073	19.46	1263	215	82.33	17.67
		R	27.525	0.9713	1.50	0.0262	5.46				
	700	A	25.375	0.9756	0.34	0.0059	24.08	668	1178	31.04	68.96
		R	27.525	0.9713	0.18	0.0031	45.39				

[a]The crystallite size was calculated by using Sherrer's equation.

[b]The anatase content was calculated by applying Spurr-Myers equation.

[c]The rutile content was calculated by 100% - Anatase%.

1.1.3 Raman spectroscopy

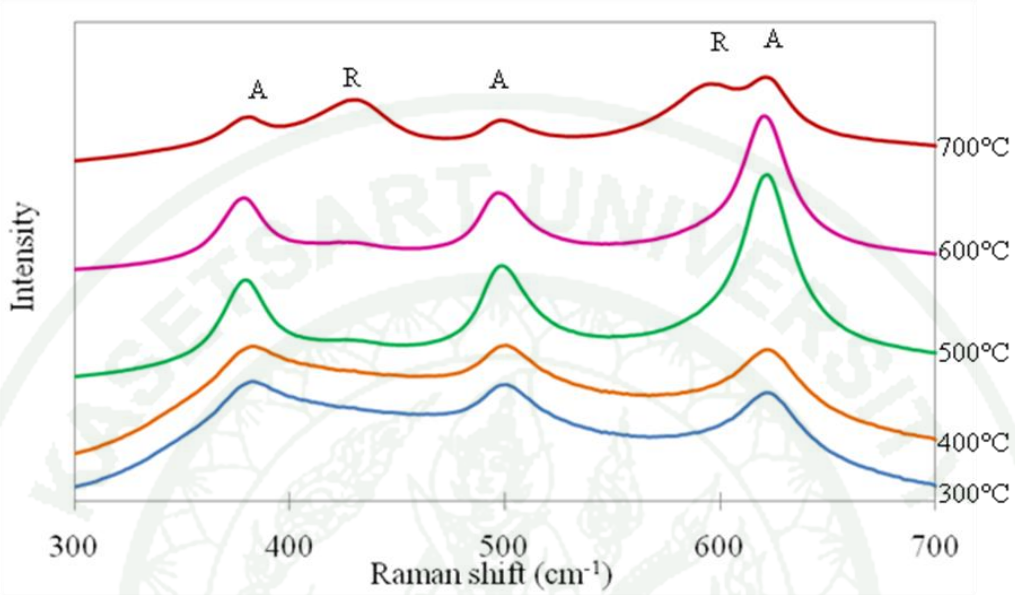

Figure 8 The Raman spectra of N-S co-doped TiO_2 using titanium(IV) tetra-isopropoxide as a titania precursor with different calcination temperatures. ("A" for anatase phase and "R" for rutile phase)

Figure 8 shows the spectra of N-S co-doped TiO_2. At lower calcination temperature (300 and 400°C) shows anatase phase which can be confirmed by the presence of Raman shift of 399 cm^{-1}, 519 cm^{-1} and 639 cm^{-1}, respectively. These bands can be attributed to Raman active modes of anatase phase with symmetries of B_{1g} (399 cm^{-1}, 519 cm^{-1}) and E_g (639 cm^{-1}) (Skiya *et al*., 2001). When the temperature increased, the N-S co-doped TiO_2 (500°C) structure was transformed into the rutile phase which could be identified at Raman shift of 447 cm^{-1}(E_g) and 612 cm^{-1}(A_{1g}) (Ma *et al*., 2007).

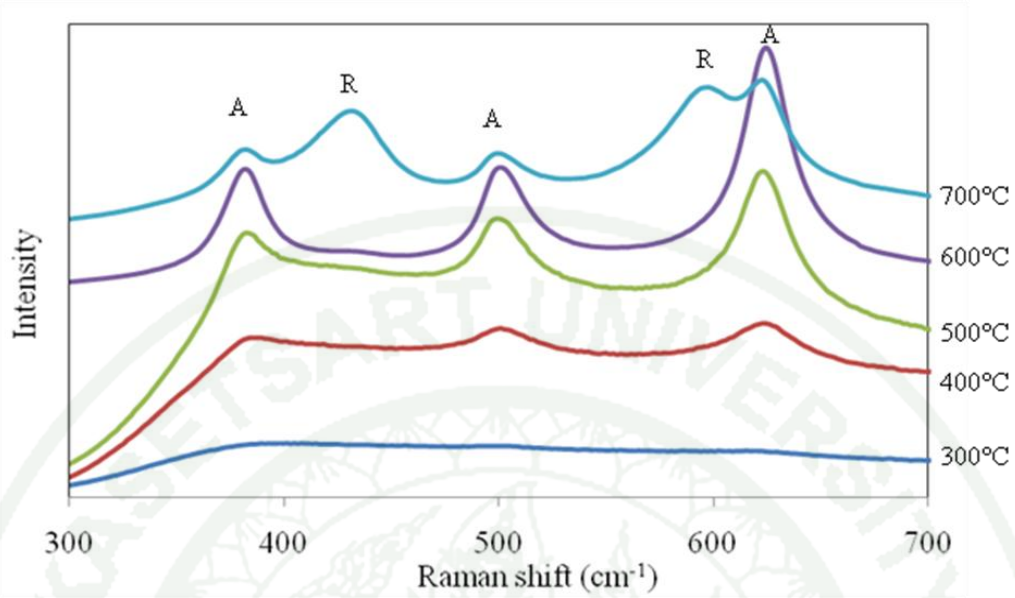

Figure 9 The Raman spectra of N-S co-doped TiO_2 using titanium(IV) tetra-n-butoxide as a titania precursor with different calcination temperatures. ("A" for anatase phase and "R" for rutile phase)

The Raman spectra of N-S co-doped TiO_2 in Figure 9, shows the anatase phase at 400°C and 500°C can be observed the Raman shift at 399 cm^{-1}, 519 cm^{-1} and 639 cm^{-1}, respectively. At higher temperature (600°C), the structure was transformed into the rutile phase which can be attributed to the Raman shift at 447 cm^{-1} and 612 cm^{-1} with the symmetries of E_g and A_{1g}.

This result confirmed the XRD patterns of the N-S co-doped TiO_2 using both of the titania precursors. The anatase-rutile phase transformation of N-S co-doped TiO_2 using titanium(IV) tetra-n-butoxide starts phase changes at 600°C was slower than N-S co-doped TiO_2 using titanium(IV) tetraisopropoxide shows phase changes at 500°C.

1.1.4 Diffusion Reflectance UV-Vis Spectroscopy (UV-Vis/DR)

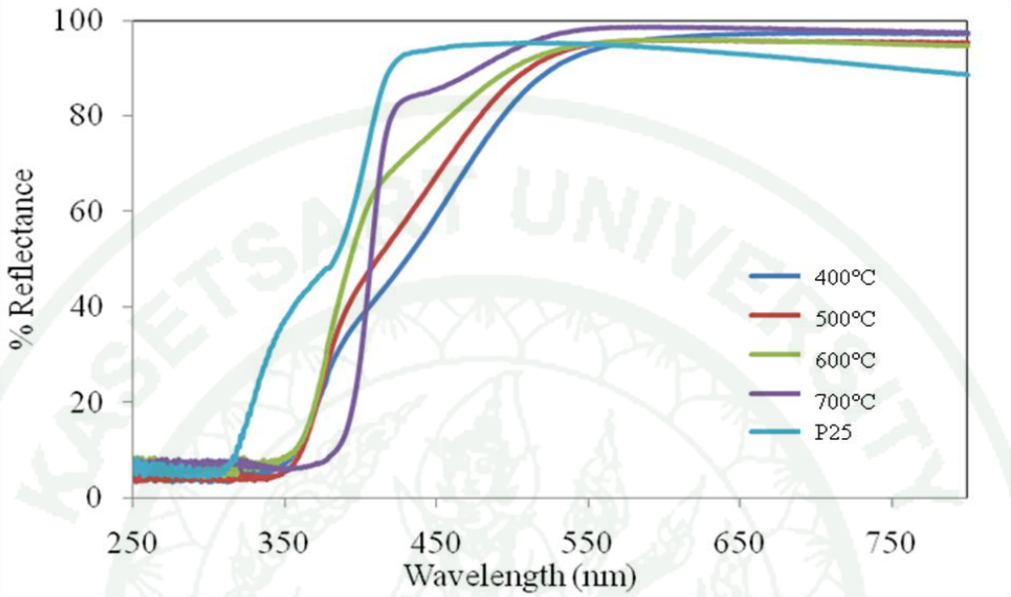

Figure 10 UV-Vis/DR spectra of N-S co-doped TiO_2 using titanium(IV) tetraisopropoxide as a titania precursor.

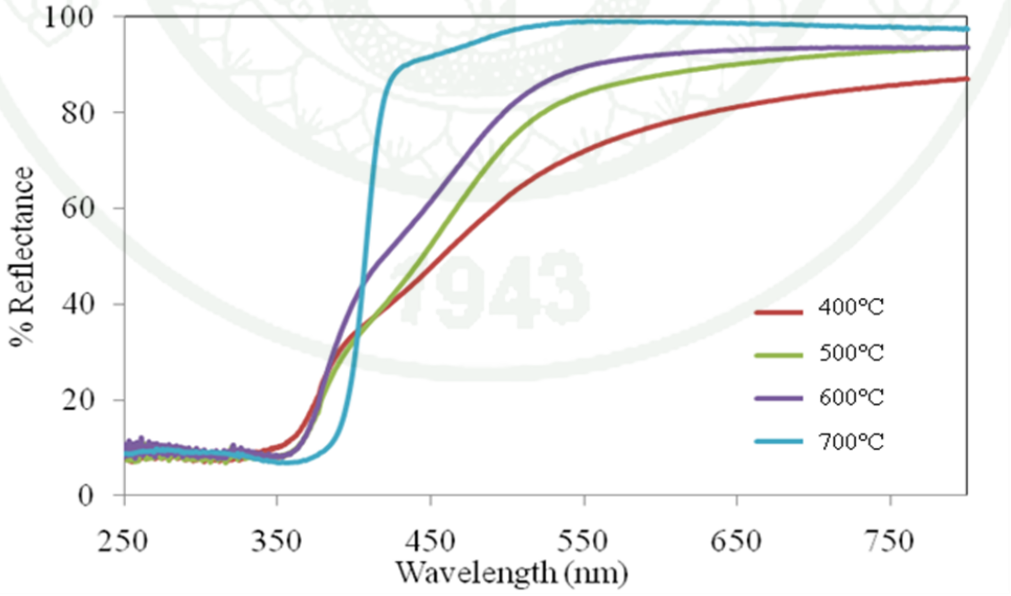

Figure 11 UV-Vis/DR spectra of N-S co-doped TiO_2 using titanium(IV) tetra-n-butoxide as a titania precursor.

Figure 10 and 11 show UV-Vis spectra of N-S co-doped TiO_2 with different calcinations temperature using two types of titania precursors and Degussa P25. The spectra of co-doped TiO_2 show the two absorption edge. The first absorption edge in the UV region is related to the band structure of anatase phase. The second absorption in the visible region of 400-550 nm indicates that nitrogen and sulfur codoping had a significant on the band structure of TiO_2.

In addition, the band gap can be calculated from absorption edge which resulted from UV-Vis reflectance spectra. The summarization is shown in Table 5. The band gap of the catalyst could be determined by the equation as follows (Li *et al*., 2008);

$$Eg = \frac{1239.8}{\lambda}$$

where E_g is band gap energy (eV)

λ is wavelength (nm)

Table 5 Energy gap (E_g) values of all N-S co-doped TiO_2 and Degussa P25.

Titania precursors	Calcination temperature (°C)	λ_1 (nm)	E_{g1} (eV)	λ_2 (nm)	E_{g2} (eV)
Titanium(IV) tetraisopropoxide	400	390	3.18	530	2.34
	500	386	3.21	516	2.40
	600	395	3.14	514	2.41
	700	420	2.95	530	2.34
Titanium(IV) tetra-n-butoxide	400	392	3.16	545	2.27
	500	390	3.18	527	2.35
	600	395	3.14	525	2.36
	700	420	2.95	518	2.39
Degussa P25	-	420	2.95	-	-

All of the first observed absorption edges can be elaborated in terms of charge transition corresponding to the excitation of electrons from the valence band (O 2p) to the conduction band (Ti 3d). Meanwhile, the second absorption edges originated from the excitation of electrons from N 2p and S 3p located above valence band O 2p to conduction band Ti 3d (Li *et al*., 2008). Therefore, having the nitrogen and sulfur content in TiO_2 lattice will improve the absorption ability of photocatalysts in the visible region.

1.1.5 Elemental Analysis (EA)

In this characterization technique, it focused on measuring the amount of both nitrogen and sulfur. The N-S co-doped TiO_2 using titanium(IV) tetraisopropoxide showed 0.391% of nitrogen and 1.766% of sulfur at 300°C as shown in Table 6. This suggests that heating at 120°C was not enough to evaporate the hydrolyzed organic species at high extent. Therefore, the amounts of nitrogen and sulfur decreased with increasing calcination temperature. At 600°C, The nitrogen contents in the catalyst could not be detected which suggested the absence of nitrogen species in TiO_2 lattice. There were not capable of existing with high temperature.

N-S co-doped TiO_2 using titanium(IV) tetra-n-butoxide (Table 6) shows high nitrogen and sulfur contents at 300°C. This indicated that there were high organic contents after drying process (120°C) owing to titania precursor was more difficult to be hydrolyzed and organic species were not evaporate at low temperature. However, with increasing calcination temperature the nitrogen and sulfur contents were decreased. Because of the decomposition of unhydrolyzed organic species in titanium alkoxide chains and organic species adsorbed on TiO_2 surface. Therefore, very small amount of nitrogen and sulfur were detected at 700°C.

In addition, N-S co-doped TiO_2 using titanium(IV) tetra-n-butoxide shows higher amount of nitrogen and sulfur than N-S co-doped TiO_2 using titanium(IV) tetraisopropoxide in the same calcination temperature. Since the N-S co-doped TiO_2 using titanium(IV) tetra-n-butoxide was more difficult to be hydrolyzed than titanium(IV) tetraisopropoxide as a precursor.

Table 6 The amount of nitrogen and sulfur of N-S co-doped TiO_2 with different types of titania precursors.

Titania precursors	calcination temperature (°C)	Nitrogen content (%)			Average nitrogen content (%)	Sulfur content (%)			Average sulfur content (%)
		N_1	N_2	N_3	$N_{average}$	S_1	S_2	S_3	$S_{average}$
Titanium(IV) tetraisopropoxide	300	0.401	0.380	0.392	0.391±0.011	1.783	1.755	1.761	1.766±0.015
	400	0.069	0.071	0.060	0.067±0.006	0.598	0.606	0.602	0.602±0.004
	500	0.033	0.036	0.016	0.028±0.011	0.181	0.182	0.169	0.177±0.007
	600	0.000	0.000	0.000	ND*	0.058	0.064	0.069	0.064±0.006
	700	0.000	0.000	0.000	ND*	0.033	0.026	0.020	0.026±0.007
Titanium(IV) tetra-n-butoxide	300	0.752	0.736	0.743	0.744±0.008	1.965	1.949	1.963	1.959±0.009
	400	0.291	0.279	0.286	0.285±0.006	0.643	0.633	0.631	0.636±0.006
	500	0.131	0.122	0.127	0.127±0.005	0.357	0.359	0.354	0.357±0.003
	600	0.060	0.056	0.079	0.065±0.123	0.123	0.110	0.103	0.112±0.010
	700	0.013	0.003	0.009	0.008±0.005	0.048	0.047	0.037	0.044±0.006

(* ND for not detected)

1.2 Effect of solvent

1.2.1 Thermal Gravimetric Analysis

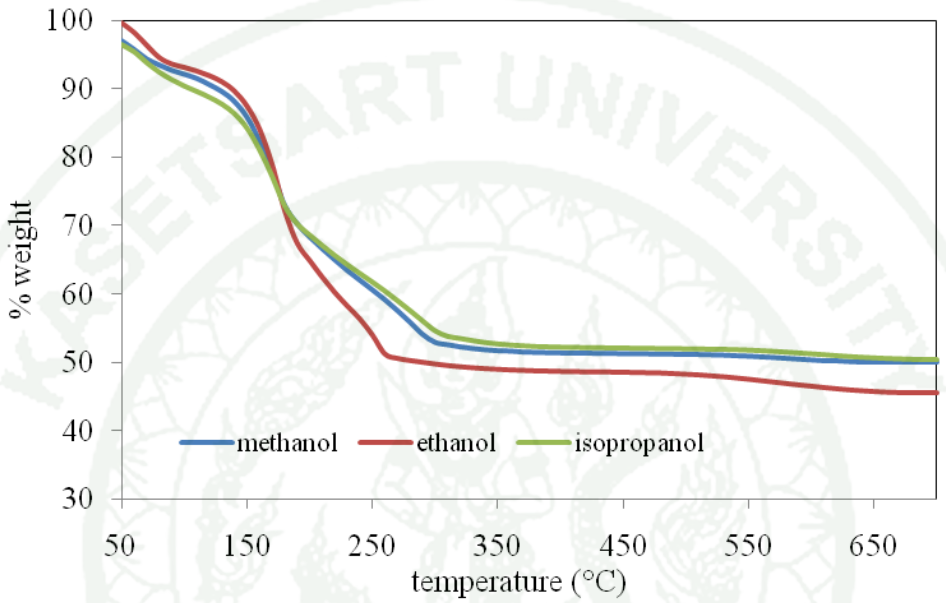

Figure 12 The TG curve of the as-prepared N-S co-doped TiO_2 using titanium(IV) tetraisopropoxide as a titania precursor with three of preparation solvents.

Figure 12 shows two stages of weight loss in the TG curve of N-S co-doped TiO_2 with different solvents. Firstly, it was observed that ~15% weight loss occurred in the temperature range 50-150°C owing to the elimination of water and solvent in the catalyst. Secondly, the temperature range of 150-300°C, weight loss of ~28% was observed. This is attributed to the removal of latent species in the TiO_2 structure.

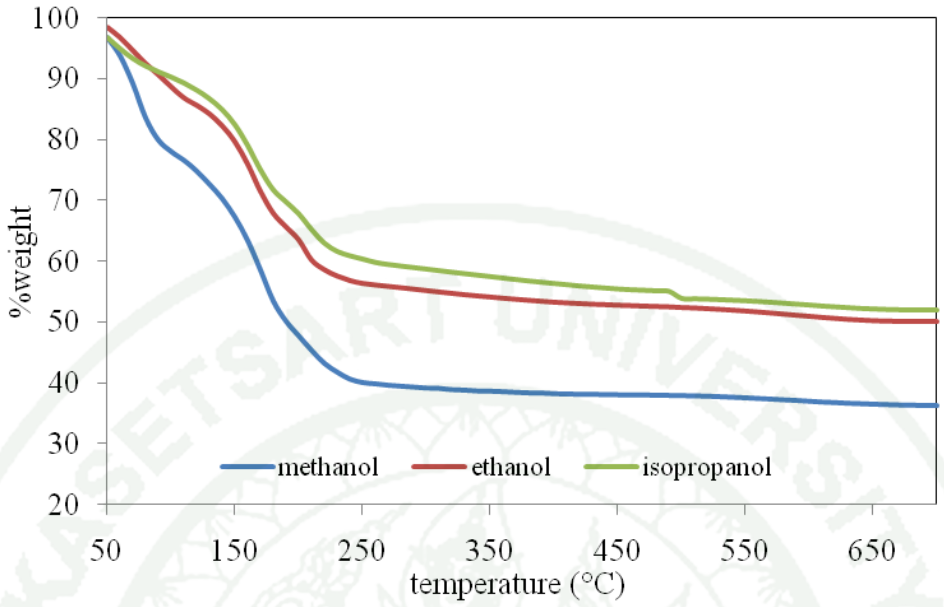

Figure 13 The TG curve of the as-prepared N-S co-doped TiO_2 using titanium(IV) tetra-n-butoxide as a titania precursor with three of preparation solvents.

The TG curve (Figure 13) exhibits two stages of weight loss. The first stage between 50 and 150°C is due to the removal of weakly-adsorbed species on TiO_2 surface. The second stage between 150 and 300°C originated from the release of strongly-adsorbed species in the TiO_2 structure. Moreover, N-S co-doped TiO_2 which prepared by using methanol as solvent shows higher weight loss than other solvent. This may be attributed to the lower solubility of titanium(IV) tetra-n-butoxide in methanol, which is ascribed the disappearance of unhydrolyzed organic species in metal alkoxide.

Compared to the previous study (section 1.1.1), all TG curves of catalysts can be implied that the first stage of weight loss was associated with hydrolyzed organic species that were weakly adsorbed on the surface. The second stage of weight loss was involved in dormant organic molecule of titania precursors and organic species difficult to be hydrolyzed.

1.2.2 X-ray powder diffraction

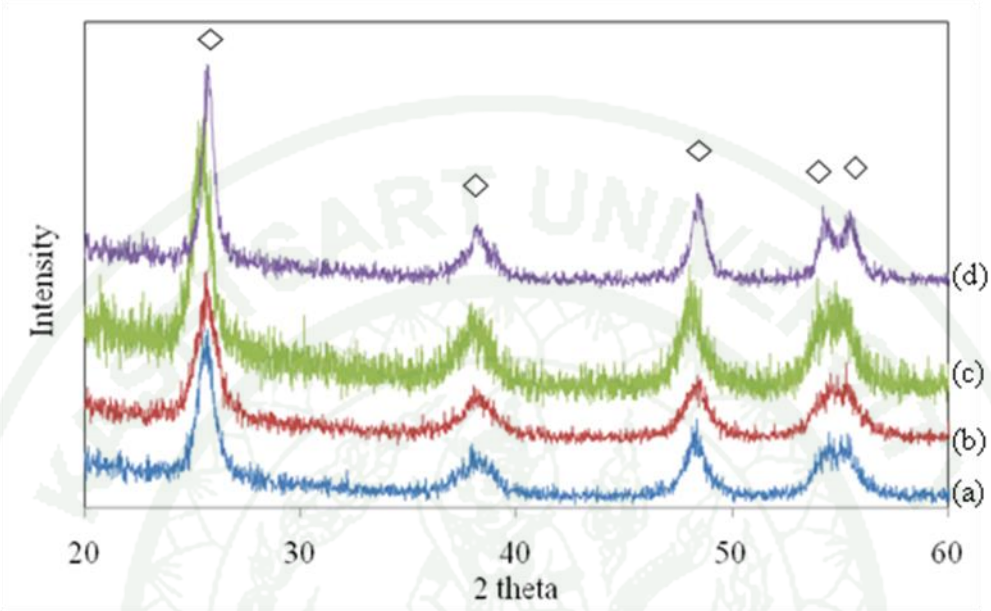

Figure 14 The XRD patterns of N-S co-doped TiO_2 calcined at 400°C using titanium(IV) tetraisopropoxide as a titania precursor with three of preparation solvents and undoped TiO_2; (a) methanol, (b) ethanol (c) isopropanol and (d) undoped TiO_2.
(◇ for the anatase phase)

The XRD patterns of the N-S co-doped TiO_2 calcined at 400°C with different solvent (methanol, ethanol and isopropanol) and undoped TiO_2 are shown in Figrue 14. The diffraction peak at 2θ of 25.4°, 38.1°, 48.2°, 53.9° and 55.1 °C corresponding to the anatase phase (JCPDS file. NO.21-1276) are observed in all the samples. The crystallite sizes of these samples are listed in Table 7, the undoped TiO_2 provided the largest crystallite size around 11 nm. It are suggested that the crystallite size decreased after N and S codoping.

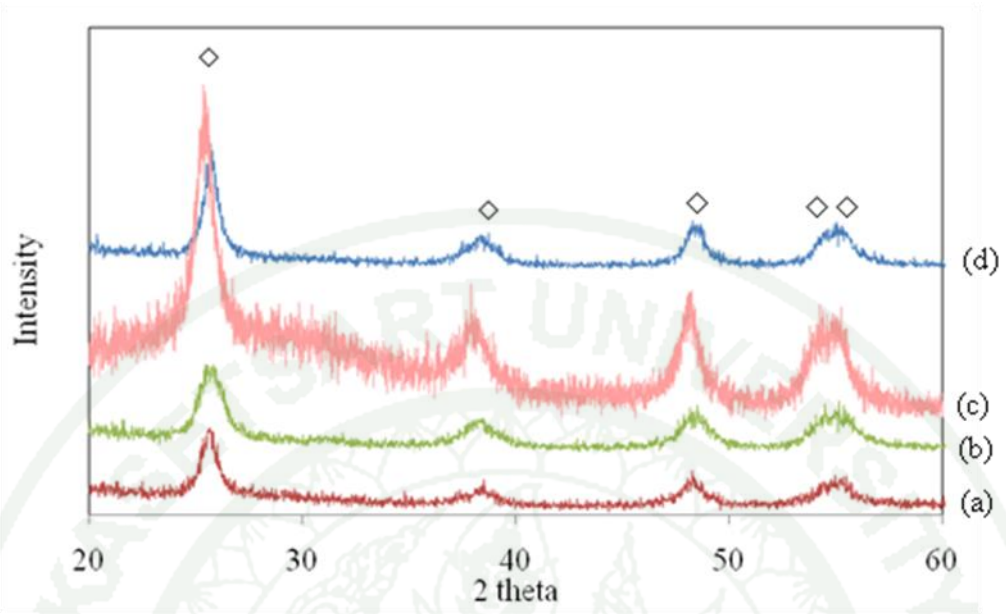

Figure 15 The XRD patterns of N-S co-doped TiO_2 calcined at 400°C using titanium(IV) tetra-n-butoxide as a titania precursor with three of preparation solvents and undoped TiO_2; (a) methanol, (b) ethanol (c) isopropanol and (d) undoped TiO_2.
(◇ for the anatase phase)

The XRD patterns (Figure 15) of all the samples with different solvents showed the presence of anatase crystal structure of TiO_2, and no rutile phase. The crystallite size of undoped TiO_2 and N-S co-doped TiO_2 used methanol, ethanol and isopropanol as a solvent are 9.9, 7.5, 5.1 and 6.9, respectively.

From the XRD patterns, the crystallite size of undoped TiO_2 using two titania precursors exhibited the larger crystallite size than N-S co-doped TiO_2. This result may be indicated that the codoping blocked particle agglomeration of the TiO_2 during the heat treatment. However, solvent had less effect on the structure and size of N-S co-doped TiO_2.

Table 7 Effect of solvent on the crystallite sizes of N-S co-doped TiO_2 and undoped TiO_2 calcined at 400°C.

Titania precursor	solvent	Phase	2θ (degree)	Cosθ	β (degree)	β (radian)	Crystallite size (nm)
Titanium(IV) tetraisopropoxide	methanol	A	25.710	0.9749	0.90	0.01571	9.01
	ethanol	A	25.650	0.9751	1.18	0.02060	6.90
	isopropanol	A	25.535	0.9753	1.13	0.01973	7.21
	undoped TiO_2	A	25.690	0.9749	0.74	0.01292	11.02
Titanium(IV) tetra-n-butoxide	methanol	A	25.670	0.9750	1.08	0.01885	7.53
	ethanol	A	25.450	0.9754	1.58	0.02758	5.15
	isopropanol	A	25.355	0.9756	1.18	0.02060	6.90
	undoped TiO_2	A	25.710	0.9479	0.82	0.01431	9.97

Table 8 The lattice parameters (nm) and unit cell volumn (nm^3) of the N-S co-doped TiO_2 and undoped TiO_2 calcined at 400°C.

Titania precursors	solvent	Phase	Lattice parameters (nm)			Unit cell volume (nm^3)
			a	b	c	
Titanium(IV) tetraisopropoxide	methanol	A	0.3718	0.3718	0.9472	0.1301
	ethanol	A	0.3729	0.3729	0.9453	0.1314
	isopropanol	A	0.3746	0.3746	0.9481	0.1330
	undoped TiO_2	A	0.3725	0.3725	0.9416	0.1307
Titanium(IV) tetra-n-butoxide	methanol	A	0.3748	0.3748	0.8724	0.1226
	ethanol	A	0.3780	0.3780	0.8739	0.1249
	isopropanol	A	0.3776	0.3776	0.8995	0.1282
	undoped TiO_2	A	0.3943	0.3943	0.8627	0.1341

Table 8 shows the lattice parameter of N-S co-doped TiO_2 calcined at 400°C with various solvent and undoped TiO_2. The lattice parameters of the c-axis is a little larger than of undoped TiO_2, indicating a lattice expansion along the c-axis due to the incorporation of nitrogen and sulfur atoms. These results hints that nitrogen atoms may substitute the sites of oxygen atoms in the lattice of anatase (Chen *et al*., 2007) and sulfur atoms may be interstitial in the lattice. To consider in term of ionic radius of atoms, the larger ionic radius of S^{2-} (1.7 Å) compared to that of O^{2-} (1.22 Å).

1.2.3 Raman spectroscopy

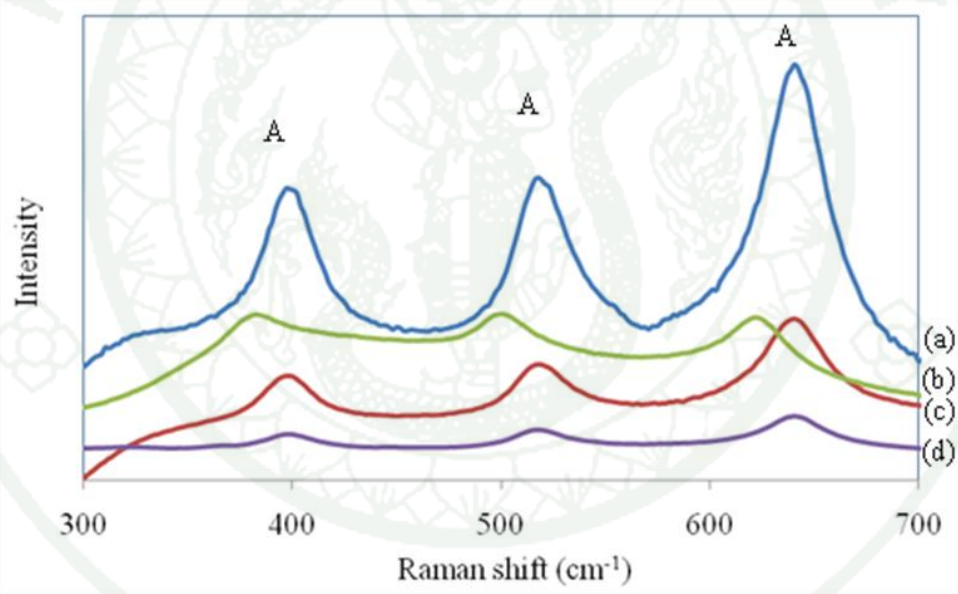

Figure 16 The Raman spectra of N-S co-doped TiO_2 using titanium(IV) tetra isopropoxide as a titania precursor with three of preparation solvents; (a) methanol, (b) isopropanol, (c) ethanol and (d) undoped TiO_2. ("A" for the anatase phase)

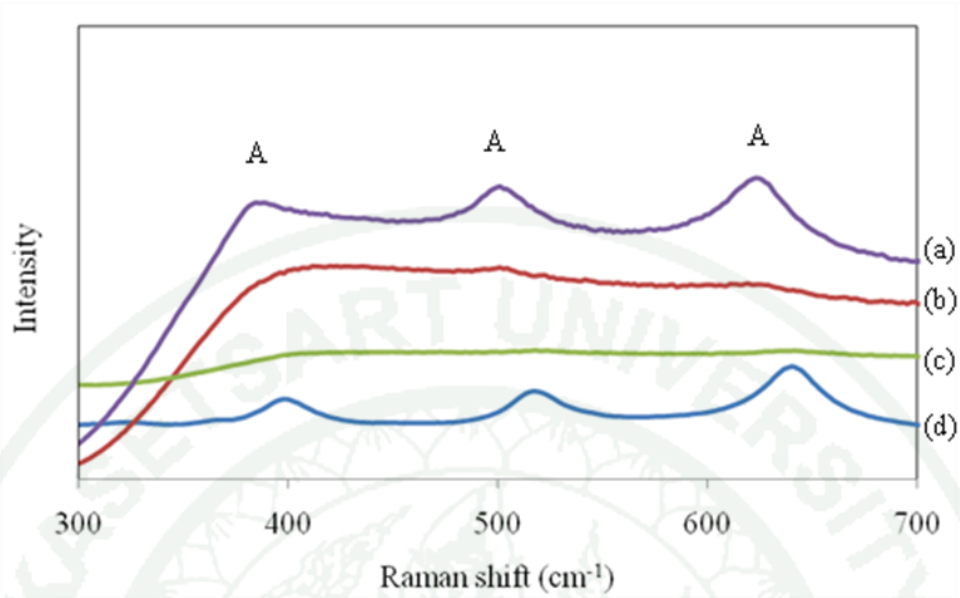

Figure 17 The Raman spectra of N-S co-doped TiO_2 using titanium(IV) tetra -n-butoxide as a titania precursor with three of preparation solvents; (a) isopropanol, (b) ethanol, (c) methanol and (d) undoped TiO_2. ("A" for the anatase phase)

Table 9 Raman shift of N-S co-doped TiO_2 prepared at various solvents and undoped TiO_2 calcined at 400°C.

Titania precursors/caltalyst	solvents	Raman shift (cm^{-1}) of Ti-O bond		
		1	2	3
undoped TiO_2		397.63	517.95	638.27
Titanium(IV) tetraisopropoxide	methanol	396.86	517.65	640.14
	ethanol	399.51	519.49	641.16
	isopropanol	384.17	500.78	622.46
Titanium(IV) tera-n-butoxide	methanol	broad	broad	broad
	ethanol	broad	517.68	642.73
	isopropanol	401.07	504.16	625.84

Figure 16 and 17 show the Raman spectra of the N-S co-doped TiO_2 using two titania precursors at various solvent and undoped TiO_2 calcined at 400°C. The observed peaks at 399, 519 and 639 cm^{-1}which could be assigned to the anatase phase compared to Ranam spectrum of undoped TiO_2 (397.63, 517.95 and 638.27 cm^{-1}). From the Raman spectra of N-S co-doped TiO_2, indicated that all samples show the characteristic Raman bands of anatase phase, with no evidence for the corresponding bands of rutile phase. However, the spectrum of N-S co-doped TiO_2 using titanium(IV)tetra-n-butoxide as a precursors and methanol and ethanol as a solvent show the broad spectrum, indicated that there were less of Ti-O bond forming and catalyst have high percentage of amorphous solid.

The slightly shifted to the lower frequency of the 639 cm^{-1} of E_g peak (the stretching vibration mode of Ti-O) of the N-doped TiO_2 as compared with undoped TiO_2 was reported by Lee *et al*. 2010. Since the stretching wave numbers are related to the lengths of the bonding. It ascribed to the increase in Ti-O bond length corresponding to the estimated Ti-O bond length of the substitutional of N doped TiO_2. In this work found that the spectrum of 638 cm^{-1} slightly shifted to the lower frequency as compared to undoped TiO_2. This may be indicated that nitrogen could be substituted for some oxygen atoms in the titania lattice. Moreover, found that the spectrum of some catalyst show the slightly shifted to the higher frequency indicated that the Ti-O bond was shorter and stronger due to the bond contraction via N-S codoping. This may be because the size of sulfur atom much larger oxygen atom, therefore sulfur should incorporated into the interstitial size of TiO_2.

1.2.4 Diffusion Reflectance UV-Vis Spectroscopy (UV-Vis/DR)

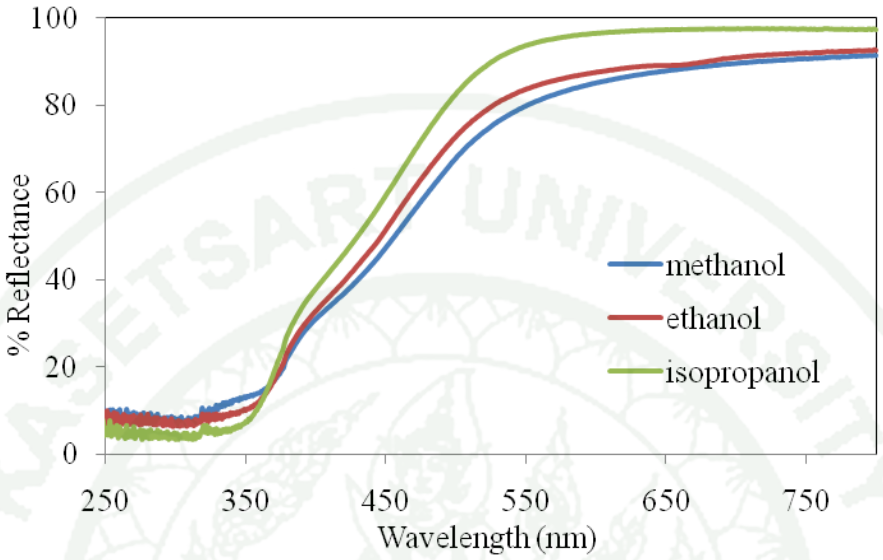

Figure 18 UV-Vis/DR spectra of N-S co-doped TiO_2 using titanium(IV) tetraisopropoxide as a titania precursor with three of preparation solvents calcined at 400°C.

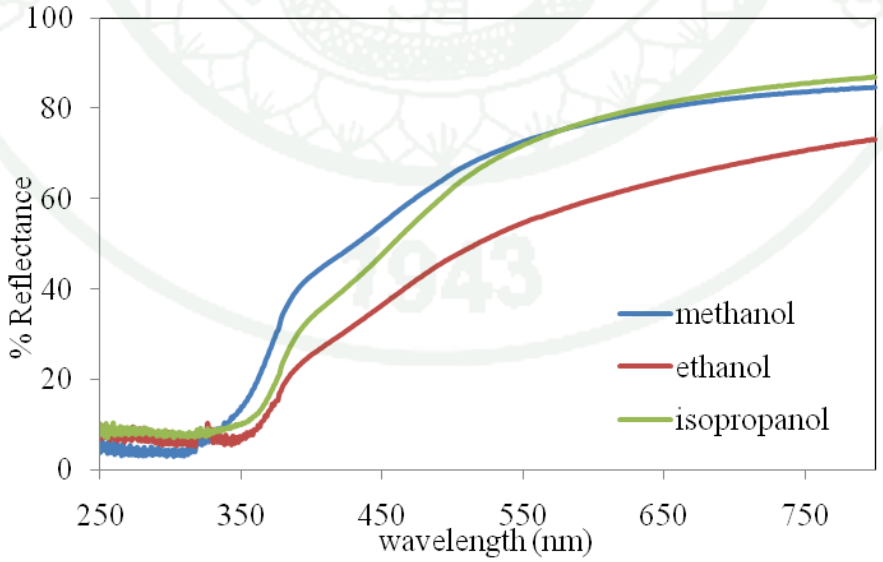

Figure 19 UV-Vis/DR spectra of N-S co-doped TiO_2 using titanium(IV) tetra-n-butoxide as a titania precursor with three of preparation solvents calcined at 400°C.

Table 10 Energy gap (E_g) values of all N-S co-doped TiO_2 calcined at 400°C.

Titania precursors	Solvent	λ_1 (nm)	E_{g1} (eV)	λ_2 (nm)	E_{g2} (eV)
Titanium(IV)	methanol	390	3.18	550	2.25
tetraisopropoxide	ethanol	395	3.14	530	2.34
	isopropanol	390	3.18	530	2.34
Titanium(IV)	methanol	387	3.20	550	2.25
tetra-n-butoxide	ethanol	390	3.18	550	2.25
	isopropanol	392	3.16	545	2.27

The diffuse reflectance spectra of N-S co-doped TiO_2 using two titania precursors with different solvents are shown in Figure 18 and 19. The spectra of all the samples show two absorption edges. In contrast, the undoped TiO_2 sample shows only one absorption edge at 362 nm (Phatinavin, 2009). Consequently, the absorption spectra of the N-S co-doped TiO_2 show a stronger absorption in the UV-light region (530 – 550 nm) and a red shift in the band gap. Thus, the optical absorption in the visible region was enhanced due to the co-doping.

Table 10 shows energy gap of the calalysts prepared at different preparation solvents which have similar proportion. The band gap energy are 2.25, 2.25 and 2.27 eV for methanol, ethanol and isopropanol as solvent using titanium(IV) tetra-n-butoxide. It suggested that the solvent had no influence on the optical absorption edge.

1.2.5 Elemental Analysis (EA)

From the EA data, it suggested that the N-S co-doped TiO_2 using titanium(IV) tetra-n-butuxide with three preparation of solvents show higher amount of nitrogen and sulfur than N-S co-doped TiO_2 using titanium(IV) tetraisopropoxide as a precursor. It may be implied that N-S co-doped TiO_2 using titanium(IV) tetra-n-butoxide was more interacted with thiourea than N-S co-doped TiO_2 using titanium(IV) tetraisopropoxide as precursors. N-S co-doped TiO_2 prepared with titanium(IV) tetraisopropoxide and isopropanol as a solvent and N-S co-doped TiO_2 using titanium(IV) tetra-n-butoxide with methanol as a solvent show higher percentage of sulfur than other prepared solvent.

Table 11 The amount of nitrogen and sulfur of N-S co-doped TiO_2 with different solvents.

Titania precursors	Solvents	Nitrogen content (%)			Average nitrogen content (%)	Sulfur content (%)			Average sulfur content (%)
		N_1	N_2	N_3	$N_{average}$	S_1	S_2	S_3	$S_{average}$
Titanium(IV) tetraisopropoxide	methanol	0.344	0.312	0.282	0.313±0.031	0.425	0.463	0.516	0.468±0.046
	ethanol	0.212	0.225	0.228	0.222±0.009	0.463	0.443	0.450	0.452±0.010
	isopropanol	0.069	0.071	0.060	0.067±0.006	0.598	0.606	0.602	0.602±0.004
Titanium(IV) tetra-n-butoxide	methanol	0.377	0.365	0.356	0.366±0.011	0.932	0.884	0.898	0.905±0.025
	ethanol	0.390	0.388	0.384	0.387±0.003	0.706	0.713	0.700	0.706±0.007
	isopropanol	0.291	0.279	0.286	0.285±0.006	0.643	0.633	0.631	0.636±0.006

1.3 Morphology

To determine the surface morphology and element composition of catalyst were investigated by Scanning Electron Microscope (SEM), Energy Dispersive X-Ray Spectroscope (EDX) and EDX spectra mapping.

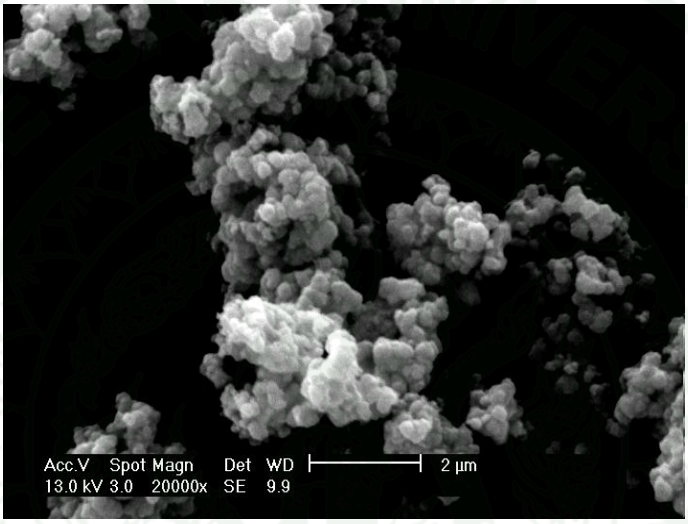

Figure 20 SEM image of N-S co-doped TiO_2 using titanium(IV) tetraisopropoxide as a titania precursor calcined at 300°C.

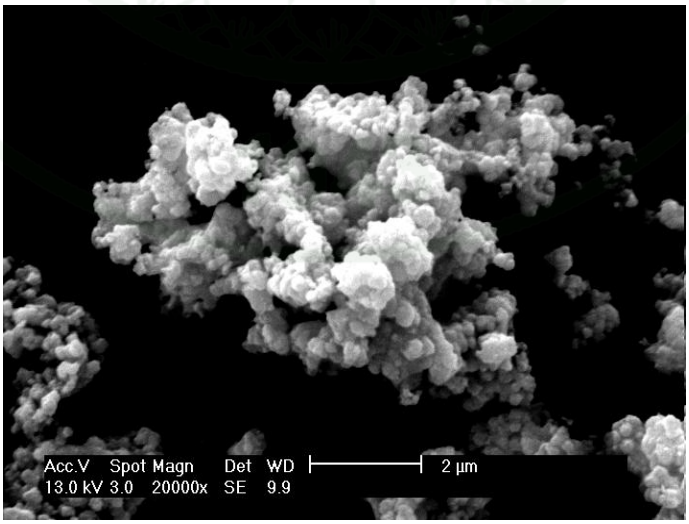

Figure 21 SEM image of N-S co-doped TiO_2 using titanium(IV) tetraisopropoxide as a titania precursor calcined at 400°C.

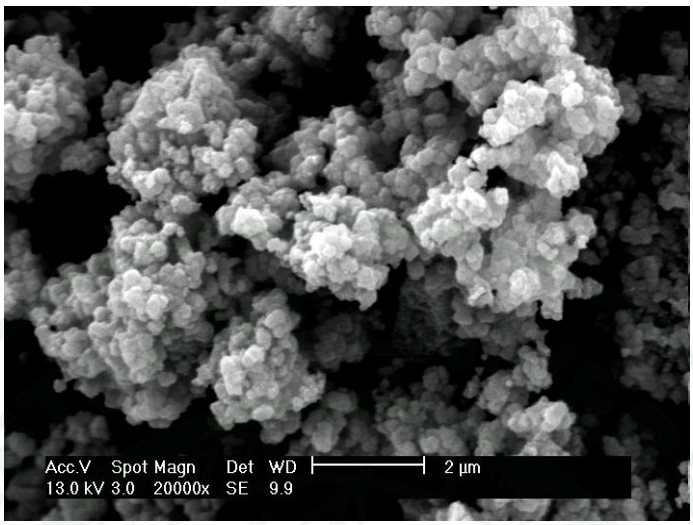

Figure 22 SEM image of N-S co-doped TiO_2 using titanium(IV) tetraisopropoxide as a titania precursor calcined at 500°C.

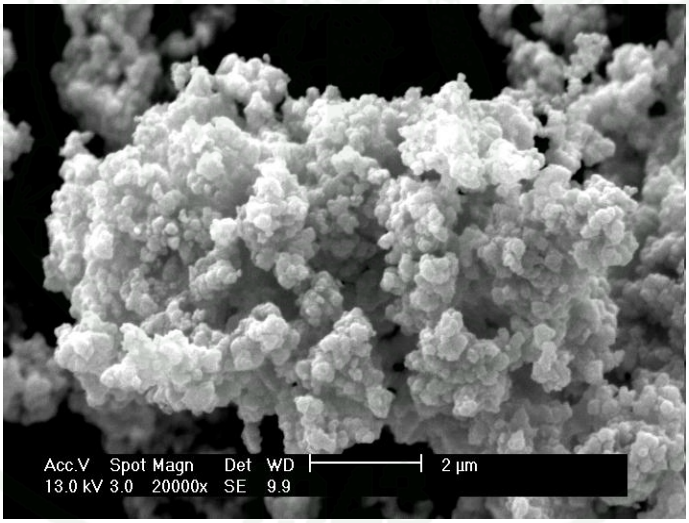

Figure 23 SEM image of N-S co-doped TiO_2 using titanium(IV) tetraisopropoxide as a titania precursor calcined at 600°C.

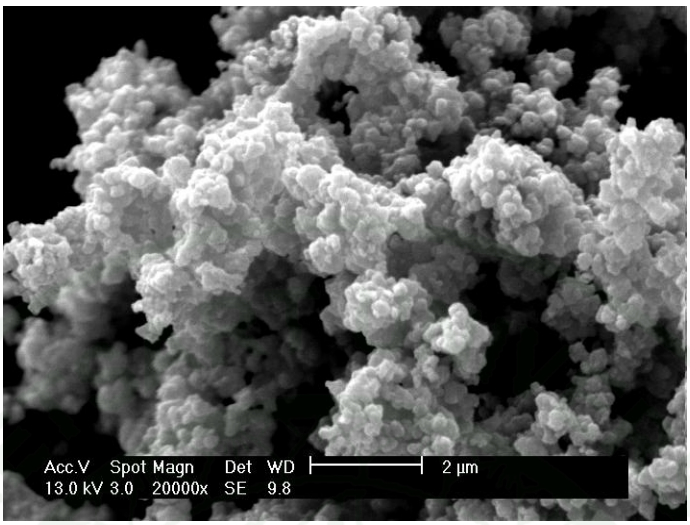

Figure 24 SEM image of N-S co-doped TiO_2 using titanium(IV) tetraisopropoxide as a titania precursor calcined at 700°C.

The SEM images of N-S co-doped TiO_2 using titanium(IV) tetraisopropoxide with different calcination temperature are shown in Figure 20-24. The SEM images show that the surface morphology of all the co-doped titania powders are very rough and fluffy grains. In addition, it is obvious that the crystalline of prepared photocatalyst was agglomerated when the temperature was increased. These results are in good agreement with the XRD results. On the other hand, N-S co-doped TiO_2 using titanium(IV) tetra-n-butoxide provided that the similar morphology with titanium(IV) tetraisopropoxide (Sirisaksoontorn, 2008) and their morphology like fluffy powders.

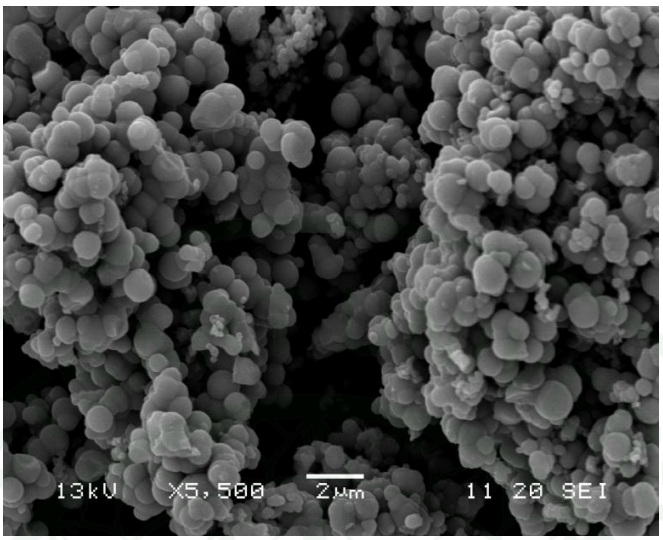

Figure 25 SEM image of N-S co-doped TiO_2 using titanium(IV) tetraisopropoxide as a titania precursor and methanol as a solvent calcined at 400°C.

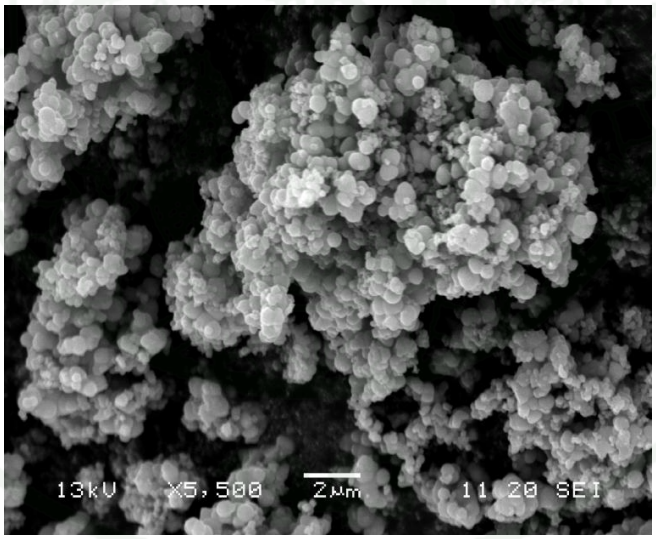

Figure 26 SEM image of N-S co-doped TiO_2 using titanium(IV) tetraisopropoxide as a titania precursor and ethanol as a solvent calcined at 400°C.

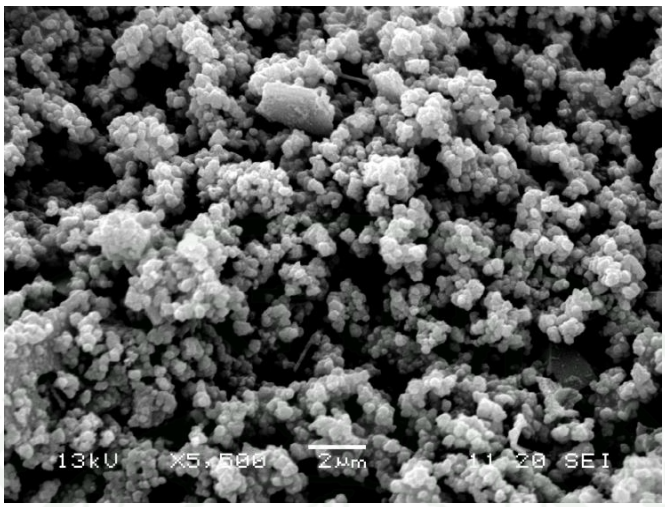

Figure 27 SEM image of N-S co-doped TiO_2 using titanium(IV) tetraisopropoxide as a titania precursor and isopropanol as a solvent calcined at 400°C.

The surface morphology of N-S co-doped TiO_2 at various solvents are presented in Figure 25-27. It exhibits that the surface morphology of all samples are roughly monodispered and fluffy powders. Moreover, the catalyst using isopropanol as a solvent reveals that the particles are more disperse than using methanol as a solvent.

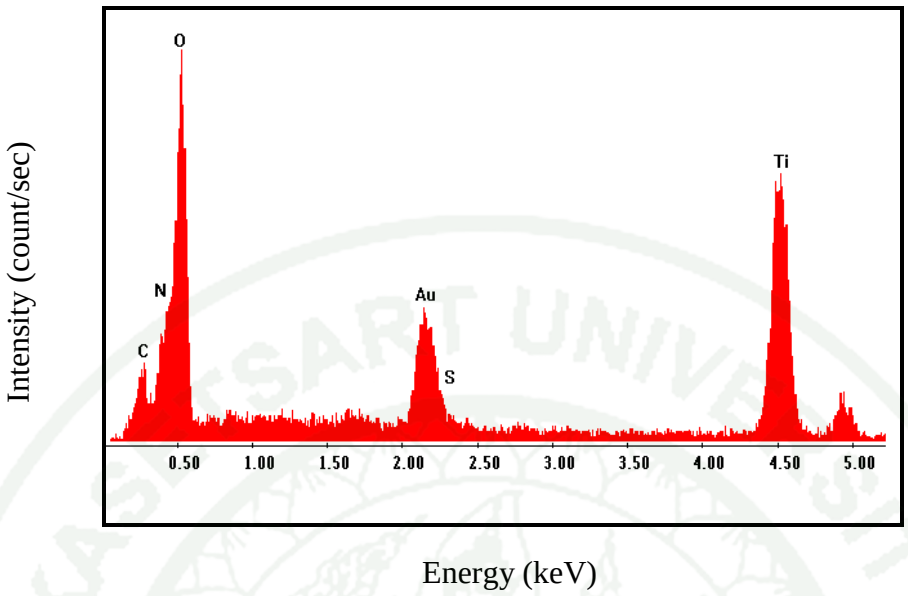

Figure 28 EDX spectrum of the N-S co-doped TiO_2 using titanium(IV) tetraisopropoxide calcined at 400 ^{o}C.

Figure 28, shows the EDX spectrum of N-S co-doped TiO_2 using titanium(IV) tetraisopropoxide calcined at 400°C. The spectrum illustrates the element composition in the prepared catalyst. It exhibits the peak of Ti, O, N, S, C and Au. The indicated the exist of N and S exist in the catalyst structures.

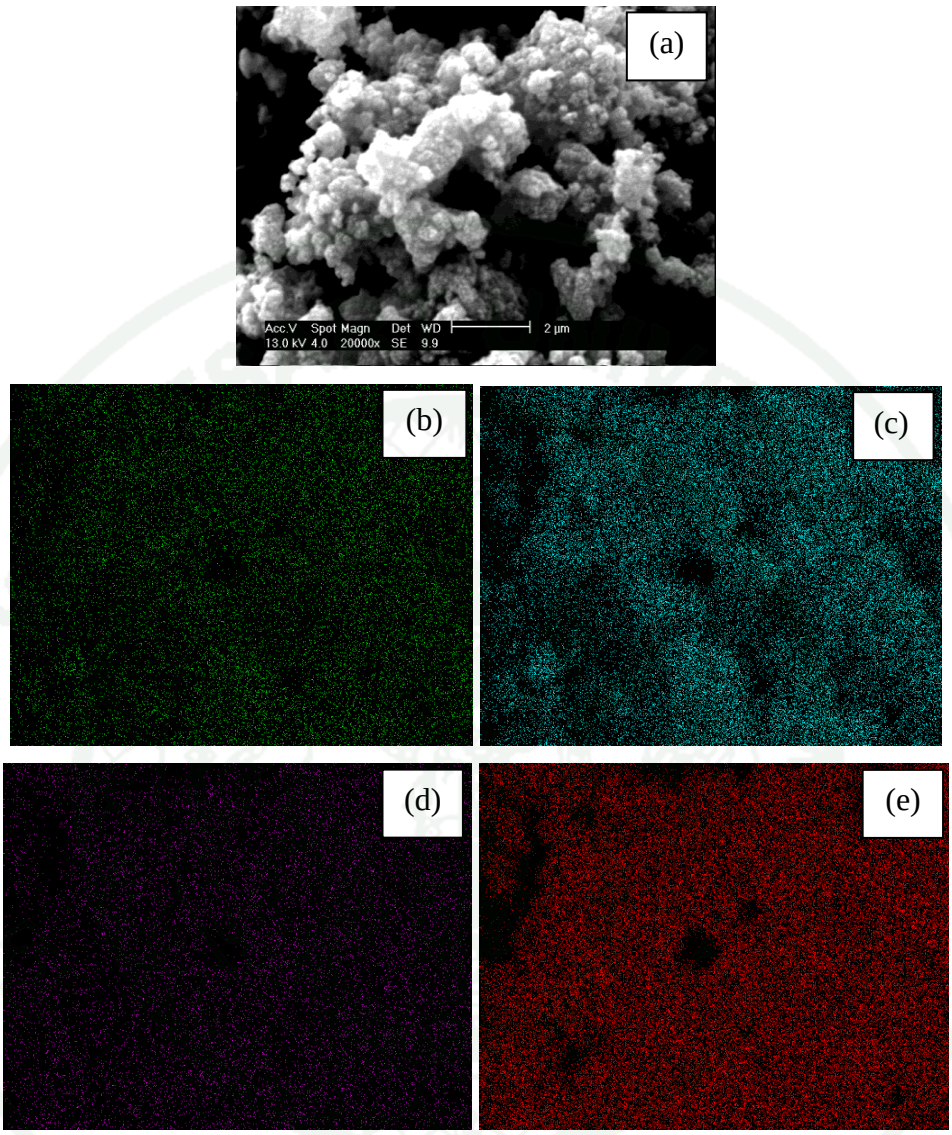

Figure 29 SEM image and mapping images of N-S co-doped TiO_2 using titanium(IV) tetraisopropoxide as a titania precursor calcined at 400ºC; (a) SEM image, (b) mapping image of N, (c) mapping image of O (d) mapping image of S and (e) mapping image of Ti.

Figure 29 shows surface morphology (Figure 29a) and mapping images (Figure 29b-e) of N-S co-doped TiO_2 prepared by titanium(IV) isopropoxide. From the SEM results, the bright spots corresponding to Ti, O, N and S atoms are distributed into the catalyst. These indicated that the elements are dispersed

homogeneously along the bulk of the catalyst. Therefore, the small amount of bright spots for N and S exhibit the smaller amount of N and S was distributed in the sample.

2. Photocatalytic activity

2.1 Photodegradation of benz[a]anthracene

2.1.1 Calibration curve of standard benz[a]anthracene

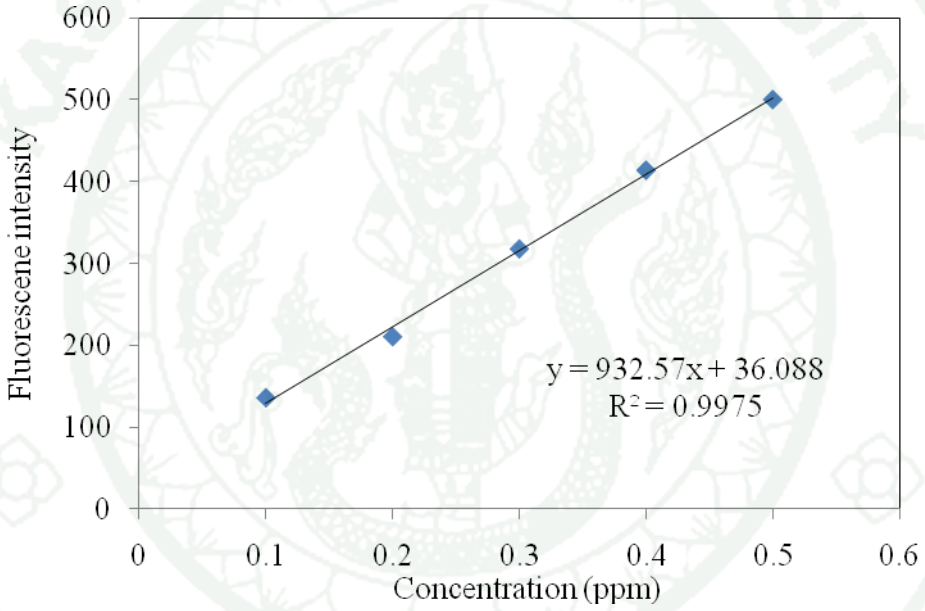

Figure 30 Calibration curve of benz[a]anthracene at concentration from 0.1-0.5 ppm.

Figrue 30 shows a series of solution of benz[a]anthracene which were quantified by fluorescene spectroscopy. The intensity of excitation wavelength at 264 nm and emission wavelength at 527 nm were plotted against concentration of benz[a]anthracene from 0.1 to 0.5 ppm.

2.1.2 Photocatalytic activity of N-S co-doped TiO_2

The visible photocatalytic activity of N-S co-doped TiO_2 photocatalysts were evaluated by measuring the decomposition of benz[a]anthracene under visible light irradiation for 5 h. The 0.1 g of samples were used to degrade benz[a]anthracene from 125 ml of 20 ppm benz[a]anthracene solutions. Figure 31, 32, 33, 34 showed the photodegradation of benz[a]anthracene by without catalyst, undoped TiO_2, N-doped TiO_2 and N-S co-doped TiO_2, respectively. N-S co-doped TiO_2 photocatalysts showed higher % of degradation than in others conditions. The undoped TiO_2 and without catalyst reveal that no change in the relative concentration of benz[a]anthracene. Because of the fact that undoped TiO_2 have the large band-gap energy and larger crystallite size. N-doped TiO_2 and N-S co-doped TiO_2 show the high photocatalytic efficiency under visible light due to nitrogen and sulfur doping can evidently narrow the band gap of TiO_2 which indicates that the doping TiO_2 could improve the catalytic activity of TiO_2 under visible light.

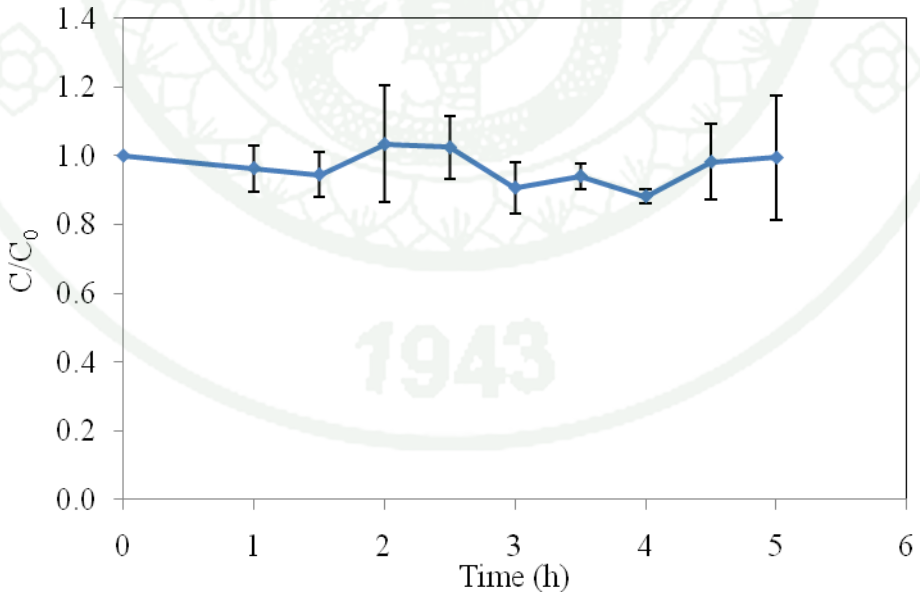

Figure 31 Photodegradation of 20 ppm benz[a]anthracene without catalyst under visible light.

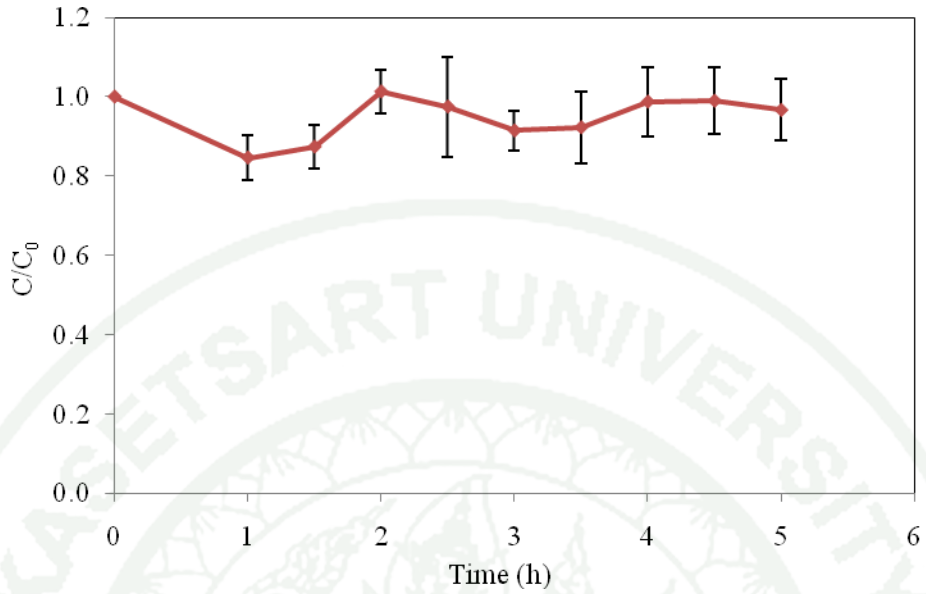

Figure 32 Photodegradation of 20 ppm benz[a]anthracene by undoped TiO_2 calcined at 400°C under visible light.

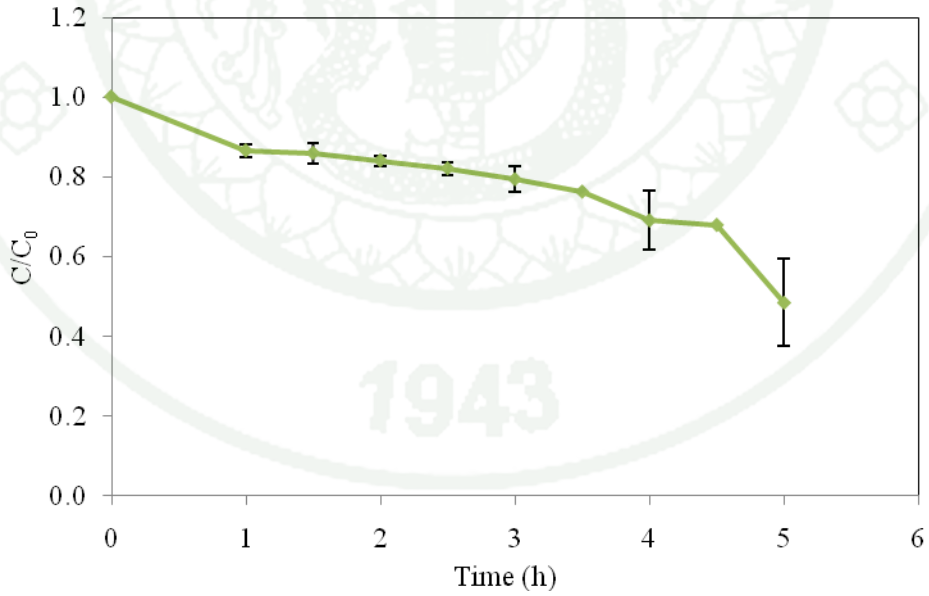

Figure 33 Photodegradation of 20 ppm benz[a]anthracene by N-doped TiO_2 calcined at 400°C under visible light.

Source: Sirisaksoontorn. (2008)

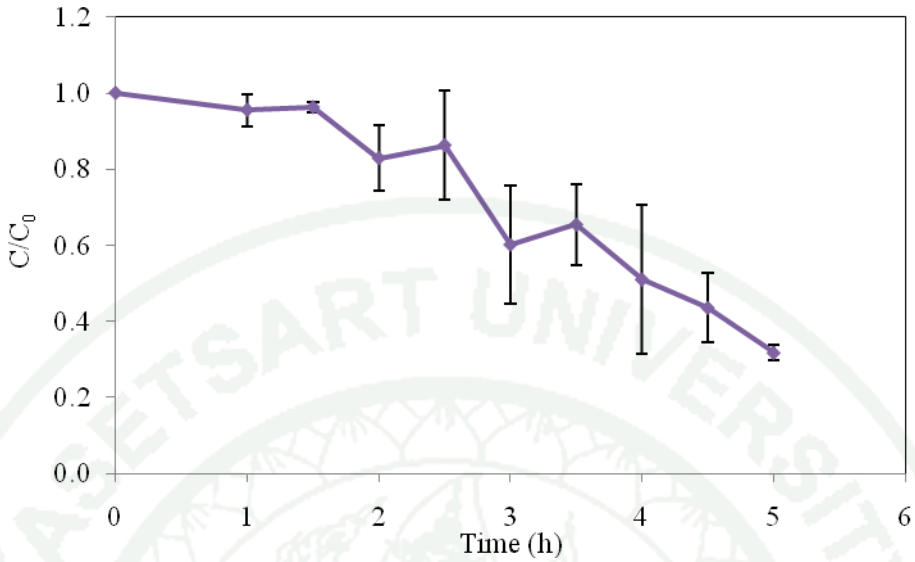

Figure 34 Photodegradation of 20 ppm benz[a]anthracene by N-S co-doped TiO_2 calcined at 400°C under visible light.

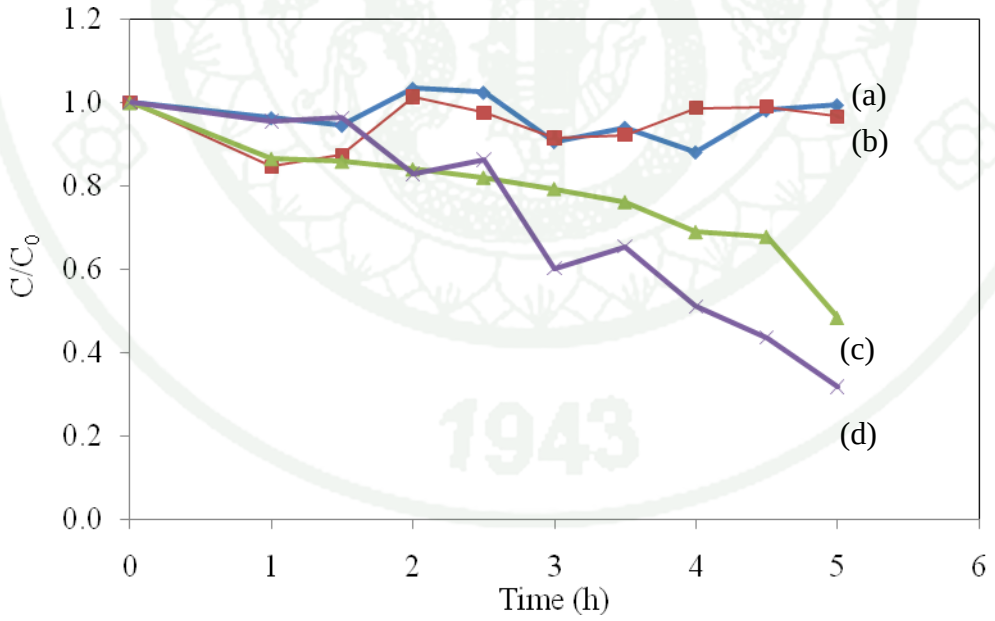

Figure 35 Photodegradation of 20 ppm benz[a]anthracene by without catalyst, undoped TiO_2, N-doped TiO_2 and N-S co-doped TiO_2 calcined at 400°C under visible light; (a) without catalyst, (b) undoped TiO_2, (c) N-doped TiO_2 and (d) N-S co-doped TiO_2.

Table 12 %Degradation and rate constants of photodegradation reactions of 20 ppm benz[a]anthracene by without catalyst, undoped TiO_2, N-doped TiO_2 and N-S co-doped TiO_2 calcined at 400^oC under visible light.

Catalysts	% Degradation[a]	Rate constant (h^{-1})	Relation coefficient (R^2)
Without catalyst	-	-	-
undoped TiO_2	-	-	-
N-doepd TiO_2	52.00±10.91	0.1192	0.7416
N-S co-doped TiO_2	68.20±2.05	0.2721	0.9192

[a]%degradation was calculated from ($C_{initial}$- C_{final}/ $C_{initial}$) x 100

The rate constant (h^{-1}) of photocatalytic degradation of benz[a]anthracene with different catalysts are shown in Table 12. Propose that the rate of degradation was the first order reaction from the plotting between ln(C_0/C) and time, the rate constant (h^{-1}) is related to the slope of the plot which can be calculated by assumption that the degradation of benz[a]anthacene is the first order reaction. The procedure to calculate rate constant is also shown in Appendix F. To compare the photocatalytic activity of mono-doped TiO_2 and co-doped TiO_2, Sirisaksoontorn 2008 found that the N-doped TiO_2 showed high photodegradation of benz[a]anthracene. Moreover, the %degradation and rate constant of N-S co-doped TiO_2 is 68% and 0.2721 h^{-1}, while 52% degradation and rate constant is 0.1192 h^{-1} of N-doped TiO_2. The results indicated that the improvement in smaller crystallite size and stronger absorption in visible region than N-doped TiO_2 and codoping (N, S) made the N-S co-doped TiO_2 more effective for degradation of benz[a]anthracene than N-doped TiO_2.

The N-S co-doped TiO_2 with different calcination temperatures of two titania precursors were used to degrade benz[a]anthracene in the same condition under visible light.

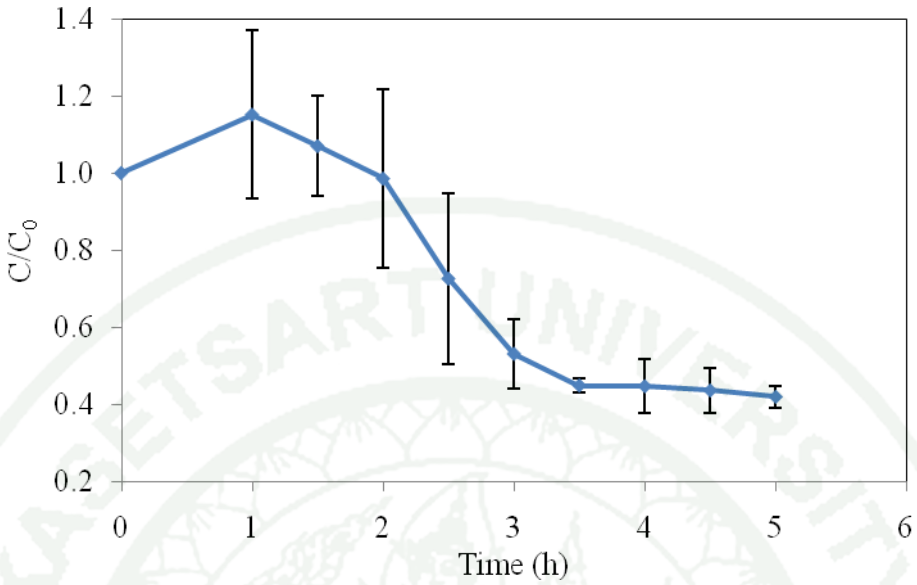

Figure 36 Photodegradation of 20 ppm benz[a]anthracene by N-S co-doped TiO_2 using titanium(IV) tetraisopropoxide calcined at 300°C under visible light.

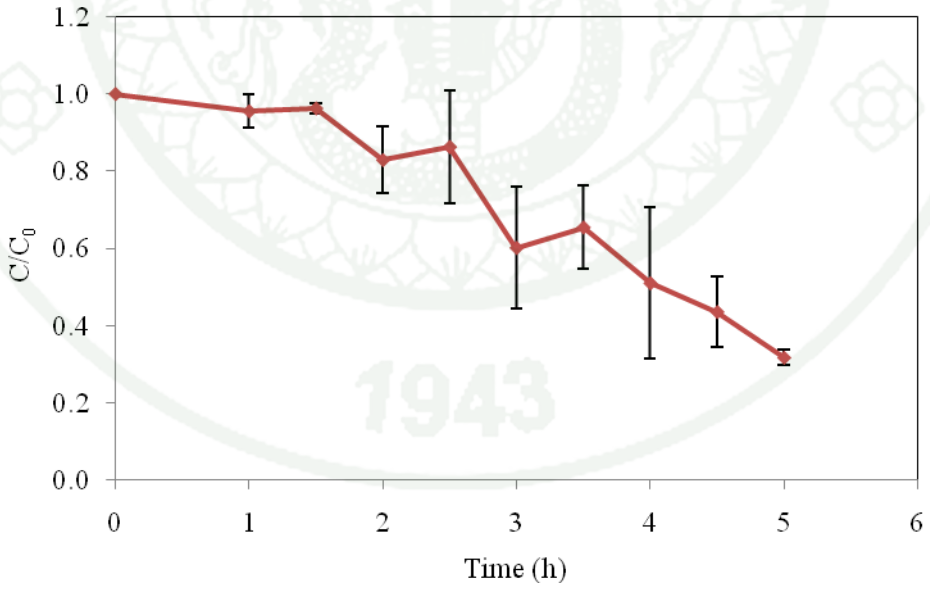

Figure 37 Photodegradation of 20 ppm benz[a]anthracene by N-S co-doped TiO_2 using titanium(IV) tetraisopropoxide calcined at 400°C under visible light.

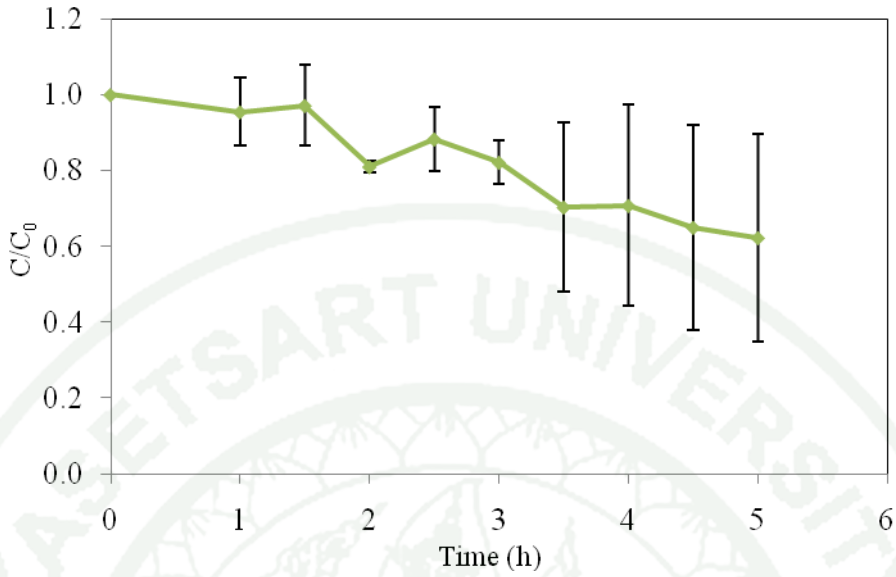

Figure 38 Photodegradation of 20 ppm benz[a]anthracene by N-S co-doped TiO_2 using titanium(IV) tetraisopropoxide calcined at 500°C under visible light.

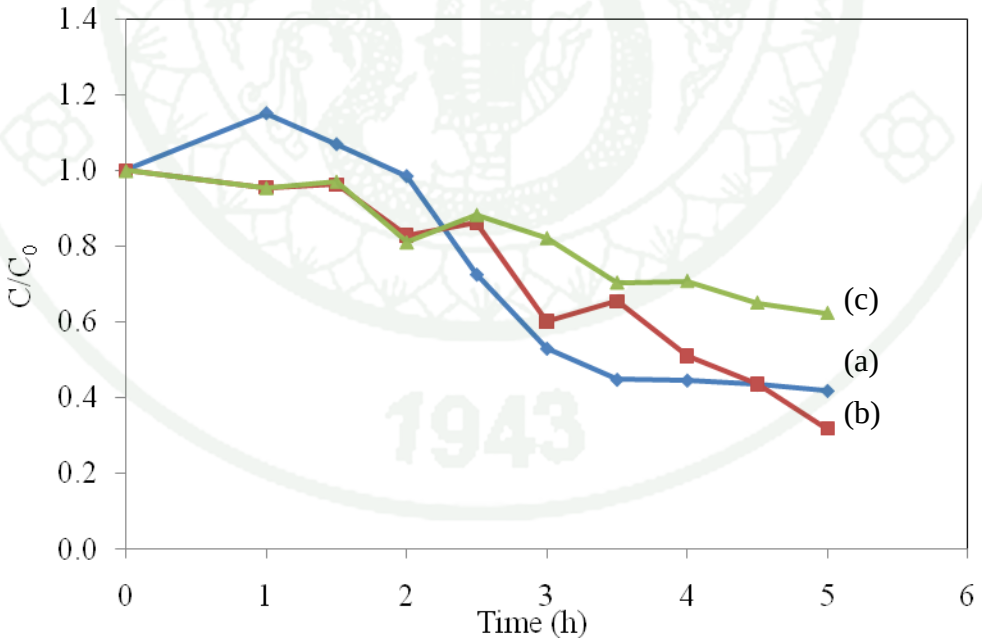

Figure 39 Photodegradation of 20 ppm benz[a]anthracene by N-S co-doped TiO_2 using titanium(IV) tetraisopropoxide with different calcination temperatures under visible light; (a) calcined at 300°C, (b) calcined at 400°C and (c) calcined at 500°C.

Figure 39 shows the photodegradation of benz[a]anthracene by using titanium(IV) tetraisopropoxide as precursor calcined 300°C, calcined at 400°C, calcined at 500°C. The N-S co-doped TiO_2 photocatalysts calcined 400°C shows higher %degradation than the other calcination temperature.

From the results of N-S co-doped TiO_2 using titanium(IV) tetraisopropoxide with calcination temperature, the N-S co-doped TiO_2 calcined at 400°C shows the highest catalytic efficiency. The % degradation of catalysts are 58.14%, 68.20% and 37.70% for N-S co-doped TiO_2 calcined at 300°C, 400°C and 500°C, respectively. Generally, the photocatalytic activity increased initially and decreased with the increasing calcinations temperature (Xie *et al*., 2008). This can be implied that, firstly, the calcination temperatures are affected on the crystallinity, crystallite size and surface area which consequently resulted in the different recombination rate of electron-hole pair. When the calcination temperature increased then, the crystallinity and crystallite size increased and surface area decreased. Thus, the N-S co-doped TiO_2 calcined at 300°C shows smaller crystallite size indicate that the higher surface area. Therefore, it can adsorb a higher number of organic molecules. Secondly, the phase composition of catalyst is a factor which can improve the phocatalytic activity. Anatase phase of titania has been reported to be more photocatalytically active than the rutile phase because the absorption affinity of the organic molecule toward the anatase phase is stronger compared to that of rutile phase. The N-S co-doped TiO_2 calcined at 400°C shows higher crystallintiy of anatase phase than calcined at 300°C. However, the N-S co-doped TiO_2 calcined at 500°C exhibited the mixed phase (anatase/rutile). Thirdly, the N-S co-doped TiO_2 indicated a new strong absorption band in the visible, and with the decreasing calcinations temperature the absorption edge shifted toward higher wavelength. The enhancement of absorbance in the UV-Vis region increase the number of photogenerated electrons and holes to participate in the photocatalytic activity reaction, which can enhance the photodegradation of TiO_2.

Table 13 %Degradation and rate constants of photodegradation reactions of 20 ppm benz[a]anthracene by N-S co-doped TiO_2 using titanium(IV) tetraisopropoxide with different calcination temperatures under visible light.

Catalysts	Calcination temperature (°C)	% Degradation[a]	Rate constant (h^{-1})	Relation coefficient (R^2)
N-S co-doped TiO_2	300	58.14±2.79	0.2910	0.9028
	400	68.20±2.05	0.2721	0.9192
	500	37.70±27.34	0.1366	0.9209

[a]%degradation was calculated from ($C_{initial}$- C_{final}/ $C_{initial}$) x 100

Table 13 shows the degradation rate of N-S co-doped TiO_2, it reveal that The N-S co-doped TiO_2 calcined at 300°C shows high rate constant (0.2910 h^{-1}) and %degradation is 58.14%. Moreover, the N-S co-doped TiO_2 exhibits the highest % degradation of benz[a]anthracene (68.20% degradation) and rate constant is 0.2721 h^{-1}due to the high crystallinity.

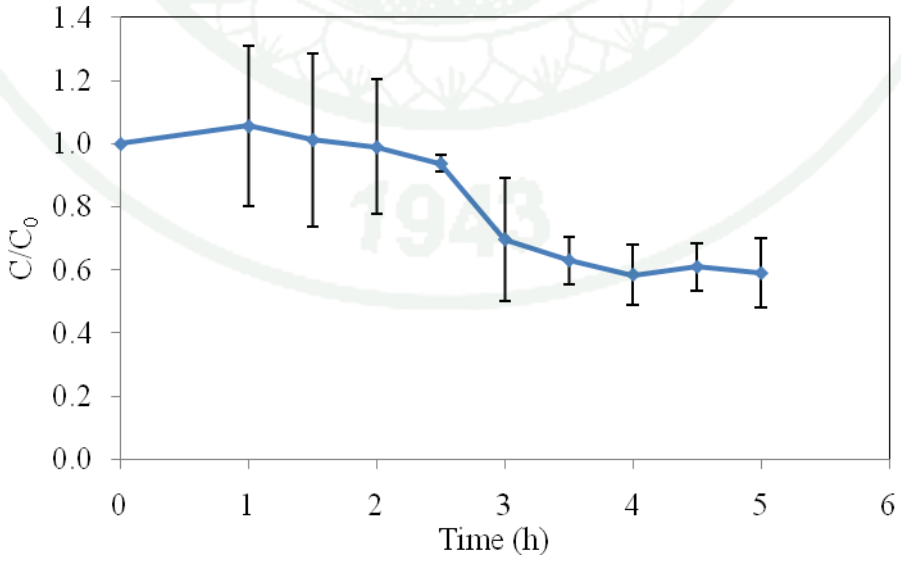

Figure 40 Photodegradation of 20 ppm benz[a]anthracene by N-S co-doped TiO_2 using titanium(IV) tetra-n-butoxide calcined at 300°C under visible light.

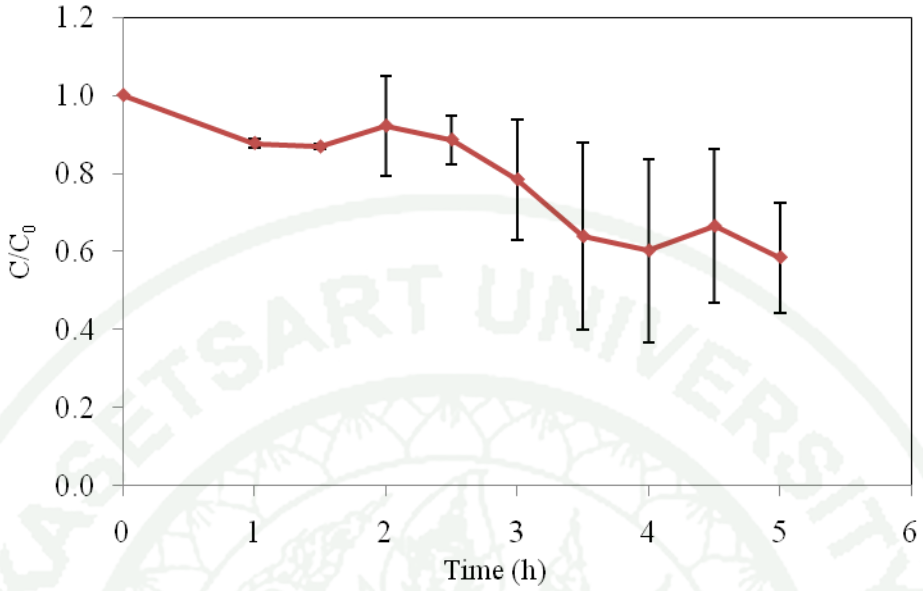

Figure 41 Photodegradation of 20 benz[a]anthracene by N-S co-doped TiO_2 using titanium(IV) tetra-n-butoxide calcined at 400°C under visible light.

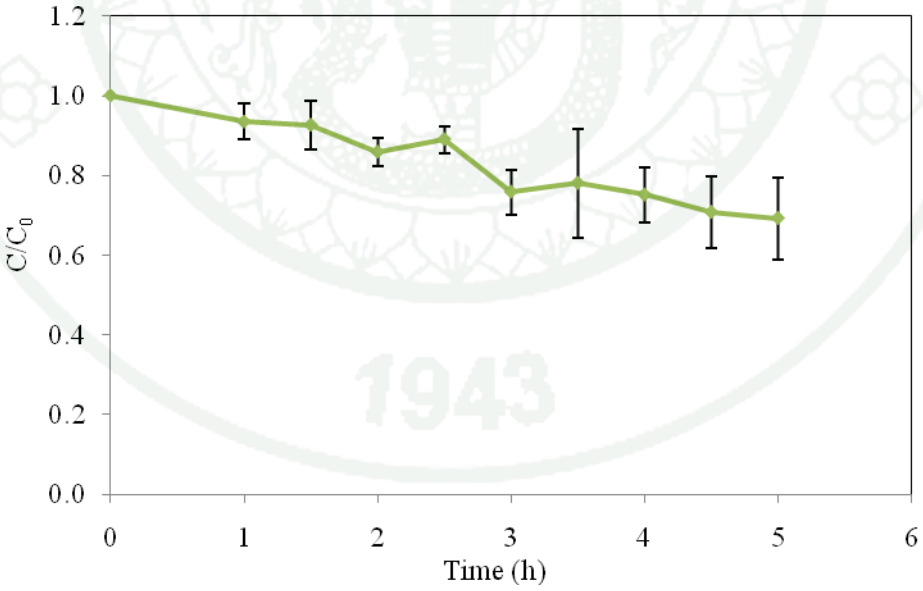

Figure 42 Photodegradation of 20 ppm benz[a]anthracene by N-S co-doped TiO_2 using titanium(IV) tetra-n-butoxide calcined at 500°C under visible light.

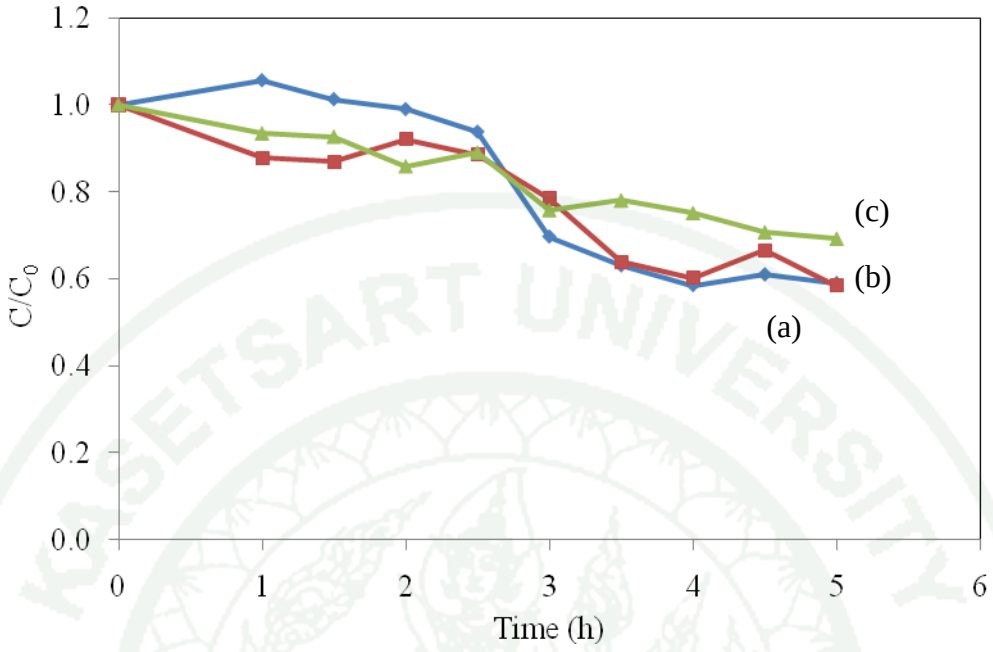

Figure 43 Photodegradation of 20 ppm benz[a]anthracene by N-S co-doped TiO_2 using titanium(IV) tetra-n-butoxide with different calcination temperatures under visible light; (a) calcined at 300°C, (b) calcined at 400°C and (c) calcined at 500°C.

Table 14 %Degradation and rate constants of photodegradation reactions of 20 ppm benz[a]anthracene by N-S co-doped TiO_2 using titanium(IV) tetra-n-butoxide with different calcination temperatures under visible light.

Catalysts	Calcination temperature (°C)	% Degradation[a]	Rate constant (h^{-1})	Relation coefficient (R^2)
N-S co-doped TiO_2	300	41.09±10.90	0.1742	0.8763
	400	41.55±14.10	0.1299	0.7968
	500	30.78±10.37	0.0822	0.9233

[a]%degradation was calculated from ($C_{initial}$- C_{final}/ $C_{initial}$) x 100

The photocatalytic activities of titanium(IV) tetra-n-butoxide with different calcination temperatures (Figure 40-42) and rate constant are shown in Table 14. The results exhibit the similar photoactivity of N-S co-doped TiO_2 calcined at 300°C and 400°C. Its catalytic efficiency determined by the degradation of benz[a]anthracene is 41.09% for N-S co-doped TiO_2 calcined at 300°C, 41.55% for N-S co-doped TiO_2 calcined at 400°C and 30.78% for N-S co-doped TiO_2 calcined at 500°C. Anyhow, N-S co-doped TiO_2 calcined at 300°C showed amorphous solid in XRD and Raman shift.

From these results, it suggested that the N-S co-doped TiO_2 calcined at 400°C provided the high photocatalytic efficiency of benz[a]anthracene using titanium(IV) isopropoxide and titanium(IV) tetra-n-butoxide. Therefore, it was selected as the photocatalyst for further experiment.

The N-S co-doped TiO_2 with different solvents of two titania precursors were used to degrade 20 ppm of benz[a]anthracene in the same condition under visible light.

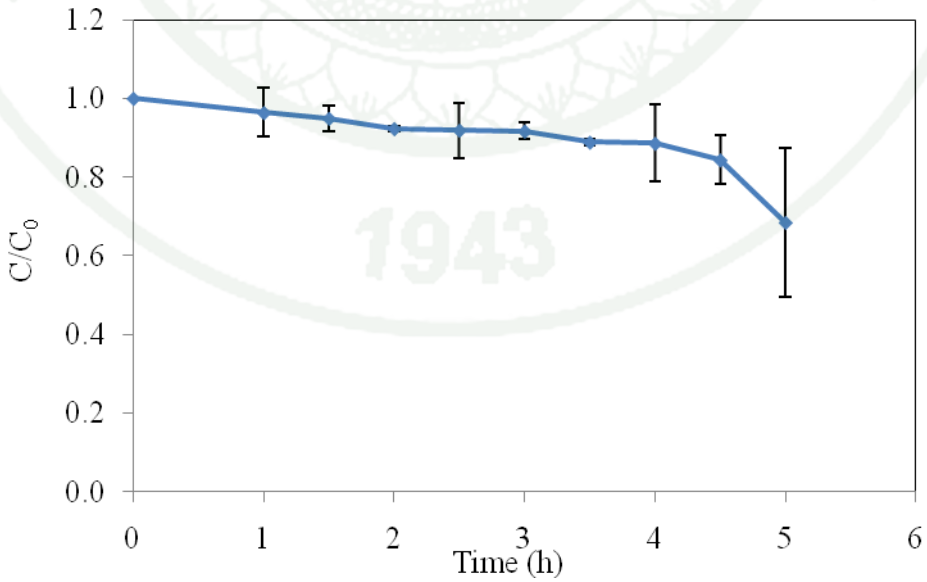

Figure 44 Photodegradation of 20 ppm benz[a]anthracene by N-S co-doped TiO_2 using titanium(IV) tetraisopropoxide and methanol as a solvent calcined at 400°C under visible light.

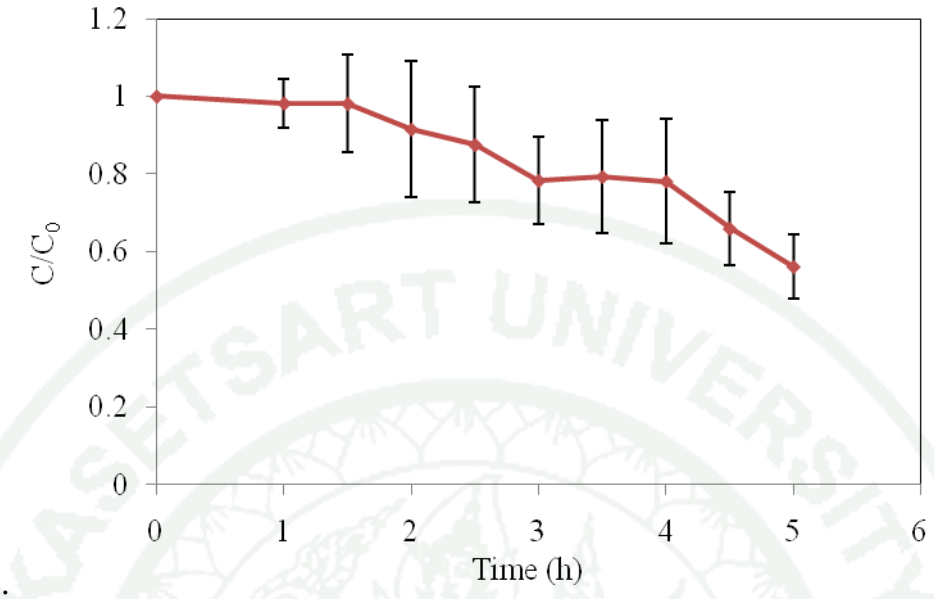

Figure 45 Photodegradation of 20 ppm benz[a]anthracene by N-S co-doped TiO_2 using titanium(IV) tetraisopropoxide and ethanol as a solvent calcined at 400°C under visible light.

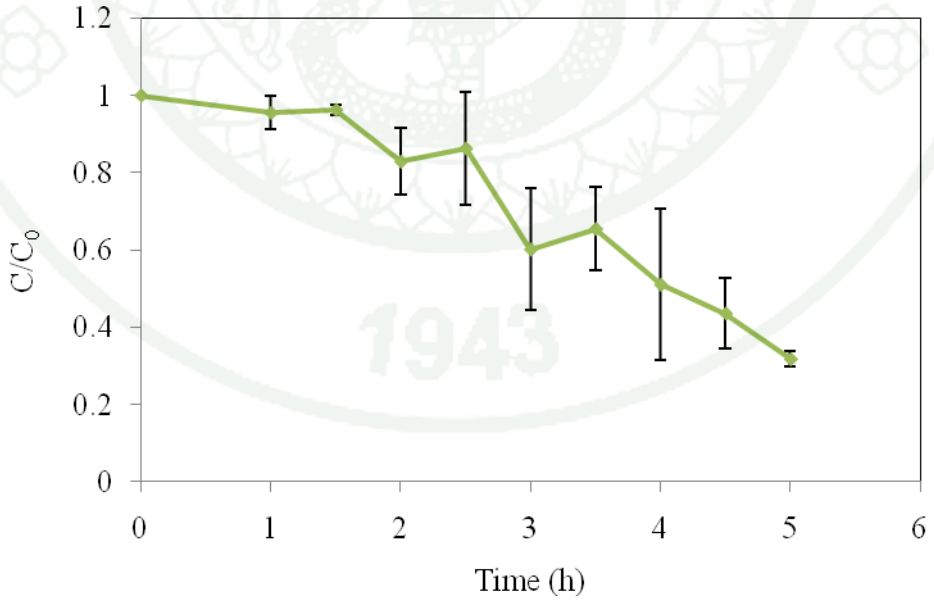

Figure 46 Photodegradation of 20 ppm benz[a]anthracene by N-S co-doped TiO_2 using titanium(IV) tetraisopropoxide and isopropanol as a solvent calcined at 400°C under visible light.

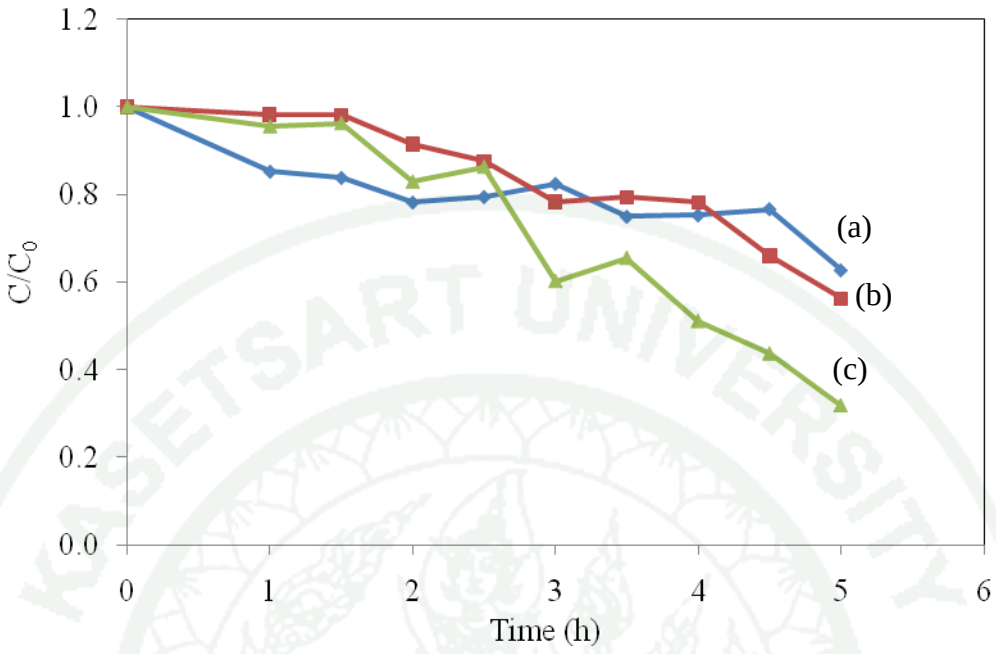

Figure 47 Photodegradation of 20 ppm benz[a]anthracene by N-S co-doped TiO_2 using titanium(IV) tetraisopropoxide with three of preparation solvents and calcined at 400°C under visible light; (a) methanol, (b) ethanol and (c) isopropanol.

The N-S codoped TiO_2 by titanium(IV) tetraisopropoxide with different solvents are shown in Figure 48. The %degradation of benz[a]anthacene with methanol, ethanol and isopropanol as solvents are 31.49%, 43.83% and 68.2%, respectively. It reveals that N-S co-doped TiO_2 using isopropanol as a solvent shows the highest photocatalytic efficiency. The effect of solvents on photocatalytic activity of N-S co-doped TiO_2 could be confirmed by ANOVA. ANOVA can also be used in situations where is more than one source of random variation. It can be estimated in two ways, one involving the variation within the samples and the other the variation between the samples can be calculated by equation as follow (James and Jane., 2005);

Within-sample estimate of σ_0^2 $= \Sigma\,\Sigma\,(x_{ij} - \bar{X}_i^2)/h(n\text{-}1)$

Between–sample estimate of σ_0^2 $= n\,\Sigma\,(\bar{X}_i - \bar{X})^2/(h\text{-}1)$

where x is sample

$\bar{X}$ is sample mean

h is amount of sample mean

n is replicate of sample

If it is incorrect, the between-sample estimated of σ_0^2 will be greater than the within-sample estimate. To test whether it is significantly greater, a one-sided F-test is used by equation as follow;

$$F = s_1^2/s_2^2$$

where s_1^2 is between–sample estimate

s_2^2 is within-sample estimate

If the calculated value of F exceeds a certain critical value (obtained from table of F for a two-tailed test) (P=0.05) then the sample data is rejected. In addition, a significant result in ANOVA can arise for several different reason and can indicated that all the means may differ from each other. The data is to arrange the means in increasing order and compare the difference between adjacent values with a quantity called the least significant difference. This is given by;

$$s\sqrt{(\frac{2}{n})}\, t_{h(n-1)}$$

where s is within-sample estimate

h(n-1) is the number of degrees of freedom of this estimate

If the least significant difference exceeds certain the value suggests that result which no differ significantly from each other.

From the calculatation, the F calculated is 47.34 greater than 7.26 of the critical value indicating the %degradation of three solvent are differ

significantly. The calculated value of %degradation between methanol and ethanol are 6.56 (this value is 43.83%-37.25%) less than the least significant difference of 14.437. It indicate that %degradation of methanol and ethanol as solvents are no differing significantly. However, the value calculated of %degradation between isopropanol and ethanol are 24.37 (this value is 68.2%-43.83%) suggesting the %degradation of isopropanol and ethanol are differ significantly.

These results may be implied that the steric ligand of titania precursor and solubility of solvent. Isopropanol exhibited that slowly to be hydrolyzed in sol-gel process. The crystallite size of N-S co-doped TiO_2 used isopropanol (7 nm) had smaller than crystallite size of N-S co-doped TiO_2 used methanol (9 nm) as a solvent.

Table 15 %Degradation and rate constants of photodegradation reactions of 20 ppm benz[a]anthracene by N-S co-doped TiO_2 using titanium(IV) tetraisopropoxide prepared in different solvents and calcined at 400°C under visible light.

Catalysts	solvents	% Degradation[a]	Rate constant (h^{-1})	Relation coefficient (R^2)
N-S co-doped TiO_2	methanol	37.25±6.67	0.0537	0.6615
	ethanol	43.83±8.39	0.1292	0.9108
	isopropanol	68.20±2.05	0.2721	0.9192

[a]%degradation was calculated from ($C_{initial}$- C_{final}/ $C_{initial}$) x 100

From table 15, the rate constant of photodegradation using N-S co-doped TiO_2 with different solvents show N-S co-doped TiO_2 used isopropanol as a solvent is higher than other the samples. It indicated that catalyst using isopropanol was more effective. Conclude that solvent had little effect on the photodegradation efficiency of benz[a]anthracene.

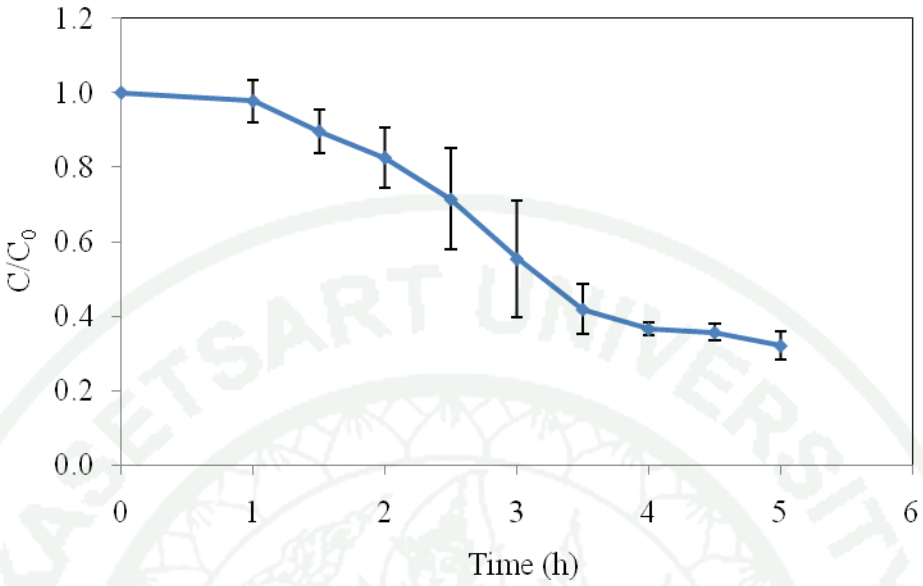

Figure 48 Photodegradation of 20 ppm benz[a]anthracene by N-S co-doped TiO_2 using titanium(IV) tetra-n-butoxide and methanol as a solvent calcined at 400°C under visible light.

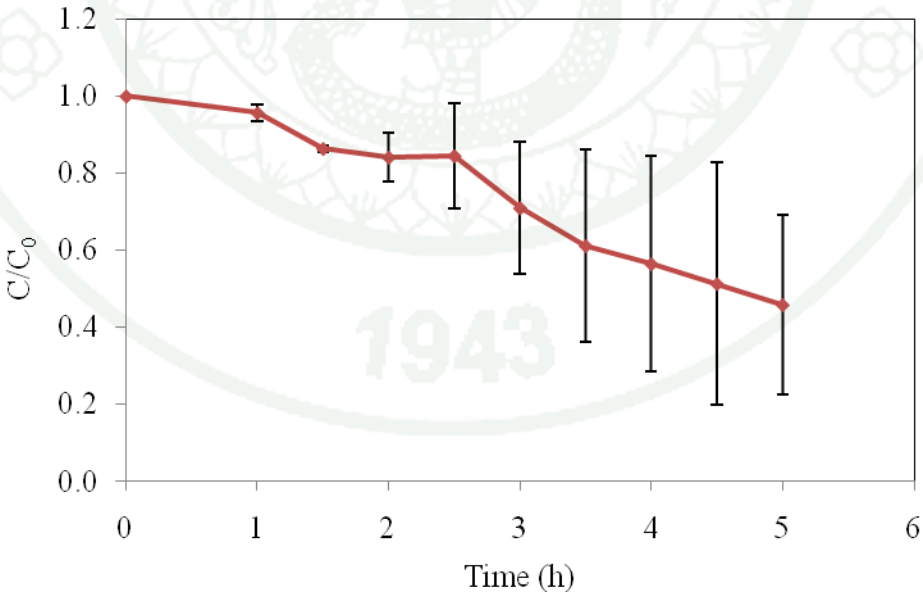

Figure 49 Photodegradation of 20 ppm benz[a]anthracene by N-S co-doped TiO_2 using titanium(IV) tetra-n-butoxide and ethanol as a solvent calcined at 400°C under visible light.

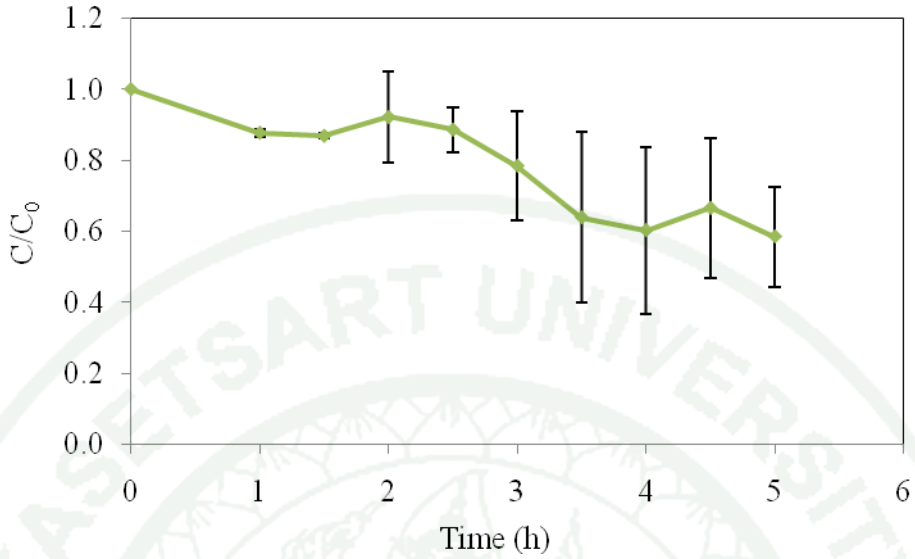

Figure 50 Photodegradation of 20 ppm benz[a]anthracene by N-S co-doped TiO_2 using titanium(IV) tetra-n-butoxide and isopropanol as a solvent calcined at 400°C under visible light.

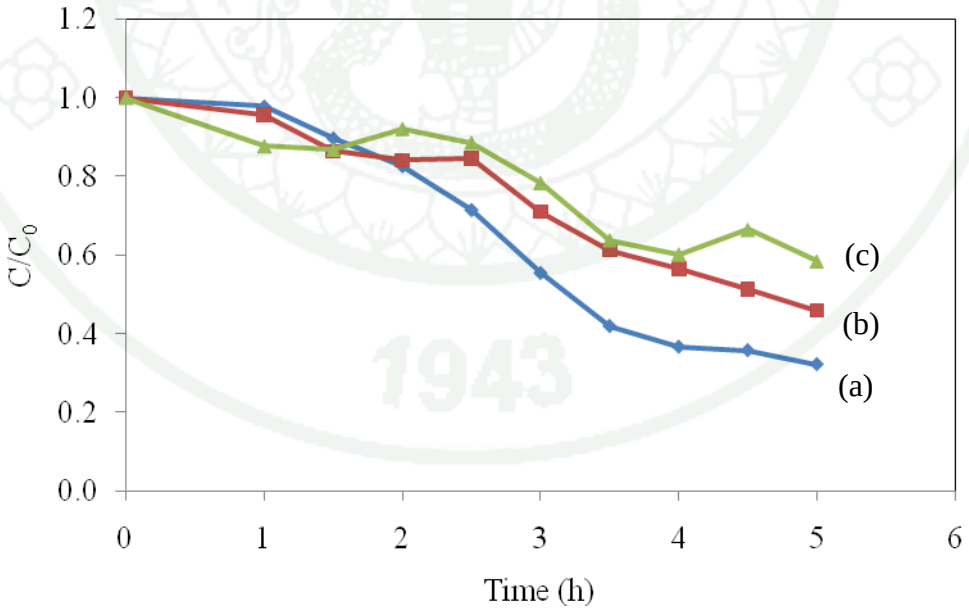

Figure 51 Photodegradation of 20 ppm benz[a]anthracene by N-S co-doped TiO_2 using titanium(IV) tetrabutoxide with three of preparation solvents and calcined at 400°C under visible light; (a) methanol, (b) ethanol and (c) isopropanol.

Figrue 51 show photocatalytic activtiy of N-S co-doped TiO_2 with different solvents. The %degradation of benz[a]anthracene are 67.86% for methanol, 54.19% for ethanol and 41.55% for isopropanol as solvent. The N-S co-doped TiO_2 prepared with methanol as a solvent shows high photocatalytic activity. Anova was used to confirm the effect of solvent on photocatalytic activity. It found that the calculated value of %degradation is 0.7898 is less than 7.26 of the critical value which indicates the % degradation of three preparation solvents are no differ significantly. The calculated value of %degradation between methanol and ethanol are 13.1 and ethanol and isopropanol are 13.67 less than 30.13 of the least significant difference. This result indicates N-S co-doped TiO_2 prepared with each solvent are no differing significant. This may be ascribed to less steric ligand of titania precursor. Thus, solvent had no influence on the photocatalytic efficiency.

Table 16 %Degradation and rate constants of photodegradation reaction of 20 ppm benz[a]anthracene by N-S co-doped TiO_2 using titanium(IV) tetra-n-butoxide prepared in different solvents calcined at 400°C under visible light.

Catalysts	solvents	% Degradation[a]	Rate constant (h^{-1})	Relation coefficient (R^2)
N-S co-doped TiO_2	methanol	67.86±3.76	0.3127	0.9651
	ethanol	54.19±23.40	0.2165	0.9589
	isopropanol	41.55±14.10	0.1299	0.7968

[a]%degradation was calculated from ($C_{initial}$- C_{final}/ $C_{initial}$) x 100

The rate of degradation of N-S co-doped TiO_2 with various solvents are shown in Table 16. The results show that the N-S co-doped TiO_2 using methanol as a solvent exhibits the highest the degradation rate.

From these results, it suggested that the high photocatalytic efficiency are found in two titania precursors, N-S co-doped TiO_2 by titanium(IV)

tetraisopropoxide using isopropanol as a solvent showed the %degradation is 68.2% and rate constant is 0.2721 h^{-1} and 67.86% degradation rate and 0.3127 h^{-1} rate constants for the N-S co-doped TiO_2 by titanium(IV) tetrabutoxide using methanol as a solvent.

2.2 Photodegradation of methylene blue

2.2.1 Calibration curve of standard methylene blue

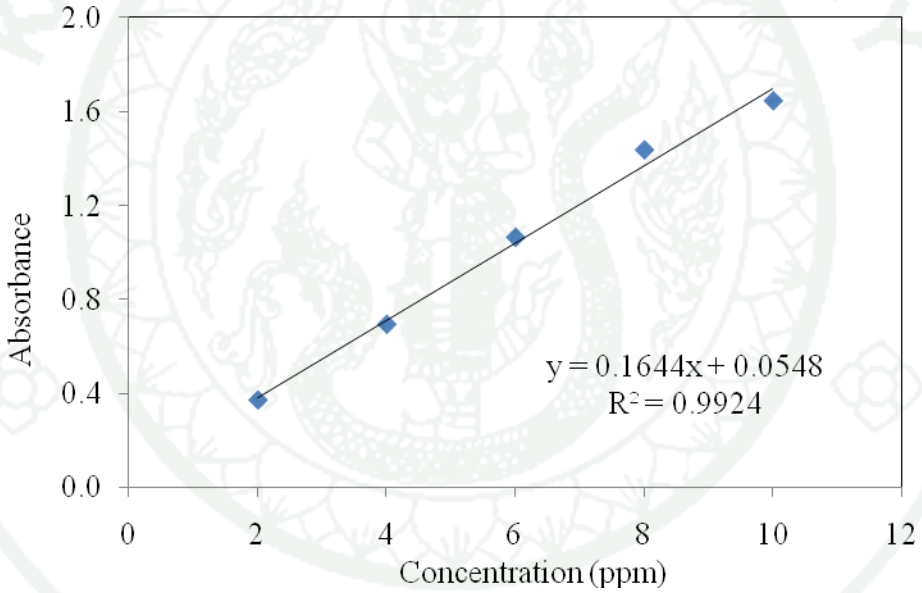

Figure 52 Calibration curve of methylene blue at concentration from 2-10 ppm.

Figrue 52 shows a series of solution of methylene blue was quantified by UV-Vis spectroscopy. The maximum spectra wavelength at 664 nm was plotted against concentration of methylene blue from 2 to 10 ppm.

2.2.2 Photocatalytic activity of methlylene blue using N-S co-doped TiO_2.

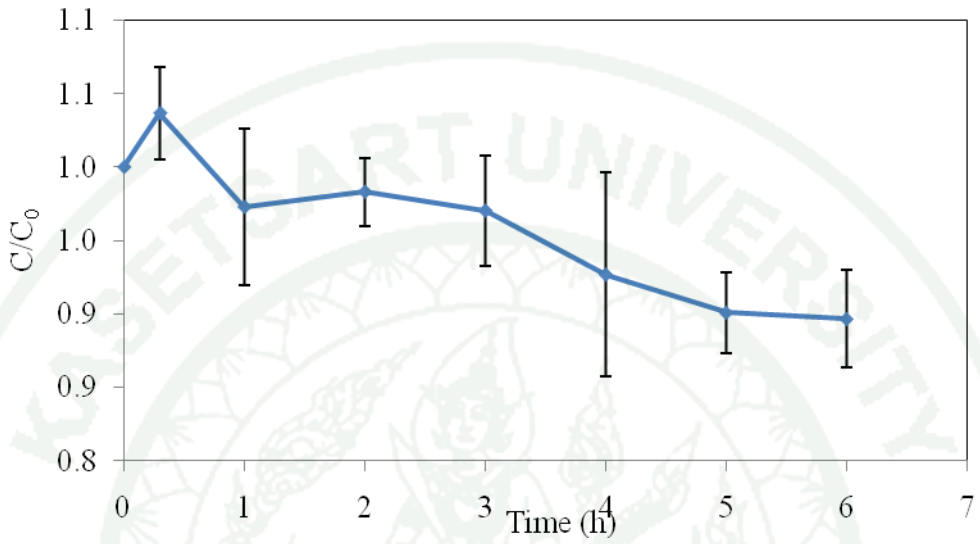

Figure 53 Photodegradation of 20 ppm methylene blue by N-S co-doped TiO_2 using titanium(IV) tetraisopropoxide and isopropanol as a solvent calcined at 400°C under visible light.

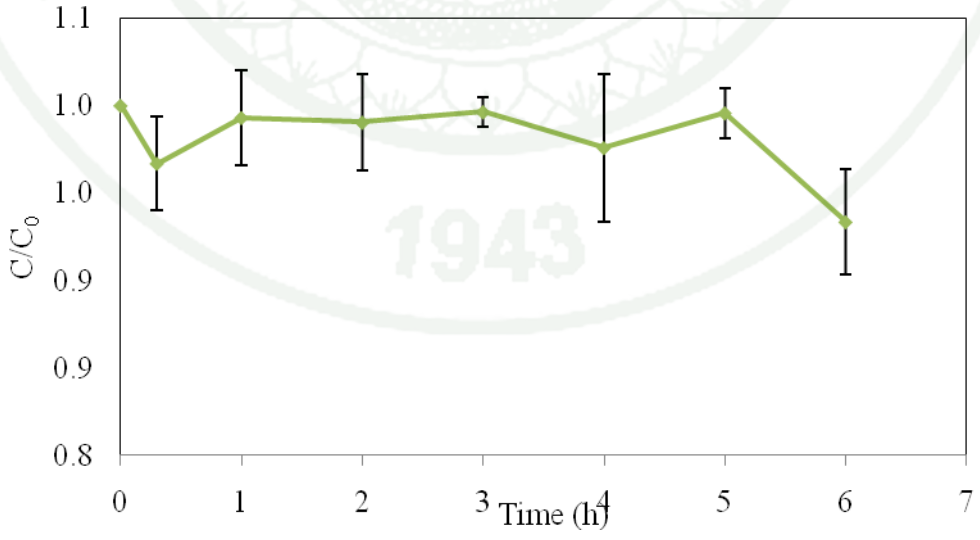

Figure 54 Photodegradation of 20 ppm methylene blue by N-S co-doped TiO_2 using titanium(IV) tetra-n-butoxide and methanol as a solvent calcined at 400°C under visible light.

Table 17 %Degradation and rate constants of photodegradation reactions of 20 ppm methylene blue by N-S co-doped TiO_2 calcined at 400°C under visible light.

Titanium precursors	% Degradation[a]	Rate constant (h^{-1})	Relation coefficient (R^2)
Titanium(IV) tetraisopropoxide	10.34	0.0238	0.8962
Titanium(IV) tetra-n-butoxide	6.67	0.0045	0.1587

[a]%degradation was calculated from $(C_{initial}- C_{final}/ C_{initial}) \times 100$

The concentrations of methylene blue after degraded in each 30 minutes interval under visible light were quantified by UV-Vis spectrophotometry at the maximum wavelength of 664 nm. The photocatalytic activity results are shown in Figrue 53-54. Percentage of degradation of methylene blue by N-S co-doped TiO_2 using titanium(IV) tetraisopropoxide and titanium(IV) tetra-n-butoxide are 10.34% and 6.67% respectively. Both two photocatalyst had low degradation rate which can be seen as shown in Table 17. This result indicates that methylene blue was more difficult to be mineralized by this photocatayst. However, the degradation rate of N-S co-doped TiO_2 using titanium(IV) tetraisopropoxide show the higher than N-S co-doped TiO_2 using titanium(IV) tetra-n-butoxide.

CONCLUSION AND RECOMMENDATIONS

Conclusion

The N-S co-doped TiO_2 photocatalyst were prepared by titanium(IV) tetraisopropoxide and titanium(IV) tetra-n-butoxide as titania precursors and using methanol, ethanol and isopropanol as solvents were prepared by sol-gel method. From all characterization techniques, it can indicated that the calcination temperature had an effect on the crystal structure, crystallite size and amount of nitrogen and sulfur. With increasing calcination temperature, the N-S co-doped TiO_2 had larger crystallite size, higher crystallinity, anatase-to-rutile phase transformation and smaller amount of nitrogen and sulfur. The codoping had effect on band structure of TiO_2 which shifted the absorption edge in the visible region.

Concerning the effect of titania precursor, N-S co-doped TiO_2 using titanium(IV) tetra-n-butoxide showed smaller crystallite size, higher amount of nitrogen and sulfur contents in catalyst and retard to phase transformation than N-S co-doped TiO_2 using titanium(IV) tetraisopropoxide. About of three preparation solvent on titania precursor, indicated that all of catalyst show the anatase phase. N-S co-doped TiO_2 using titanium(IV) tetra-n-butoxide and prepared with three solvents show higher amount of nitrogen and sulfur than N-S co-doped TiO_2 using titanium(IV) tetraisopropoxide and different solvents.

From the photocatalytic activity results, the N-S co-doped TiO_2 by titanium(IV) tetraisopropoxide used isopropanol as a solvent showed the highest %degradation of benz[a]anthracene and methylene blue under visible light. The %degradation and rate constant (h^{-1}) were 68.20% and 0.2721 h^{-1} for benz[a]anthracene and 10.34% and 0.0238 h^{-1} for methylene blue. For the %degradation of N-S co-doped TiO_2 by titanium(IV) tetraisopropoxide prepared in different solvents, implied that the solvent had effect on the photocatalytic activity.

As for the %degradation of N-S co-doped TiO_2 by titanium(IV) tetra-n-butoxide prepared with methanol as a solvent shows higher %degradation of benz[a]anthracene than the other solvents. However, from Anova, it was found that there is no solvent effect on the %degradation.

Recommendations

1. Regarding in the preparation, it should be use the high amount of solvents to dissolve of thiourea owing to thiourea hard in to dissolve in isopropanol as a solvent.

2. The studied of the effect of solvent ought to used the organic solvent in different properties such as boiling point, polarity etc. in order to investigated the different of solvent effect on the characteristics of photocatalyst and photocatalytic activity.

3. In the characterization of N-S co-doped TiO_2 photocatalyst, the surface area, pore volume and pore size distribution are important properties to the photocatalytic acitivity. Therefore, the characterization of the N-S co-doped TiO_2 photocatalyst should be determined by Brunauer-Emmett-Teller (BET) method so as to clarify the efficiency of the photocatalysts.

4. The photodegradation experiment without pre-adsorbed in the dark should perform as a blank experiment.

LITERATURE CITED

Carp, O., C.L. Huisman and A. Reller. 2004. Photoinduced reactivity of titanium dioxide. **Prog. Solid State Chem.** 32: 33-177.

Chen, X. and S. Mao. 2007. Titanium dioxide nanomaterials: synthesis, properties, modifications, and application. **Chem. Rev**. 107: 2891-2959.

Chen, D., Z. Jiang., J. Geng., Q. Wang. and D. Yang. 2007. Carbon and nitrogen co-doped TiO_2 with enhanced visible-light photocatalytic activity. **Ind. Eng, Chem. Res**. 46: 2741-2746.

Fang, X., Z. Zhang, Q. Chen., H. Ji and X. Gao. 2007. Dependence of nitrogen doping TiO_2 precursor annealed under NH_3 flow. **J. Solid State Chem**. 180: 1325-1332.

Gnaser, H., M.R. Savina, W.F. Calaway, C. Emil Tripa. I.V. Veryovkin and M.J. Pellin. 2005. Photocatalytic degradation of methylene blue on nanocrystalline TiO_2: surface mass spectrometry of reaction intermediates. **Int. J. Mass. Spectrom**. 245: 61-67.

Gombac, V., L. De Rogatis, A. Gasparotoo, G. Vicario, T. Montini, D. Barreca, G. Balducci, P. Fornasiero, E. Tondello and M. Graziani. 2007. TiO_2 nanopowders doped with boron and nitrogen for photocatalytic applications. **Chem. Phys**. 399: 111-123.

Gopal, M., W.J. Moberly Chan and L.C. De Jonghe. 1997. Room temperature synthesis of crystalline metal oxides. **J. Mater. Sci**. 32: 6001-6008.

Henner, P., M. Schiavon, J.L. Morel and E. Lichtfouse. Polycyclic aromatic hydrocarbons (PAH) occurrence and remediation methods. **Analusis Magazine**. 25: 56-59.

Ho, W., J. Yu and S. Lee. 2006. Low-temperature hydrothermal synthesis of S-doped TiO_2 with visible light photocatalytic activity. **J. Solid State Chem**. 179: 1171-1176.

Huang, D., S-J. Liao, J-M Lin, Z. Dang and L. Petrik. 2006. Preparation of visible-light responsive N-F-codoped TiO2 photocatalyst by a sol-gel-solvothermal method. **J. Photochem. Photobiol., A**. 184: 282-288.

Kanna, M. and S. Wongnawa. 2008. Mixed amorphous and nanocrystalline TiOe powders prepared by sol-gel method: characterization and photocatalytic study. **Mater. Chem. Phys**. 110: 166-175.

Katoh, M., H. Aihara, T. Horikawa and T. Tomida. 2006. Spectroscopic study for photocatalytic decomposition of organic compounds on titanium dioxide containing sulfur under visible light irradiation. **J. Colloid Interface Sci.** 298: 805-809.

Ksibi, M., S. Rossognol, J-M. Tatiouet and C. Trapalis. 2008. Synthesis and solid characterization of nitrogen and sulfur-doped TiO2 photocatalysts active under near visible light. **Mater. Lett.** 62: 4204-4206.

Li, X., R. Xiong and G. Wei. 2008. S-N co-doped TiO_2 photocatalysts with visible-light activity prepared by sol-gel method. **Catal Lett**. 125: 104-109.

Linsebigler, A.L., G. Lu, and J.T. Yates. 1995. Photocatalysis on TiO_2 surfaces: principles, mechanisms, and selected results. **Chem. Rev**. 95: 735-758.

Lv, Y., D.J. Zhou. W. Xiao and Y. Feng. 2009. Preparation, characterization, and photocatalytic activity of N, S- codoped TiO_2 nanoparticles. **J. Am. Ceram. Soc**. 92: 938-941.

Liu, S., C. Xiaoyun and C. Xi. 2006. Preparation of N-doped visible-light response nanosize TiO_2 photocatalyst using the acid-catalyzed hydrolysis method. **Chin J. Catal.** 27(8): 697-702.

_____, and X. Chen. 2008. A visible light response TiO_2 photocatalyst realized by cationic S-doping and its application for phenol degradation. **J. Hazard. Mater**. 152: 48-55.

Ma., H.L., J.Y. Yang, Y. Dai, Y.B. Zhang, B. Lu and G.H. Ma. 2007. Raman study of phase transformation of TiO2 rutile single crystal irradiated by infrared femtosecond laser. **Appl. Sur. Sci**. 253: 7497-7500.

Madarász, J., A. Brăileanu and G. Pokol. 2008. Comprehensive evolved gas analysis of amorphous precursors for S-doped titania by *in situ* TG-FTIR and TG/DTA-MS part 1. precursor from thiourea and titanium(IV)-isopropoxide. **J. Anal. Appl. Pyrolysis**. 82: 292-297.

_____, _____, M. Crişan and G. Pokol. 2009. Comprehensive evolved gas analysis (EGA) of amorphous precursors for S-doped titania by *in situ* TG-FTIR and TG/DTA-MS in air: part 2. precursor from thiourea and titanium(IV)-n-butoxide. **J. Anal. Appl. Pyrolysis**. 82: 549-556.

Miller., J.G. and J.N. Miller. 2004. **Statistic and chemometrics for analytical chemistry**. 55- 58 pages.

Ohno, T., M. Akiyoshi, T. Umebayashi, K. Asai, T. Mitsui and M. Matsumura. 2004. Preparation of S-doped TiO_2 photocatalysts and their photocatalytic activities under visible light. **Appl. Catal. A.** 265: 115-121.

Phatinavin, R. 2009. **Synthesis of summarium doped TiO_2 catalyst for photodegradation of polycyclic aromatic hydrocarbons (PAHs).** M.E. Thesis, Kasetsart university.

Periyat, P., D.E. Mccormark, S.J. Hinder and S.C. Pillai. 2009. One-pot synthesis of anionic (nitrogen) and cationic (sulfur) codoped high-temperature stable, visible light active, anatase photocatalysts. **J. Phys. Chem. C**. 113: 3246-3253.

Sekiya, T., S. Ohta, S. Kamei, M. Hanakawa and S. Kurita. 2001. Raman spectroscopy and phase transition of anatase TiO2 under ligh pressure. **J. Phys. Chem. Solids**. 62: 717-721

Shen, J., S. Zhang, J. Lian, L. Kong and J. Chen. 2007. Benz[a]anthracene heterogeneous photochemical reaction on the surface of TiO_2 particles. **Acta Phys. –Chim. Sin**. 23(10): 1531-1536.

Sheng, Y., Y. Xu, D. Jiang, L. Liang, D. Wu and Y. Sun. 2008. Hydrothermal preparation of visible-light-driven N-Br-codoped TiO_2 photocatalysts. **Int. J. Photoenergy**. 563949, 7 pages.

Shouxin, L. and C. Xiaoyun. 2008. A visible response TiO_2 photocatalyst realized by cationic S-doping and its application for phenol degradation. **J. Hazard. Mater**. 152: 48-55.

_____, _____ and C. Xi. 2006. Preparation of N-doped visible-light response nanosize TiO_2 photocatalyst using the acid-catalyzed hydrolysis method. **Chin J. Catal.** 27(8): 697-702.

Sirisaksoontorn, W. 2008. **Preparation of N-doped TiO_2 to use as catalysts in photodegradation reaction of PAHs and phenol**. M.E. Thesis, Kasetsart university.

Smith., M.F., K. Setwong, R. Tongpool, D. Onkaw, S. Na-phattalung, S. Limpijumnong and S. Rujirawat. 2007. Identification of bulk and surface sulfur impurities in TiO2 by synchrotron x-ray absorption near edge structure. **Appl. Phys. Lett.** 91: 142107.

Spurr, R.A. and H. Myers. 1957. Quantitative analysis of anatase-rutile mixtures with an X-Ray diffractometer. **Anal. Chem.** 29(5): 760-762.

Wan, L., J.F. Li, J.Y. Feng, W. Sun and Z.Q. Mao. 2007. Improved optical response and photocatalysis for N-doped titaniumoxide (TiO_2) films prepared by oxidation of TiN. **Appl. Surf. Sci**. 253: 4764-4767.

Wang, J., H. Li, H. Li and C. Zou. 2010. Mesoporous $TiO_{2-x}A_y$ (A = N, S) as a visible-light-response photocatalyst. **Solid State Sci**. 12: 490-497.

Wei, F., L. Ni and P. Cui. 2007. Preparation and characterization of N-S-co-doped TiO_2 photocatalyst and its photocatalytic activity. **J. Hazard. Mater.** 156: 135-140.

Xie, Y., Q. Zhao and X. Zhao. 2007. Low temperature preparation and characterization of N-doped and N-S co-doped TiO_2 by sol-gel route. **Catal Lett**. 188:231-237.

_____ and X. Zhao. 2008. The effects of synthesis temperature on the structure and visible-light-induced catalytic activity of F-N-codoped and S-N-codoped titania. **J Mol Cal Chem**. 285: 142-149.

Yang, G., Z. Jiang, H. Shi, M.O. Jones, T. Xiao, P.P. Edwards and Z. Yan. 2010. Study on the photocatalysis of F-S co-doped TiO_2 prepared using solvothermal method. **Appl. Catal., B**. 96: 458-465.

Yu, J., M. Zhou, B. Cheng and X. Zhao. 2005. Preparation, characterization and photocatalytic activity of in situ N,S-co-doped TiO_2 powders. **J. Mol. Catal. A: Chem**. 246: 176-184.

Zaleska, A. 2008. Doped-TiO_2: A review. **Recent patents on Engineering**. 2: 154-164.

Zhang, G., X. Ding, F. He, X. Yu, J. Zhou, Y. Hu and J. Xie. 2007. Preparation and photocatalytic properties of TiO_2-montmorillonite doped with nitrogen and sulfur. **J. Phys Chem Solid.** 69: 1102-1106.

Zhang, S., L. Limin and S. Zhang. 2009. Facile preparation of visible-light-sensitive sulfur-nitrogen-co-doped TiO_2 titanium dioxide. **React Kinet Catal Lett**. 97:199-205.

Zhuo, L., J. Beng, Y. Zhao, W. Liu, L. An and F. Chen. 2009. Preparation and characterization of N-I co-doped nanocrystal anatase TiO_2 with enhanced photocatalytic activity under visible-light irradiation. **Mater. Chem. Phys**. 117: 522-527.

Zhuo, Q., H. Ma, B. Wang and F. Fan. 2008. Degradation of methylene blue:Optimization of operating condition through a statistical technique and environmental estimate of the treated wastewater. **J. Hazard. Mater.** 153: 44–51.

APPENDICES

Appendix A

Calculation of crystallite sizes, phase identification using the Sherrer's equation

The crystallite size was also calculated applying the Sherrer's equation as shown in equation 1

$$d = \frac{k\lambda}{\beta \cos\theta_B} \qquad \text{.....(1)}$$

where d is the crystallite size (nm)

k is the constant whose value is approximately 0.9

λ is the wavelength of the X-ray radiation source (0.154 nm for Cu Kα)

β is the full width at half maximum intensity (FWHM) (radians)

θ_B is the Bragg angle at the position of the peak maximum

Figure A1 shows an example of finding all constants involved in the Sherrer's equation by fityk 0.8.9 software (a curve fitting and data analysis program).
The XRD pattern can be well fitted with Lorentzian function. The parameters for the peak were following; center of peak = 25.415º, peak area = 613.218, peak height = 758 and FWHM = 0.76.

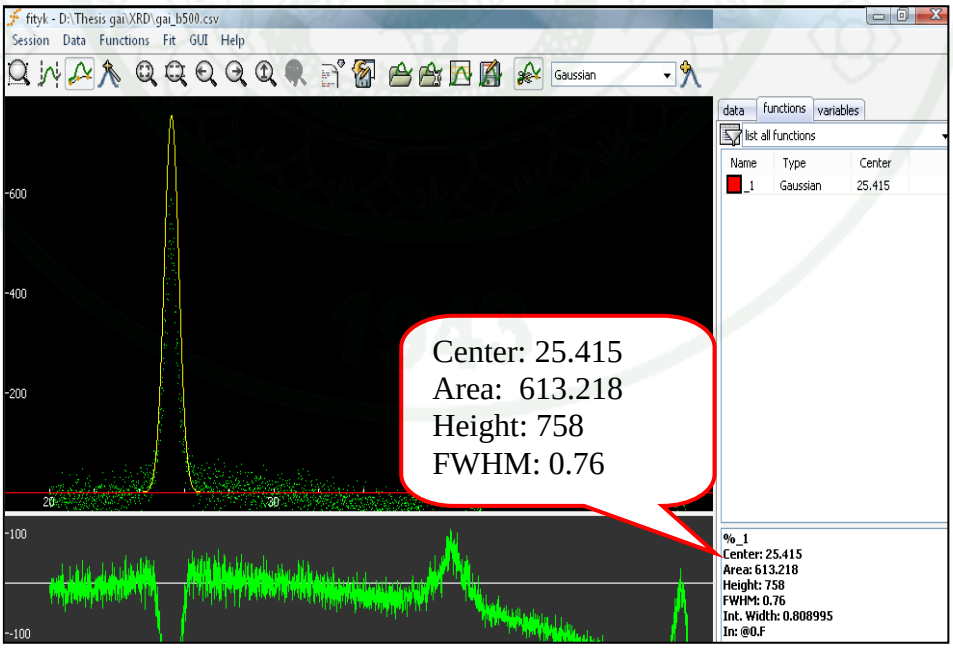

Appendix Figure A1 The fitting peak of N-S co-doped TiO_2 by titanium(IV) tetra-n-butoxide calcined at 500°C with Lorentzian function.

Appendix B

Calculation of phase composition by the Spurr-Myers eqution

The content of anatase was also calculated applying Spurr-Myers equation as shown in equation 2.

$$w_A = \frac{1}{(1+1.26\frac{I_R}{I_A})} \qquad \ldots\ldots(2)$$

where w_A is the weight fraction of anatase in the mixture

I_R is the intensity of the diffraction peak of rutile

I_A is the intensity of the diffraction peak of anatase

This is an example of finding all constants involved in the Spurr-Myers equation.

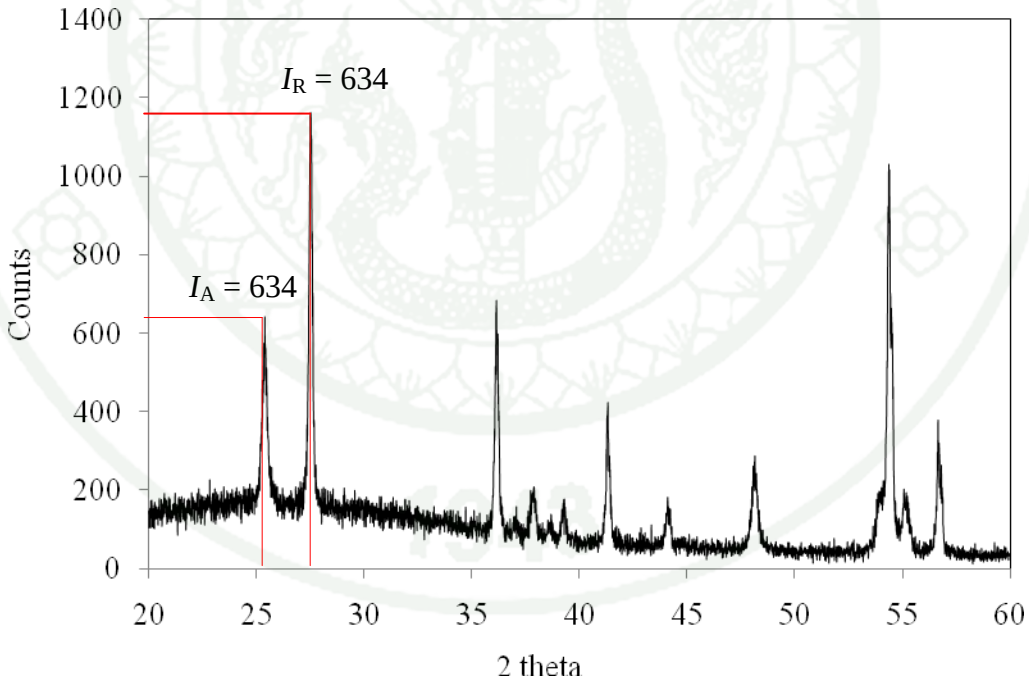

Appendix Figure B1 The XRD pattern of N-S co-doped TiO_2 using titanium(IV) tetraisopropoxide calcined at 700°C.

Appendix C

Calculation of the unit cell volume from three lattice parameters

The unit cell volume was calculated from the product of three lattice parameters (a, b and c), which can be equated for the tetragonal system (a=b≠c) as follows;

$$\frac{1}{d^2} = \frac{h^2 + k^2}{a^2} + \frac{l^2}{c^2} \quad \text{.....(3)}$$

where d is a lattice spacing between the planes in the atomic lattice

h, k and l are the Miller indices

a, b and c are the lattice parameters

This is an example of finding all constants involved in the equation 3. Firstly, a *d*-spacing value was calculated from Bragg's equation as shown below.

$$2d\sin\theta_B = n\lambda \quad \text{.....(4)}$$

where θ_B is a Bragg's angle

n is an integer determined by the order given (n = 1)

λ is the wavelength of x-rarys ($\lambda_{Cu\ K\alpha}$ = 0.154 nm)

From the XRD pattern of N-S co-doped TiO_2 using titanium(IV) tetraisopropoxide calcined 400°C exhibited $2\theta_B = 25.535^o$ of (101) plane and 37.915^o of (004) plane the *d*-spacing values were 0.3484 and 0.2370 nm, respectively. Secondly, the *d*-spacing values and the Miller indices were replaced into the equation 3.

For the (101) plane; $$\frac{1}{0.3484^2} = \frac{1^2 + 0^2}{a^2} + \frac{1^2}{c^2} \quad \text{.....(5)}$$

For the (004) plane; $$\frac{1}{0.2370^2} = \frac{0^2 + 0^2}{a^2} + \frac{4^2}{c^2} \quad \text{.....(6)}$$

Last, from the equations 5 and 6, a and c lattice constants will be obtained; a = 0.3746 nm and c = 0.9481 nm. Hence, the unit cell volume is finally equal to 0.1307 nm^3.

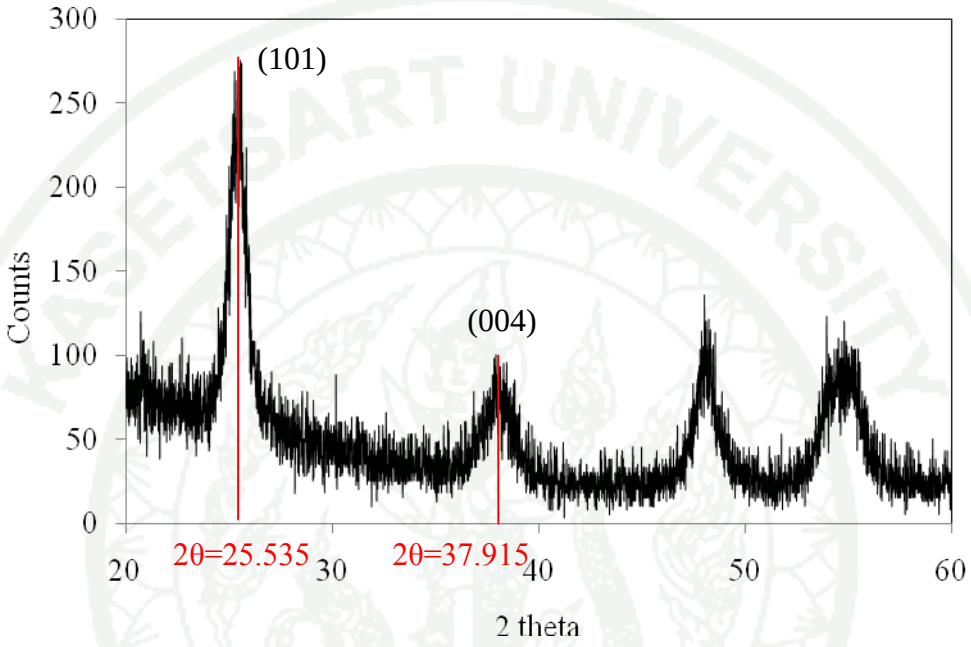

Appendix Figure C1 The XRD pattern of N-S co-doped TiO_2 using titanium(IV) tetraisopropoxide calcined at 400°C.

Appendix D

The procedure for the determination of the absorption edge of UV-Vis/DR results

The procedure that was used to find the absorption edge of each UV-Vis /DR spectrum conformed to previous research by Wan *et al.* (2007) as follows;

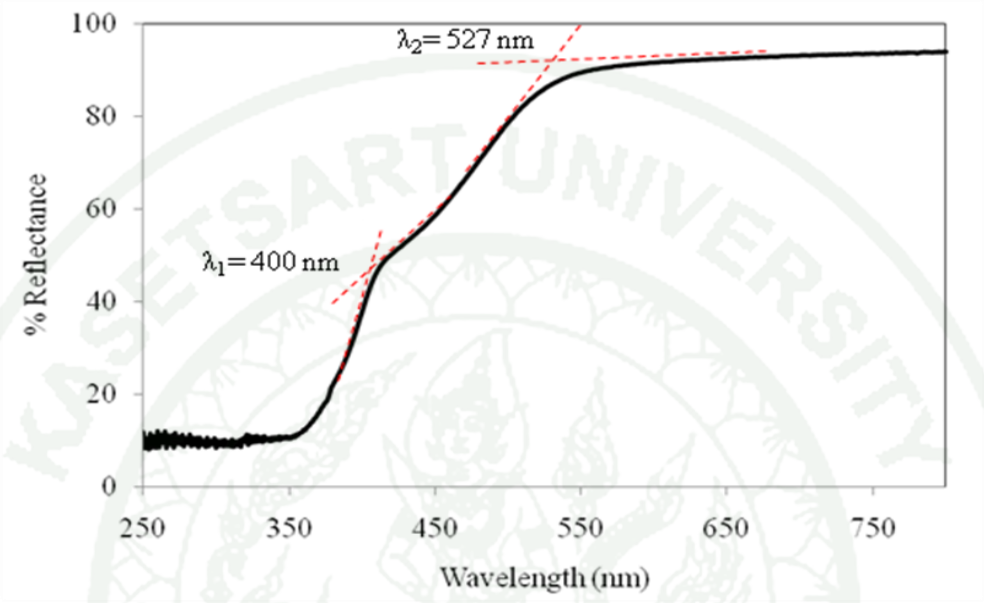

Appendix Figure D1 The UV-Vis/DR spectrum of N-S co-doped TiO_2 using titanium(IV) tetraisopropoxide calcined at 600°C.

Appendix E

Transmission Electron Microscopy (TEM) of N-S co-doped TiO_2

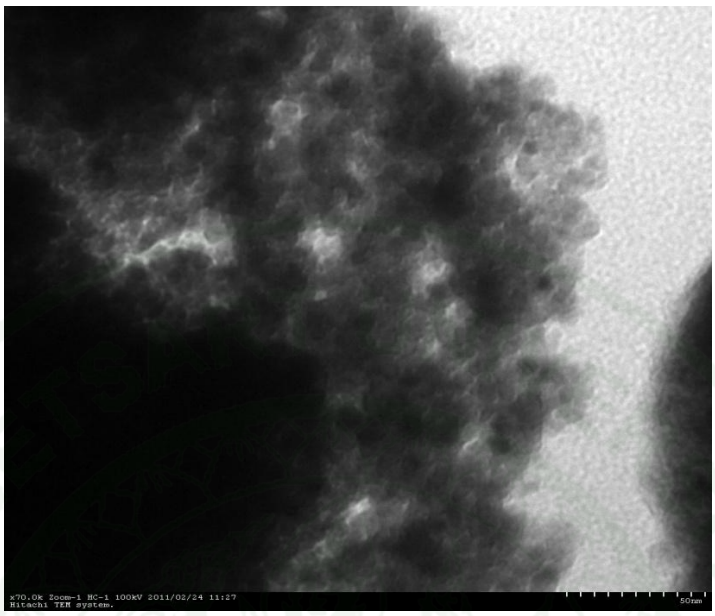

Appendix Figure E1 TEM image of the N-S co-doped TiO_2 using titanium(IV) tetraisopropoxide calcined at 400 ^{o}C.

The TEM image of the N-S co-doped TiO_2 used as titanium(IV) tetraisopropoxide as precursor. The TEM images exhibit that the spherical particle. The N-S co-doped TiO_2 had crystallite size less than 10 nm, approximately. There results were in agreement with the XRD results.

Appendix F

Calculation of rate constants of each photodegradation reactions

The procedure used to find rate constants was adapted from previous research by Fang *et al.* (2007). They assumed that the degradation of methylene blue in the presence of photocatalysts was the first-order kinetic reaction because they plotted a graph between $\ln C_o/C$ and degrading time (h). Then, they obtained the relative coefficient (R^2) was close to 1 and the slope of the graph could be considered as the rate constant of the photodegradation reaction. Therefore, this work properly modified their method to find the rate constants.The rate constants of all the photodegradation reactions as shown in Appendix Figure F1-F12.

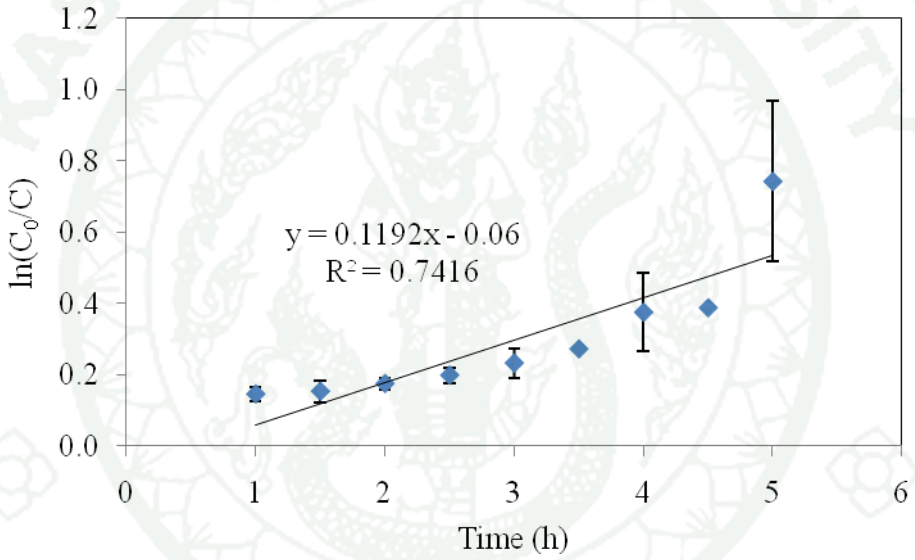

Appendix Figure F1 The relation between $\ln C_0/C$ and time (h) of photodegradation reaction of benz[a]anthracene using N-doped TiO_2 calcined at 400°C.

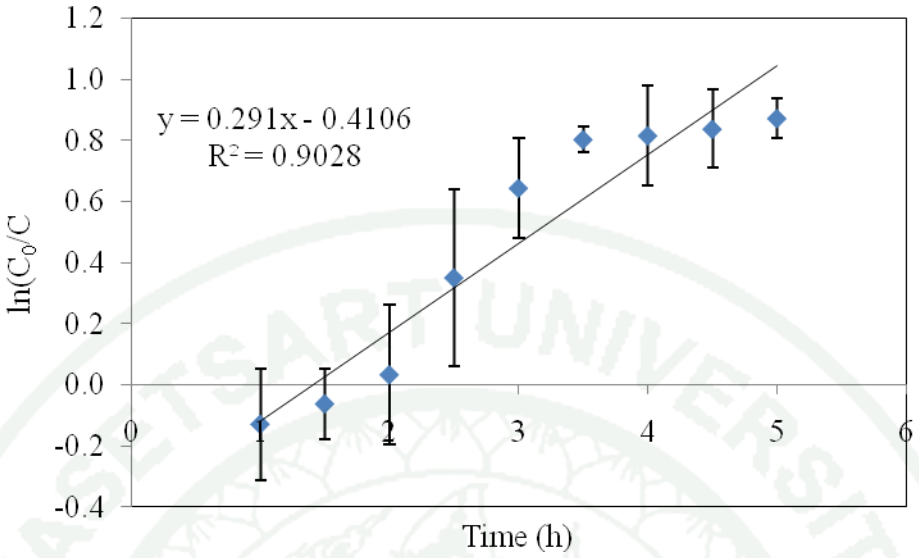

Appendix Figure F2 The relation between $\ln C_0/C$ and time (h) of photodegradation reaction of benz[a]anthracene by N-S co-doped TiO_2 using titanium(IV) tetraisopropoxide and used isopropanol as a solvent calcined at 300°C.

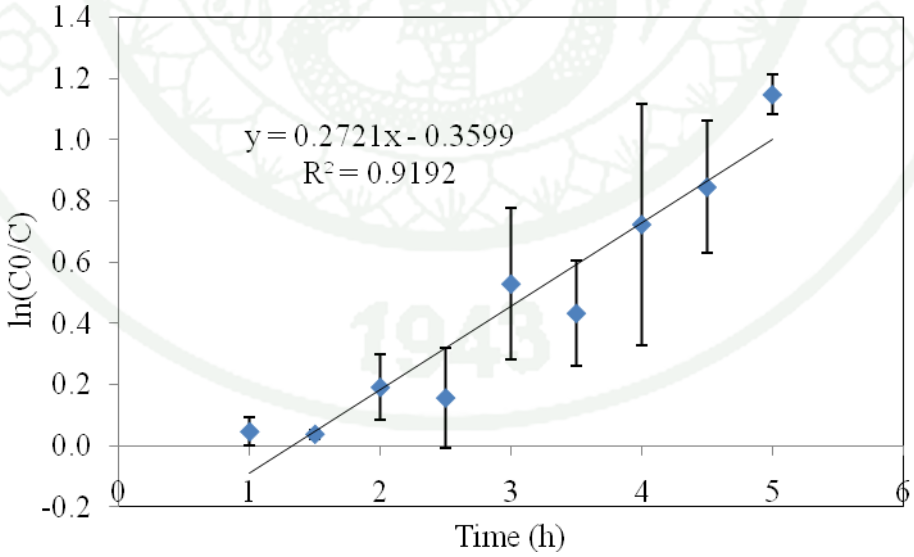

Appendix Figure F3 The relation between $\ln C_0/C$ and time (h) of photodegradation reaction of benz[a]anthracene by N-S co-doped TiO_2 using titanium(IV) tetraisopropoxide and used isopropanol as a solvent calcined at 400°C.

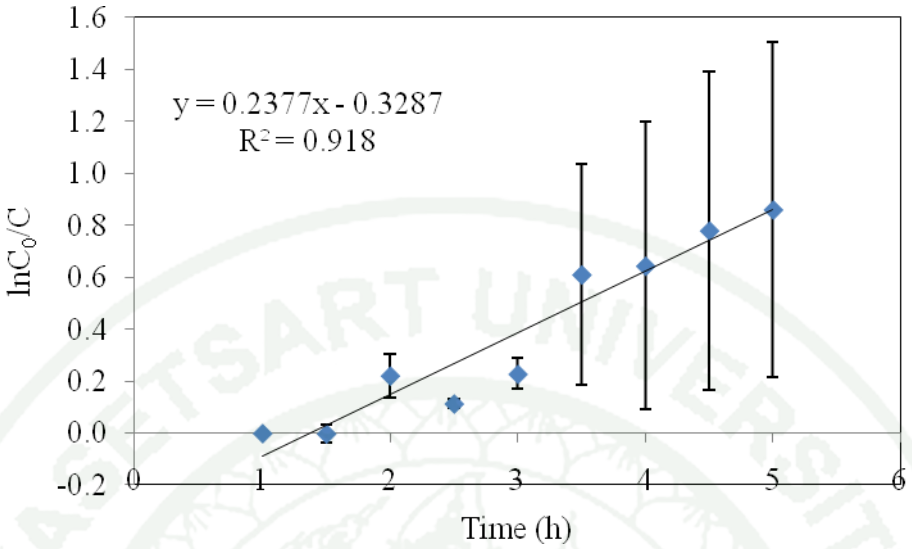

Appendix Figure F4 The relation between $\ln C_0/C$ and time (h) of photodegradation reaction of benz[a]anthracene by N-S co-doped TiO_2 using titanium(IV) tetraisopropoxide and used isopropanol as a solvent calcined at 500°C.

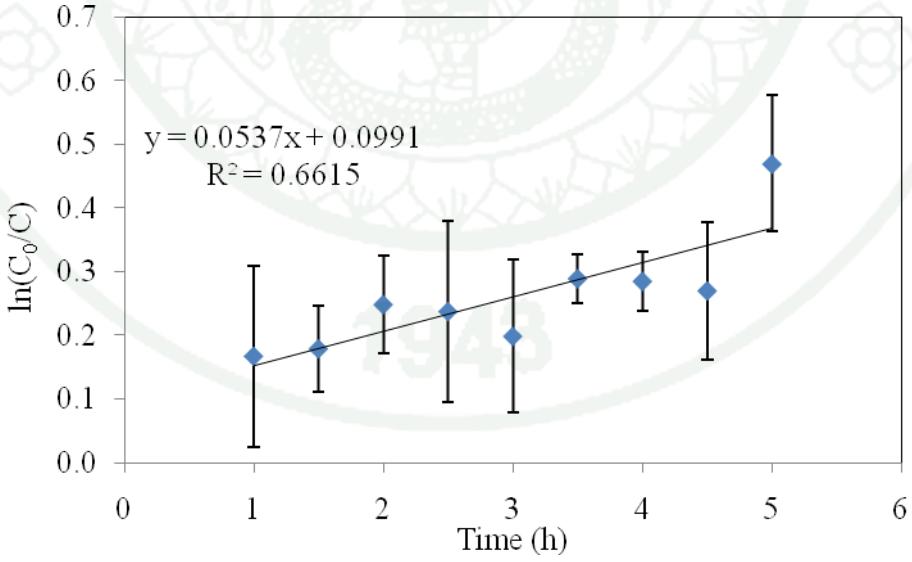

Appendix Figure F5 The relation between $\ln C_0/C$ and time (h) of photodegradation reaction of benz[a]anthracene by N-S co-doped TiO_2 using titanium(IV) tetraisopropoxide and used methanol as a solvent calcined at 400°C.

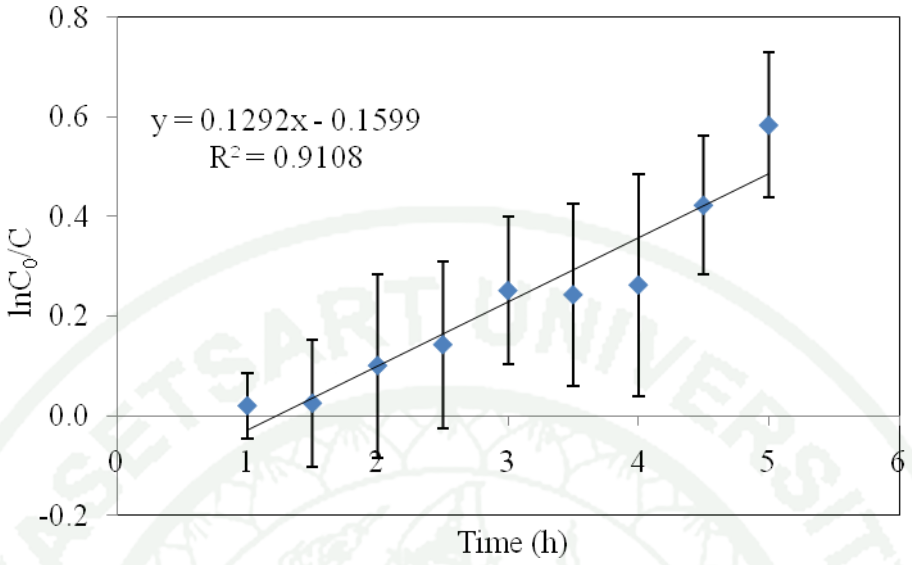

Appendix Figure F6 The relation between $\ln C_0/C$ and time (h) of photodegradation reaction of benz[a]anthracene by N-S co-doped TiO_2 using titanium(IV) tetraisopropoxide and used ethanol as a solvent calcined at 400°C.

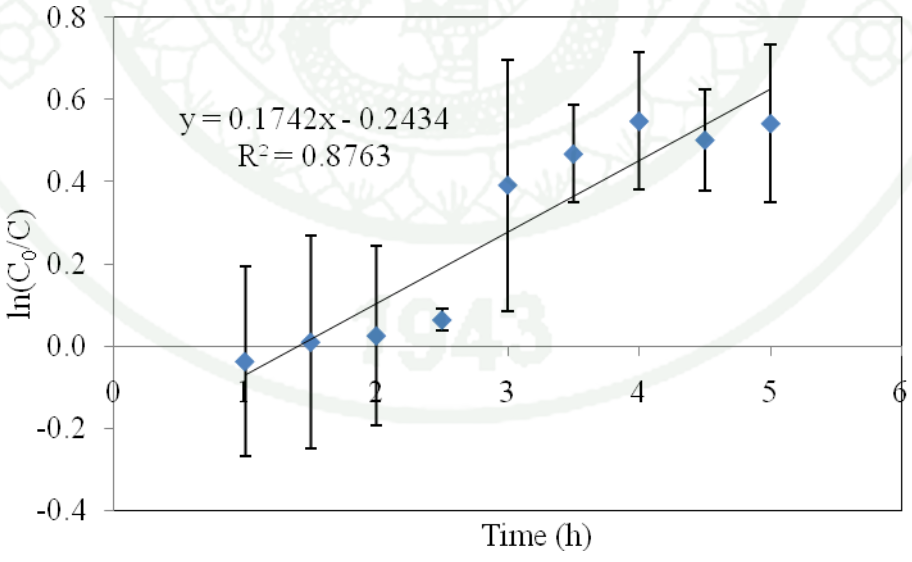

Appendix Figure F7 The relation between $\ln C_0/C$ and time (h) of photodegradation reaction of benz[a]anthracene by N-S co-doped TiO_2 using titanium(IV) tetra-n-butooxide and used isopropanol as a solvent calcined at 300°C.

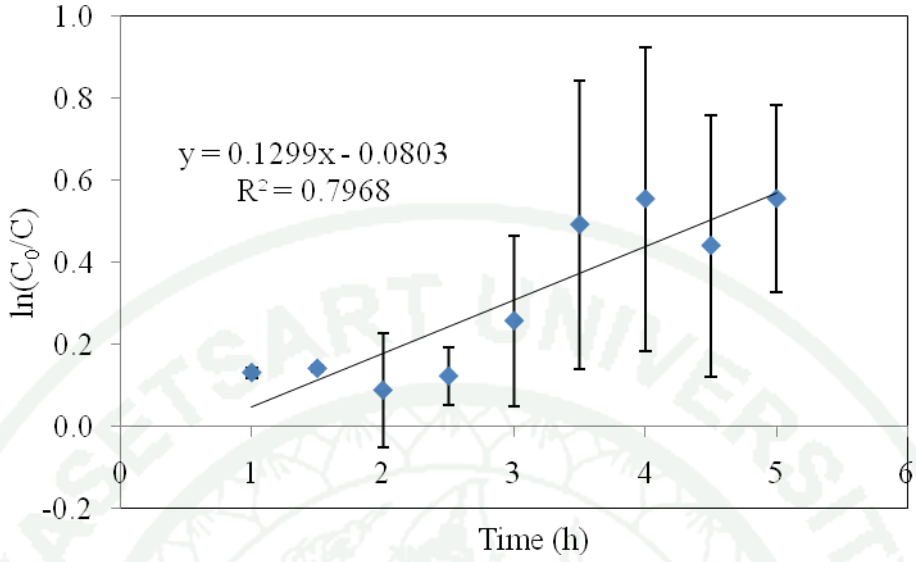

Appendix Figure F8 The relation between $\ln C_0/C$ and time (h) of photodegradation reaction of benz[a]anthracene by N-S co-doped TiO_2 using titanium(IV) tetra-n-butooxide and used isopropanol as a solvent calcined at 400°C.

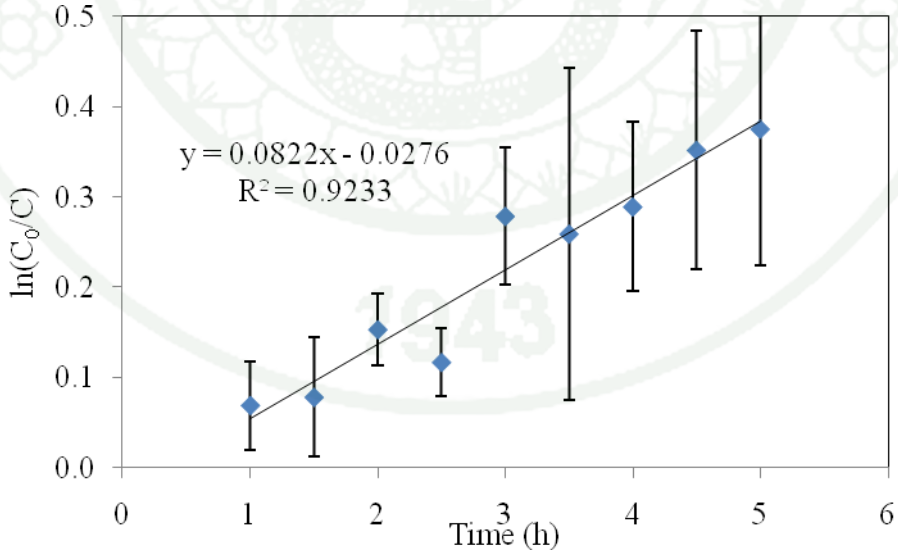

Appendix Figure F9 The relation between $\ln C_0/C$ and time (h) of photodegradation reaction of benz[a]anthracene by N-S co-doped TiO_2 using titanium(IV) tetra-n-butooxide and used isopropanol as a solvent calcined at 500°C.

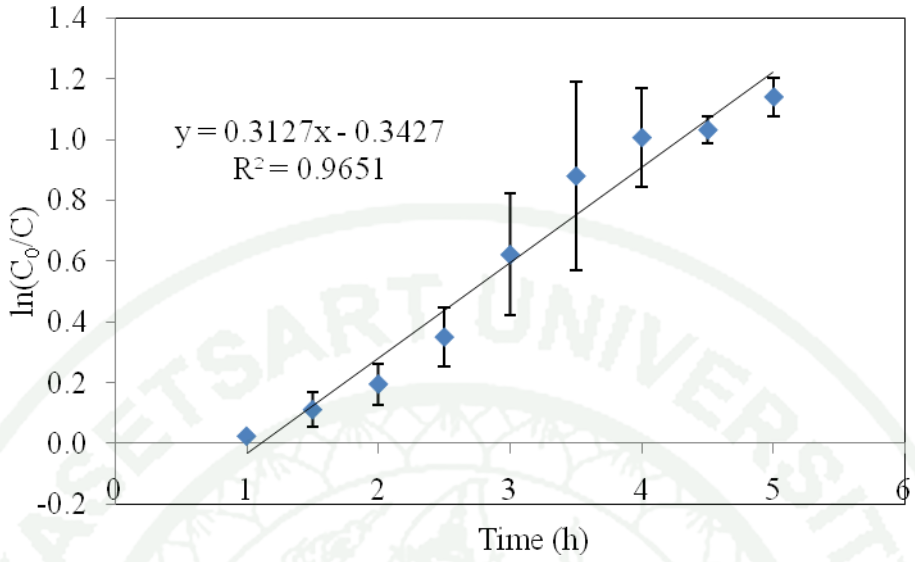

Appendix Figure F10 The relation between $\ln C_0/C$ and time (h) of photodegradation reaction of benz[a]anthracene by N-S co-doped TiO_2 using titanium(IV) tetra-n-butooxide and used methanol as a solvent calcined at 400°C.

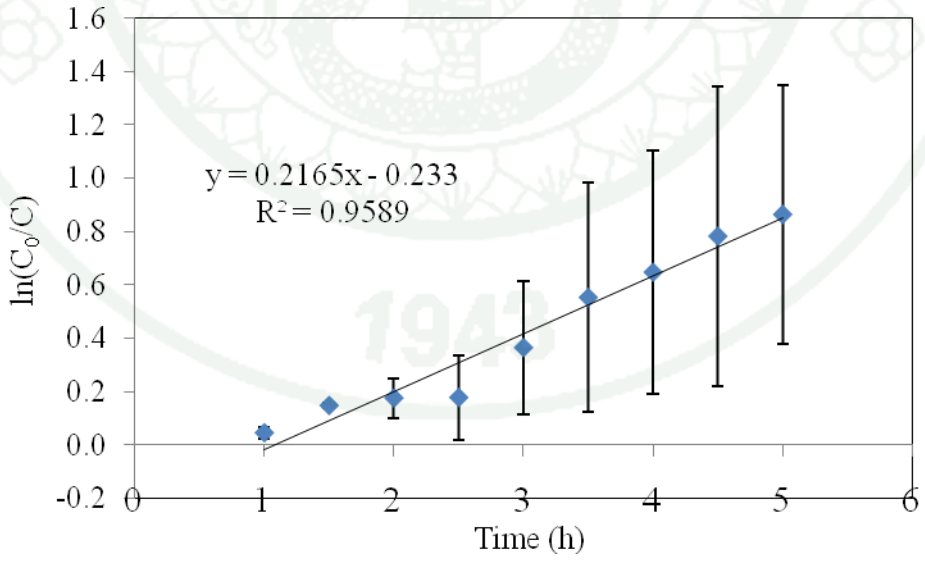

Appendix Figure F11 The relation between $\ln C_0/C$ and time (h) of photodegradation reaction of benz[a]anthracene by N-S co-doped TiO_2 using titanium(IV) tetra-n-butooxide and used ethanol as a solvent calcined at 400°C.

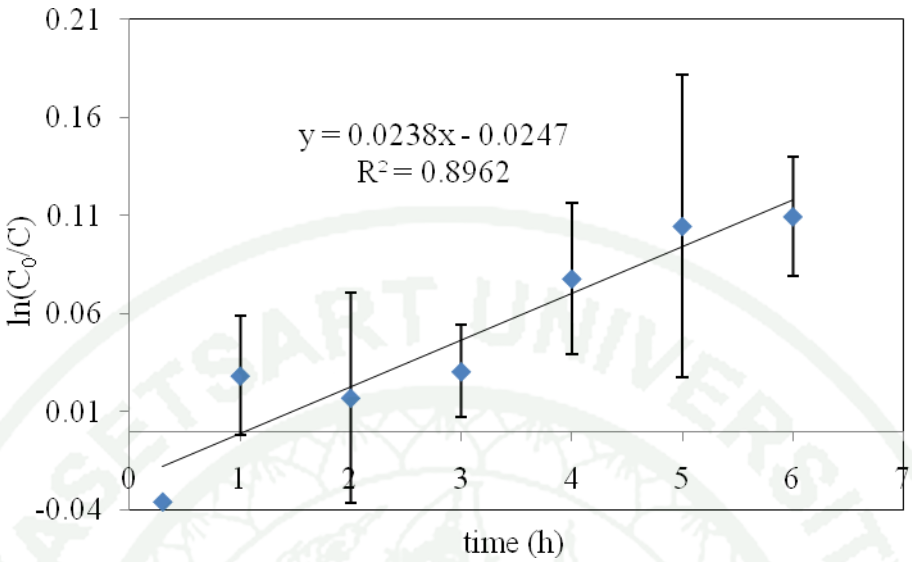

Appendix Figure F12 The relation between lnC_0/C and time (h) of photodegradation reaction of methylene by N-S co-doped TiO_2 using titanium(IV) tetraisopropoxide and used isopropanol as a solvent calcined at 400°C.

Appendix G

Raw data of all photodegradration reaction

Appendix Table G1 Raw data of the photodegradation reaction of benz[a]anthracene by N-S co-doped TiO_2 using titanium(IV) tetraisopropoxide and used isopropanol as a solvent calcined at 300°C.

Degradating time (h)	Absorbance at λ_{max} 264 nm			Concentration (ppm)			Relative concentration (C/C_0)				
	Abs_1	Abs_2	Abs_3	C_1	C_2	C_3	C_1/C_0	C_1/C_0	C_1/C_0	$(C/C_0)_{ave}$	$Std(C/C_0)$
before lamp on	345.998	365.716	336.371	16.0997	17.6731	16.0997	1	1	1	1	0
0	316.566	333.171	353.735	17.0307	15.9281	17.0307	0.90503	0.90126	1.05782	0.95470	0.08932
30	335.669	322.226	360.39	17.3875	15.3413	17.3875	0.96667	0.86806	1.07998	0.97157	0.10604
60	292.361	298.667	278.477	12.9957	14.0782	12.9957	0.82692	0.79659	0.8072	0.81024	0.01539
90	317.528	296.108	322.201	15.3400	13.9410	15.3400	0.90813	0.78882	0.95281	0.88325	0.08477
120	309.686	289.364	280.458	13.1019	13.5794	13.1019	0.88283	0.76836	0.81379	0.82166	0.05763
150	303.344	299.605	171.018	7.2343	14.1285	7.2343	0.86236	0.79943	0.44934	0.70371	0.22252
180	291.564	331.497	157.274	6.4974	15.8384	6.4974	0.82435	0.89618	0.40357	0.70803	0.26611
210	275.491	312.366	138.299	5.4801	14.8127	5.4800	0.77249	0.83815	0.34038	0.65034	0.27043
240	271.210	300.446	128.671	4.9638	14.1736	4.9638	0.75867	0.80198	0.30831	0.62299	0.27337

Appendix Table G2 Raw data of the photodegradation reaction of benz[a]anthracene by N-S co-doped TiO_2 using titanium(IV) tetraisopropoxide and used isopropanol as a solvent calcined at 400°C.

Degradating time (h)	Absorbance at λ_{max} 264 nm			Concentration (ppm)			Relative concentration (C/C_0)				
	Abs_1	Abs_2	Abs_3	C_1	C_2	C_3	C_1/C_0	C_2/C_0	C_3/C_0	$(C/C_0)_{ave}$	$Std(C/C_0)$
before lamp on	249.786	471.811	244.002	15.2774	23.3614	11.1473	1	1	1	1	1.74E+00
0	244.625	464.934	224.441	14.9084	22.9927	10.0986	0.97585	0.98422	0.90592	0.95533	0.04299
30	238.421	460.631	237.186	14.4649	22.7619	10.7819	0.94682	0.97434	0.96722	0.96279	0.01428
60	193.179	430.688	212.042	11.2305	21.1565	9.4338	0.73511	0.90562	0.84628	0.82900	0.08656
90	194.444	395.516	248.766	11.3209	19.2708	11.4027	0.74103	0.8249	1.02291	0.86295	0.14474
120	140.979	268.784	198.455	7.4987	12.4760	8.7053	0.49084	0.53405	0.78093	0.60194	0.15651
150	188.537	267.639	185.76	10.8986	12.4146	8.0247	0.71339	0.53142	0.71987	0.65489	0.10698
180	105.461	250.988	184.477	4.9595	11.5219	7.9559	0.32463	0.4932	0.7137	0.51051	0.19511
210	108.512	261.613	130.078	5.1776	12.0915	5.0393	0.33891	0.51759	0.45206	0.43619	0.09039
240	99.125	181.697	103.599	4.5065	7.8068	3.6196	0.29498	0.33418	0.32471	0.31796	0.02045

Appendix Table G3 Raw data of the photodegradation reaction of benz[a]anthracene by N-S co-doped TiO_2 using titanium(IV) tetraisopropoxide and used isopropanol as a solvent calcined at 500°C.

Degradating time (h)	Absorbance at λ_{max} 264 nm			Concentration (ppm)			Relative concentration (C/C_0)				
	Abs_1	Abs_2	Abs_3	C_1	C_2	C_3	C_1/C_0	C_2/C_0	C_3/C_0	$(C/C_0)_{ave}$	$Std(C/C_0)$
before lamp on	345.998	365.716	336.371	16.0997	17.6731	16.0997	1	1	1	1	0
0	316.566	333.171	353.735	17.0307	15.9281	17.0307	0.90503	0.90126	1.05782	0.954703	0.08932
30	335.669	322.226	360.39	17.3875	15.3413	17.3875	0.96667	0.86806	1.07998	0.97157	0.10604
60	292.361	298.667	278.477	12.9957	14.0782	12.9957	0.82692	0.79659	0.8072	0.810237	0.01539
90	317.528	296.108	322.201	15.3400	13.9410	15.3400	0.90813	0.78882	0.95281	0.883253	0.08477
120	309.686	289.364	280.458	13.1019	13.5794	13.1019	0.88283	0.76836	0.81379	0.82166	0.05763
150	303.344	299.605	171.018	7.23430	14.1285	7.23430	0.86236	0.79943	0.44934	0.70371	0.22252
180	291.564	331.497	157.274	6.49742	15.8384	6.49742	0.82435	0.89618	0.40357	0.708033	0.26611
210	275.491	312.366	138.299	5.48007	14.8127	5.48007	0.77249	0.83815	0.34038	0.65034	0.27043
240	271.21	300.446	128.671	4.96386	14.1736	4.96386	0.75867	0.80198	0.30831	0.622987	0.27337

Appendix Table G4 Raw data of the photodegradation reaction of benz[a]anthracene by N-S co-doped TiO_2 using titanium(IV) tetraisopropoxide and used methanol as a solvent calcined at 400°C.

Degradating time (h)	Absorbance at λ_{max} 264 nm			Concentration (ppm)			Relative concentration (C/C_0)				
	Abs_1	Abs_2	Abs_3	C_1	C_2	C_3	C_1/C_0	C_2/C_0	C_3/C_0	$(C/C_0)_{ave}$	$Std(C/C_0)$
before lamp on	480.782	427.859	441.306	23.8423	21.0049	21.7258	1	1	1	1	0
0	447.085	317.606	406.15	22.0357	15.0936	19.8409	0.92422	0.71857	0.91324	0.85201	0.85201
30	381.134	382.363	382.033	18.4997	18.5656	18.5479	0.77591	0.88387	0.85372	0.837833	0.83783
60	386.548	317.673	375.841	18.7900	15.0972	18.2159	0.78809	0.71874	0.83844	0.781757	0.78176
90	446.122	334.739	319.093	21.9840	16.0122	15.1733	0.92205	0.76231	0.6984	0.794253	0.79425
120	443.404	318.846	374.469	21.8383	15.1601	18.1423	0.91594	0.72174	0.83505	0.824243	0.82425
150	364.932	342.609	330.438	17.6310	16.4342	15.7816	0.73948	0.78239	0.72639	0.74942	0.74942
180	353.345	336.397	351.319	17.0098	16.1011	16.9012	0.71342	0.76654	0.77792	0.752627	0.75263
210	363.853	373.958	319.945	17.5732	18.1149	15.2190	0.73705	0.86241	0.7005	0.766653	0.76666
240	344.423	282.585	263.014	16.5314	13.2160	12.1667	0.69336	0.62918	0.56001	0.627517	0.62752

Appendix Table G5 Raw data of the photodegradation reaction of benz[a]anthracene by N-S co-doped TiO_2 using titanium(IV) tetraisopropoxide and used ethanol as a solvent calcined at 400°C.

Degradating time (h)	Absorbance at λ_{max} 264 nm			Concentration (ppm)			Relative concentration (C/C_0)				
	Abs_1	Abs_2	Abs_3	C_1	C_2	C_3	C_1/C_0	C_2/C_0	C_3/C_0	$(C/C_0)_{ave}$	$Std(C/C_0)$
before lamp on	365.923	252.617	365.011	17.6842	11.6092	17.6353	1	1	1	1	2.49E-07
0	367.96	259.158	335.325	17.7934	11.9599	16.0436	1.00617	1.0302	0.90974	0.98203	0.06375
30	402.823	246.019	319.586	19.6626	11.2555	15.1998	1.11187	0.96952	0.86189	0.98109	0.12538
60	314.558	277.488	294.683	14.9302	12.9427	13.8646	0.84427	1.11486	0.78618	0.91510	0.17541
90	378.953	218.001	281.688	18.3828	9.7533	13.1679	1.0395	0.84013	0.74667	0.87543	0.14957
120	305.378	225.59	252.67	14.4380	10.1602	11.6121	0.81643	0.87518	0.65845	0.78335	0.11208
150	349.282	203.289	252.555	16.7919	8.9645	11.6059	0.94954	0.77218	0.6581	0.79327	0.14686
180	329.609	222.041	231.961	15.7372	9.9699	10.5017	0.8899	0.85879	0.59549	0.78139	0.16174
210	288.961	164.11	240.204	13.5578	6.8639	10.9437	0.76666	0.59124	0.62055	0.65948	0.09396
240	252.816	144.214	209.98	11.6199	5.7972	9.3232	0.65708	0.49936	0.52867	0.56170	0.08388

Appendix Table G6 Raw data of the photodegradation reaction of benz[a]anthracene by N-S co-doped TiO_2 using titanium(IV) tetra-n-butoxide and used isopropanol as a solvent calcined at 300°C.

Degradating time (h)	Absorbance at λ_{max} 264 nm			Concentration (ppm)			Relative concentration (C/C_0)				
	Abs_1	Abs_2	Abs_3	C_1	C_2	C_3	C_1/C_0	C_2/C_0	C_3/C_0	$(C/C_0)_{ave}$	$Std(C/C_0)$
before lamp on	364.808	368	332.465	17.6244	17.7955	15.8903	1	1	1	1	3.08E-07
0	479.949	330.327	312.208	23.7977	15.7757	14.8042	1.35027	0.88649	0.93165	1.05614	0.25572
30	471.373	337.736	274.699	23.3379	16.1729	12.7932	1.32418	0.90881	0.80509	1.01269	0.27469
60	433.566	360.326	268.182	21.3108	17.3841	12.4437	1.20916	0.97688	0.7831	0.98971	0.21332
90	353.561	340.952	311.348	17.0214	16.3453	14.7581	0.96578	0.9185	0.92874	0.93767	0.02487
120	192.987	289.424	287.386	8.41218	13.5826	13.4734	0.4773	0.76326	0.8479	0.69615	0.19419
150	218.456	245.424	244.553	9.7777	10.6943	11.1769	0.55478	0.63069	0.70337	0.62961	0.0743
180	195.246	233.381	235.816	8.5333	10.5779	10.7084	0.48417	0.59441	0.67389	0.58416	0.09527
210	213.36	234.735	240.404	9.50448	10.6505	10.9544	0.53928	0.59849	0.68937	0.60905	0.0756
240	191.21	237.92	239.829	8.3169	10.8212	10.9236	0.47189	0.60808	0.68743	0.58913	0.10901

Appendix Table G7 Raw data of the photodegradation reaction of benz[a]anthracene by N-S co-doped TiO_2 using titanium(IV) tetra-n-butoxide and used isopropanol as a solvent calcined at 400°C.

Degradating time (h)	Absorbance at λ_{max} 264 nm			Concentration (ppm)			Relative concentration (C/C_0)				
	Abs_1	Abs_2	Abs_3	C_1	C_2	C_3	C_1/C_0	C_2/C_0	C_3/C_0	$(C/C_0)_{ave}$	$Std(C/C_0)$
before lamp on	364.808	339.034	398.836	17.6244	16.2425	19.4488	1	1	1	1	6.58E-09
0	326.374	298.11	356.571	15.5637	14.0483	17.1827	0.88308	0.86491	0.88348	0.87716	0.0106
30	323.644	298.987	348.817	15.4173	14.0954	16.7670	0.87477	0.8678	0.86211	0.86823	0.00634
60	380.479	315.741	323.801	18.4646	14.9936	15.4258	1.04767	0.92311	0.79314	0.92131	0.12727
90	349.983	288.642	351.357	16.8295	13.5407	16.9032	0.9549	0.83366	0.86911	0.88589	0.06233
120	333.836	289.338	257.373	15.9638	13.5780	11.8642	0.90578	0.83595	0.61002	0.78392	0.15459
150	336.719	182.732	223.37	16.1184	7.8623	10.0411	0.91455	0.48406	0.51628	0.63830	0.23978
180	321.594	165.498	221.29	15.3074	6.9383	9.9296	0.86853	0.42717	0.51055	0.60208	0.23448
210	313.844	173.393	288.532	14.8919	7.3616	13.5348	0.84496	0.45323	0.69592	0.66470	0.19772
240	281.631	185.748	222.021	13.1648	8.0240	9.9688	0.74696	0.49401	0.51256	0.58451	0.14099

Appendix Table G8 Raw data of the photodegradation reaction of benz[a]anthracene by N-S co-doped TiO_2 using titanium(IV) tetra-n-butoxide and used isopropanol as a solvent calcined at 500°C.

Degradating time (h)	Absorbance at λ_{max} 264 nm			Concentration (ppm)			Relative concentration (C/C_0)				
	Abs_1	Abs_2	Abs_3	C_1	C_2	C_3	C_1/C_0	C_2/C_0	C_3/C_0	$(C/C_0)_{ave}$	$Std(C/C_0)$
before lamp on	336.371	368.544	320.008	16.0997	17.8247	15.2224	1	1	1	1	1.37E-07
0	301.042	355.321	308.756	14.2055	17.1157	14.6191	0.88235	0.96023	0.96037	0.934317	0.93431
30	315.753	323.11	315.693	14.9943	15.3887	14.9911	0.93134	0.86334	0.9848	0.926493	0.92649
60	287	334.563	275.32	13.4527	16.0028	12.8264	0.83558	0.89779	0.8426	0.858657	0.85865
90	300.988	322.56	299.412	14.2026	15.3592	14.1181	0.88217	0.86168	0.92746	0.890437	0.89043
120	277.829	267.175	255.98	12.9610	12.3897	11.7895	0.80504	0.69509	0.77449	0.758207	0.7582
150	305.507	245.178	267.425	14.4449	11.2104	12.4032	0.89722	0.62893	0.8148	0.780317	0.78031
180	274.897	259.488	259.235	12.8038	11.9776	11.9640	0.79528	0.67197	0.78595	0.751067	0.75106
210	267.257	236.848	248.491	12.3941	10.7638	11.3880	0.76984	0.60387	0.74811	0.707273	0.70727
240	274.12	230.764	234.336	12.7621	10.4376	10.6291	0.79269	0.58557	0.69825	0.69217	0.69217

Appendix Table G9 Raw data of the photodegradation reaction of benz[a]anthracene by N-S co-doped TiO_2 using titanium(IV) tetra-n-butoxide and used methanol as a solvent calcined at 400°C.

Degradating time (h)	Absorbance at λ_{max} 264 nm			Concentration (ppm)			Relative concentration (C/C_0)				
	Abs_1	Abs_2	Abs_3	C_1	C_2	C_3	C_1/C_0	C_2/C_0	C_3/C_0	$(C/C_0)_{ave}$	$Std(C/C_0)$
before lamp on	345.83	501.491	382.708	16.6069	24.9527	18.5841	1	1	1	1	1.67E-07
0	357.969	485.589	357.764	17.2577	24.1001	17.2467	1.03919	0.96583	0.92803	0.97768	0.05651
30	323.378	470.262	323.387	15.4031	23.2783	15.4036	0.92751	0.93289	0.82885	0.89642	0.05857
60	318.27	384.841	319.138	15.1292	18.6984	15.1758	0.91102	0.74935	0.8166	0.82566	0.08121
90	291.208	297.503	298.388	13.6783	14.0158	14.0632	0.82365	0.56169	0.75673	0.71402	0.1361
120	248.884	212.983	242.058	11.4091	9.4842	11.0431	0.68701	0.38009	0.59422	0.55377	0.1574
150	185.494	198.79	183.004	8.0104	8.7233	7.8769	0.48235	0.34959	0.42385	0.41860	0.06653
180	144.928	204.739	169.036	5.8354	9.0422	7.1280	0.35138	0.36237	0.38355	0.36577	0.01635
210	139.055	211.407	161.547	5.5206	9.3997	6.7265	0.33242	0.3767	0.36195	0.35702	0.02254
240	141.732	196.669	132.448	5.6641	8.6095	5.1663	0.34107	0.34503	0.27799	0.32136	0.03761

Appendix Table G10 Raw data of the photodegradation reaction of benz[a]anthracene by N-S co-doped TiO_2 using titanium(IV) tetra-n- butoxide and used ethanol as a solvent calcined at 400°C.

Degradating time (h)	Absorbance at λ_{max} 264 nm			Concentration (ppm)			Relative concentration (C/C_0)				
	Abs_1	Abs_2	Abs_3	C_1	C_2	C_3	C_1/C_0	C_2/C_0	C_3/C_0	$(C/C_0)_{ave}$	$Std(C/C_0)$
before lamp on	345.83	508.424	339.968	16.2926	25.3244	16.2926	1	1	1	1	1.84E-07
0	327.037	499.054	325.036	15.4920	24.8220	15.4920	0.93932	0.98016	0.95086	0.95678	0.02105
30	306.61	442.037	296.909	13.9839	21.7650	13.9839	0.87337	0.85945	0.8583	0.86371	0.00839
60	318.559	426.181	274.898	12.8038	20.9149	12.8038	0.91195	0.82588	0.78586	0.84123	0.06443
90	343.217	377.397	285.691	13.3825	18.2993	13.3825	0.99156	0.7226	0.82138	0.84518	0.13605
120	304.766	285.831	258.729	11.9369	13.3900	11.9369	0.86742	0.52874	0.73266	0.70961	0.17051
150	305.393	210.395	217.121	9.7061	9.3455	9.7061	0.86944	0.36903	0.59573	0.61140	0.25057
180	311.108	227.527	157.669	6.5185	10.2640	6.5185	0.8879	0.4053	0.40009	0.56443	0.28014
210	307.462	190.413	138.04	5.4661	8.2741	5.4661	0.87612	0.32673	0.3355	0.51278	0.31469
240	260.162	210.644	121.548	4.5819	9.3588	4.5819	0.72342	0.36956	0.28122	0.45807	0.234

Appendix Table G11 Raw data of the photodegradation reaction of benz[a]anthracene by undoped TiO_2 calcined at 400°C.

Degrading time	Absorbance at λ_{max} 251 nm			Concentration (ppm)			Relative concentration (C/C_0)				
(h)	Abs_1	Abs_2	Abs_3	C_1	C_2	C_3	C_1/C_0	C_2/C_0	C_3/C_0	$(C/C_0)_{ave}$	Std(C/C0)
before lamp on	460.59	460.59	260.59	0.2866	0.2866	0.2866	1	1	1	1	0
0	366.693	394.475	415.651	0.2260	0.2440	0.2576	0.7887	0.85121	0.89887	0.84626	0.05525
30	399.48	431.509	382.653	0.2472	0.2679	0.2363	0.86248	0.93455	0.82461	0.87388	0.05585
60	437.871	476.965	484.335	0.272	0.2972	0.3019	0.94887	1.03684	1.05343	1.01305	0.05619
90	388.747	460.591	499.118	0.2403	0.2866	0.3115	0.83832	1	1.0867	0.97501	0.12605
120	417.5771	447.105	403.153	0.2589	0.2779	0.2496	0.9032	0.96965	0.87074	0.91453	0.05041
150	399.376	406.79	472.518	0.2471	0.2519	0.2943	0.86224	0.87893	1.02684	0.92267	0.09059
180	441.537	498.441	424.847	0.2743	0.3110	0.2636	0.95712	1.08517	0.91956	0.98728	0.08682
210	416.371	491.399	460.139	0.2581	0.3065	0.2863	0.90049	1.06933	0.99898	0.9896	0.0848
240	416.247	483.658	437.089	0.2580	0.3015	0.2715	0.90021	1.05191	0.94711	0.96641	0.07766

Appendix Table G12 Raw data of the photodegradation reaction of benz[a]anthracene by N-doped TiO_2 calcined at 400°C.

Degrading time	Absorbance at λ_{max} 251 nm			Concentration (ppm)			Relative concentration (C/C_0)				
(h)	Abs_1	Abs_2	Abs_3	C_1	C_2	C_3	C_1/C_0	C_2/C_0	C_3/C_0	$(C/C_0)_{ave}$	$Std(C/C_0)$
before lamp on	769.41	757.86	657.71	5.3772	5.2947	4.5797	1	1	1	1	5.95E-08
0	655.24	658.16	582.36	4.5621	4.5829	4.0418	0.84842	0.86557	0.88254	0.86551	0.01706
30	680.52	657.59	548.74	4.7426	4.5789	3.8018	0.88198	0.8648	0.83013	0.85897	0.02641
60	649.17	648.74	547.26	4.5188	4.5157	3.7912	0.84036	0.85287	0.82782	0.84035	0.01252
90	621.94	637.67	542.31	4.3243	4.4367	3.7558	0.80421	0.83794	0.82011	0.82075	0.01687
120	585.71	614.88	540.33	4.0657	4.2739	3.7417	0.7561	0.80721	0.81702	0.79344	0.0327
150	-	-	505.07	-	-	3.4900	-	-	0.76205	0.76205	-
180	475.44	539.87	500.24	3.2784	3.7384	3.4555	0.6097	0.70607	0.75452	0.69010	0.07372
210	-	-	451.63	-	-	3.1085	-	-	0.67875	0.67875	-
240	372.85	298.13	399.67	2.5460	2.0126	2.7375	0.47349	0.38012	0.59775	0.48379	0.10918

Appendix Table G13 Raw data of the photodegradation reaction of benz[a]anthracene without catalyst.

Degradating time (h)	Absorbance at λ_{max} 264 nm			Concentration (ppm)			Relative concentration (C/C_0)				
	Abs_1	Abs_2	Abs_3	C_1	C_2	C_3	C_1/C_0	C_2/C_0	C_3/C_0	$(C/C_0)_{ave}$	$Std(C/C_0)$
before lamp on	365.716	238.71	335.043	17.6731	10.8636	16.0285	1	1	1	1	0
0	330.047	243.646	327.24	15.7606	11.1282	15.6102	0.89179	1.02436	0.97389	0.96335	0.06691
30	328.097	241.476	315.955	15.6561	11.0119	15.0051	0.88587	1.01365	0.93615	0.94522	0.06437
60	333.366	284.439	327.217	15.9386	13.3154	15.6089	0.90185	1.22568	0.97382	1.03378	0.17003
90	341.016	260.288	347.461	16.3488	12.0205	16.6943	0.92506	1.10649	1.04153	1.02436	0.09192
120	311.079	235.907	304.76	14.7437	10.7133	14.4049	0.83424	0.98616	0.8987	0.90637	0.07625
150	358.074	227.355	305.495	17.2633	10.2548	14.4443	0.97681	0.94396	0.90116	0.94064	0.03793
180	330.32	209.66	303.759	15.7753	9.3061	14.3512	0.89261	0.85663	0.89535	0.88153	0.02161
210	353.16	258.988	300.397	16.9999	11.9508	14.171	0.9619	1.10007	0.8841	0.98202	0.10938
240	332.104	280.094	299.331	15.8709	13.0824	14.1138	0.89803	1.20424	0.88054	0.99427	0.18204

Appendix Table G14 Raw data of the photodegradation reaction of methylene blue by N-S co-doped TiO_2 using titanium(IV) tetraisopropoxide and used isopropanol as a solvent calcined at 400°C.

Degradating time (h)	Absorbance at λ_{max} 264 nm			Concentration (ppm)			Relative concentration (C/C_0)				
	Abs_1	Abs_2	Abs_3	C_1	C_2	C_3	C_1/C_0	C_2/C_0	C_3/C_0	$(C/C_0)_{ave}$	$Std(C/C_0)$
before lamp on	0.99	0.99	1.06	9.4809	9.4809	10.1905	1	1	1	1	0
30 min	1.032	1.049	1.062	9.9067	10.0790	10.2108	1.04491	1.06308	1.00199	1.03666	0.03137
1	1.022	0.935	1.003	9.8053	8.9233	9.6127	1.03421	0.94118	0.94329	0.972893	0.05311
2	0.997	0.972	1.021	9.5519	9.2984	9.7952	1.00748	0.98075	0.9612	0.983143	0.02323
3	0.997	0.963	0.992	9.5519	9.2072	9.5012	1.00748	0.97112	0.93235	0.970317	0.03757
4	0.953	0.965	0.906	9.1058	9.2274	8.6293	0.96043	0.97326	0.84679	0.926827	0.06961
5	0.922	0.899	0.932	8.7915	8.5583	8.8929	0.92728	0.90269	0.87266	0.900877	0.02735
6	0.929	0.88	0.932	8.8625	8.3657	8.8929	0.93477	0.88237	0.87266	0.8966	0.03341

Appendix Table G15 Raw data of the photodegradation reaction of methylene blue by N-S co-doped TiO_2 using titanium(IV) tetra-n-butoxide and used methanol as a solvent calcined at 400°C.

Degradating time (h)	Absorbance at λ_{max} 264 nm			Concentration (ppm)			Relative concentration (C/C_0)				
	Abs_1	Abs_2	Abs_3	C_1	C_2	C_3	C_1/C_0	C_2/C_0	C_3/C_0	$(C/C_0)_{ave}$	$Std(C/C_0)$
before lamp on	1.06	1.06	1.06	10.1905	10.1905	10.1905	1	1	1	1	0
30 min	1.036	0.996	1.048	9.9472	9.5417	10.0689	0.97612	0.93633	0.98806	0.96684	0.02708
1	1.077	1.023	1.059	10.3629	9.8154	10.1804	1.01691	0.96319	0.999	0.99303	0.02735
2	1.081	1.026	1.044	10.4034	9.8459	10.0283	1.02089	0.96617	0.98408	0.99038	0.02789
3	1.05	1.066	1.053	10.0892	10.2514	10.1196	0.99005	1.00596	0.99303	0.99635	0.00846
4	1.079	0.994	1.034	10.3832	9.5214	9.9270	1.0189	0.93434	0.97413	0.97579	0.0423
5	1.072	1.044	1.051	10.3122	10.0283	10.0993	1.01193	0.98408	0.99104	0.99568	0.01449
6	0.977	0.974	1.028	9.34914	9.31873	9.8661	0.91743	0.91444	0.96816	0.93334	0.03019

CIRRICULUM VITAE

NAME : Miss Wanlapa Chitchiaranai

BIRTH DATE : March 27, 1985

BIRTH PLACE : Chonburi, Thailand

EDUCATION :	**YEAR**	**INSTITUTE**	**DEGREE/DIPLOMA**
	2008	Kasetsart Univ.	B.Sc. (General Science)

POSITION/TITLE : Postgraduate student

WORKPLACE : Faculty of Science, Kasetsart University

SCHOLARSHIP/AWARDS : Center for Innovation in Chemistry: Postgraduate Education and Research Program in Chemistry (PERCH-CIC)